



## ReSource—a new web service for authors and referees

Tracking the progress of journal articles is about to become a whole lot easier for RSC authors and referees, thanks to the launch of a new online service: ReSource. Designed to provide a user-friendly entry point, the ReSource homepage allows access to an extensive range of online publishing services *via* a single ID and password.

The ReSource services for referees were launched earlier this year and allow referees to download articles for review, upload their reports, view their refereeing history, and update research interest information. These referee services are available to any current RSC referee.

Now ReSource has been integrated with the RSC online services for authors. New and current authors can register to use ReSource to view and access all the

information and tools they need to submit their manuscripts. Existing ReSource users (referees) do not need to register again; they automatically have access to all author services using their existing ID.

Electronic submission has been available to RSC authors for several years. ReSource takes this several steps further, allowing authors to track their manuscript through the various stages of the peer review and publication process and then collect their free electronic reprints. Over time, authors will be able to build up a valuable record of their publication history. A further development will also provide electronic collection of article proofs.

In the past, authors had the chore of photocopying and mailing bulky

manuscripts, then often seeing them delayed in the post for days. Online submission saw a dramatic saving in time and costs, and ReSource will make life even simpler for authors by enabling them to see the progress of their article from submission through to publication.

We hope that you will discover ReSource for yourself as soon as possible, as an author, a referee, or both! ReSource services can be accessed from [www.rsc.org/resource](http://www.rsc.org/resource). Feedback on the ReSource site and suggestions for improvements are very welcome; please contact [resource@rsc.org](mailto:resource@rsc.org).

**Harp Minhas**  
Managing Editor  
*Green Chemistry*



## Highlights

Markus Hölscher reviews some of the recent literature in green chemistry

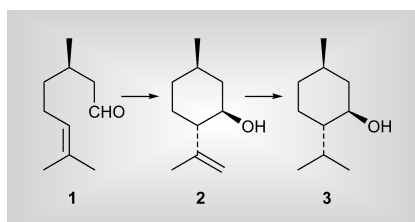
### Synthesis of chiral mesoporous silica

Shape selective processes in catalysis and separation media add to the tool box of modern sustainable technology. Although chirality is widely abundant in many biologically active molecules it was not possible until recently to synthesize mesoporous materials with large-scale chiral pores. Che *et al.* from Shanghai Jiao Tong University have succeeded in creating a template approach for the formation of chiral micelles, which enables the formation of chiral mesoporous silica (*Nature* 2004, **429**, 281–284). The successful formation of this material is based on the careful choice of appropriate micelle forming agents: *N*-trimethoxysilylpropyl-*N,N,N*-trimethylammonium chloride (TMAPS), 3-aminopropyltrimethoxysilane (APS) and *N*-miristoyl-*L*-alanine sodium salt (C14-*L*-AlaS), partially neutralized with HCl. The alkoxy silane sites of TMAPS are co-condensed with tetraethoxysilane (TEOS) and in this way form the silica framework. X-Ray diffraction patterns of the calcined material showed peaks between 1.5 and 6° (2  $\theta$ ) and according to TEM pictures the material has a hexagonal mesoscopic structure with lattice constant *a* amounting to 4.4 nm. The Barrett–Joyner–Halenda (BJH) pore diameter was determined to be 2.2 nm and the Brunauer–Emmett–Teller surface was 600 m<sup>2</sup> g<sup>-1</sup>. The material has a morphology consisting of chiral rods with mesoporous channels inside, which were used for the production of chiral cobalt and platinum nanowires. CD-spectra of the synthesis gel showed bands around 210–250 nm with positive sign, whereas synthesis gels with racemic C14-*L*-AlaS contained no bands, proving the existence of chiral micelles.

### Menthol synthesis using Ir-beta zeolites

As menthol is used on large scales for flavouring applications and in the pharmaceutical industries, it is desirable to produce it according to the general rules

of sustainability. One of the current main routes is the conversion of enantiopure (*R*)-citronellal **1** to (–)-isopulegol **2** using a ZnBr<sub>2</sub> catalyst. A subsequent hydrogenation yields the target molecule (–)-menthol **3**.

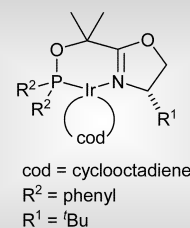


In avoiding generation of salt by-products, a bifunctional Ir/H-beta zeolite opens a possible route to a more selective and greener process, as was shown by Jacobs *et al.* from the University of Leuven (*Chem. Commun.* 2004, 1292–1293). Ir/H-beta zeolite (and for comparison also H-mor, Ir/H-mor and H-beta) was impregnated with iridium and used as catalyst for citronellal isomerization in a first step. The Ir/H-beta zeolite was the most active of all catalysts studied yielding only **2** and its stereoisomers (selectivity: 75%:20%:4% isopulegol:neoisopulegol:iso-isopulegol). The subsequent reduction with H<sub>2</sub> is also efficient, as was shown in different experiments in which a range of reaction conditions were varied. Of these variables, the H<sub>2</sub> pressure was found to be crucial. With a 3% Ir/H-beta zeolite, a full citronellal conversion is reached with menthol yield amounting to 93% (H<sub>2</sub> pressure is 0.8 Mpa). 17 g of menthol could be synthesized in this way using 1 g of catalyst in one single run. Recycling experiments showed the catalyst maintained its activity and selectivity.

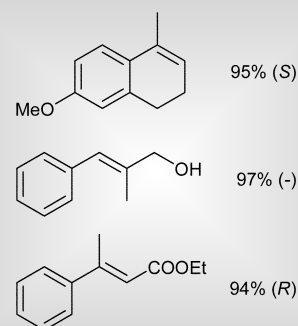
### Asymmetric hydrogenation of olefins using simple PHOX-iridium catalysts

In addition to rhodium and ruthenium hydrogenation catalysts, a recently developed class of iridium compounds can also be used for highly efficient and enantioselective hydrogenations of C–C double bonds. In an extension to earlier work,

Pfaltz *et al.* from the University of Basel have developed novel P,N-ligand core structures, which were called Simple-PHOX ligands because they can be prepared in only two steps from simple precursors (*Org. Lett.* 2004, **6**, 2023–2026). The versatility of the resulting iridium complexes in hydrogenations of olefins is impressive, since trisubstituted, unfunctionalized olefins could be hydrogenated with full conversion and ee's of up to 99%.



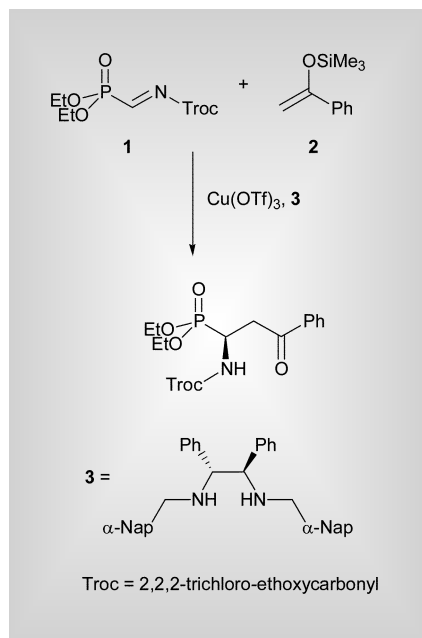
Terminal and functionalized olefins also performed well as substrates, with complete conversions and ee's in the 90% range. A selection of substrates and reported ee-values for the hydrogenated products is shown below.



### Enantioselective synthesis of $\alpha$ -amino phosphonates

One important class of analogues of  $\alpha$ -amino acids are  $\alpha$ -amino phosphonates, which are considered to have potential as bioactive compounds for medical applications. Synthetic methods for the production of these compounds are not very

abundant, which makes the recent progress reported by Kobayashi *et al.* from the University of Tokyo an interesting contribution (*J. Am. Chem. Soc.* 2004, **126**, 6558–6559). The authors developed an enantioselective method for the addition of silicon enolates to N-acyl  $\alpha$ -iminophosphonates catalyzed by a chiral  $\text{Cu}^{\text{II}}$  complex.



Interestingly the reaction proceeded with only moderate enantioselectivity, albeit high yield of the desired product,

when no proton source was present (ee 49%, yield 78%). By adding hexafluoroisopropyl alcohol (HFIP), yield and ee increased substantially (ee 65%, yield 87%). This result could be further improved by adding the reactants slowly to the reaction mixture over a period of 8 h. A much greener alternative is the use of molecular sieve 3A, which provided almost the same yield and enantioselectivity as the best result with HFIP (ee 91%, yield 86%). These results were rationalized based upon the reaction mechanism. Upon exchanging the phenyl substituent on the silicon enolate with various other groups, the authors were able to synthesize 12 different  $\alpha$ -amino phosphonates with yields between 70 and 88% and enantioselectivities varying between 76 and 94%. Some of the products obtained were further transformed to known biologically important compounds.

### Direct hydrogen peroxide synthesis with palladium resin catalysts

Hydrogen peroxide is used in many different technology fields as its oxidising abilities make it a suitable bleaching agent and also an appropriate oxidizing agent in many chemical transformations. However, its usage could not be expanded to bulk scale chemical processes since its synthesis, which commonly is accomplished *via* the

anthraquinone process, is neither cheap nor green. Fierro *et al.* from the Institute of Catalysis and Petrochemistry, Madrid, have recently reported on a catalytic process for the conversion of hydrogen into hydrogen peroxide using palladium modified polystyrene resins (*Chem. Commun.*, 2004, 1184–1185). Mesoporous ion-exchange resins functionalized with sulfonic groups were impregnated with solutions of Pd- and Pd/Pt-salts. The surface areas of the resulting catalysts ranged between 35 and 40  $\text{m}^2 \text{g}^{-1}$ , the pore diameter amounted to 70 nm and the loading with Pd was 1.49, 1.34 and 1.37 wt%, with the third catalyst also incorporating 0.14 wt% of Pt. According to photoelectron spectra, PdO clusters were present in the resins as well as  $\text{Pd}^{\text{II}}$  ions interacting with the  $\text{SO}_3\text{H}$  groups. For catalytic testing, autoclaves were charged with the catalyst, a methanol-water mixture and HBr (12 ppm). The autoclaves were heated to 313 K and subsequently pressurized with a  $\text{H}_2:\text{O}_2:\text{N}_2$  mixture (2:48:50) and stirred to initiate the reaction. Hydrogen consumption was high in all cases (>90%) and the reaction proceeded at a constant rate. Most interestingly, the hydrogen peroxide production rate was very high (*ca.* 1100  $\text{mol H}_2\text{O}_2 \text{h}^{-1} (\text{mol Pd})^{-1}$ ) and much higher than data acquired previously using an acid-free solvent. The catalyst with the highest surface density of sulfonic groups proved to be the most effective.



## Triflic acid-catalysed cyclisation of unsaturated alcohols

Lydie Coulombel<sup>a</sup> and Elisabet Duñach<sup>\*a,b</sup>

<sup>a</sup>Laboratoire Arômes, Synthèses et Interactions, UMR CNRS 6001 Université de Nice-Sophia Antipolis, Parc Valrose, 06108 Nice cedex 2, France

<sup>b</sup>Laboratoire de Chimie Bio-Organique, UMR CNRS 6001 Université de Nice-Sophia Antipolis, Parc Valrose, 06108 Nice cedex 2, France. E-mail: dunach@unice.fr

Received 10th June 2004, Accepted 8th September 2004

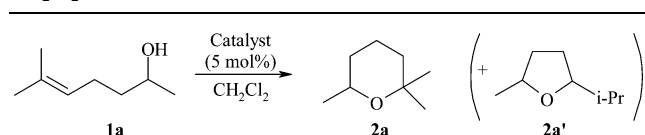
First published as an Advance Article on the web 28th September 2004

**In the presence of a catalytic amount of trifluoromethanesulfonic acid, substituted tetrahydrofurans and tetrahydropyrans have been efficiently and selectively obtained from the corresponding unsaturated alcohols.**

The preparation of differently substituted tetrahydrofurans and tetrahydropyrans constitutes an important and attractive subject in organic synthesis. Indeed, these heterocyclic skeletons are found in polyether antibiotics and other biologically active natural products.<sup>1</sup> They are also used as perfuming or flavouring ingredients in foodstuffs.<sup>2,3</sup> Cyclisation of unsaturated alcohols is one of the most straightforward route to the synthesis of cyclic ethers. In general, the reaction is promoted by an electrophile such as iodine,<sup>4</sup> phenylselenium chloride,<sup>5</sup> mercuric<sup>6</sup> or palladium salts.<sup>7</sup> Nevertheless, a second step is needed to remove the electrophile. The direct intramolecular cyclisation of alkenyl alcohols in strong acidic media is a well-known reaction, but occurs mainly with over-stoichiometric amounts of acid or with the acid used as the solvent.<sup>8</sup> To our knowledge, only a few acid-catalysed cyclisations have been described in the literature.<sup>9,10</sup> The reaction that we present here combines both the atom-economy concept and the use of a catalytic amount of “super-acid” such as trifluoromethanesulfonic acid or triflic acid (TfOH). Both these concepts are important issues in green chemistry procedures. Moreover, the triflic acid-catalysed cyclisation can also be run in the absence of solvent, it avoids the use of large excess of protic acid which is used to effect this transformation.

As shown in Table 1, we first selected 6-methyl-5-hepten-2-ol (**1a**) as a model substrate and compared the cyclisation efficiency with catalytic amounts (5 mol%) of various strong protic acids in refluxing CH<sub>2</sub>Cl<sub>2</sub>. When sulfuric acid (entry 1) or trifluoroacetic acid (entry 2) were employed, no reaction occurred after 1.5 and 3.5 h, respectively. Treatment of **1a** with

**Table 1** Acid-catalysed (5 mol%) cyclisation of **1a** in refluxing CH<sub>2</sub>Cl<sub>2</sub><sup>a</sup>



Entry	Catalyst (5 mol%)	Time/h	% Conversion (% GC yield of <b>2a</b> )
1	H <sub>2</sub> SO <sub>4</sub>	1.5	0
2	CF <sub>3</sub> CO <sub>2</sub> H	3.5	0
3	H <sub>3</sub> PO <sub>4</sub>	4	2 (1.5)
4	<i>p</i> -TsOH·H <sub>2</sub> O	4	6 (4.6)
5	TfOH	1.5	100 (100 <sup>b</sup> )

<sup>a</sup> See ref. 11 for general cyclisation procedure. <sup>b</sup> **2a** was isolated in 80% yield.

phosphoric or *p*-toluenesulfonic acid under the same conditions gave tetrahydropyran **2a** in very low conversions of 2% and 6% after 4 h, respectively (entries 3 and 4). However, in the presence of a catalytic amount of triflic acid, we observed the clean and quantitative cyclisation of **1a**, obtained in excellent isolated yield (80%) to the corresponding tetrahydropyran **2a** in 1.5 h (entry 5). The cyclisation was completely regioselective. Tetrahydropyran **2a** was the only product formed; the isomeric 2-isopropyl-5-methyltetrahydrofuran **2a'** was not detected, the cyclisation occurring exclusively at the more substituted carbocation intermediate.

We further examined the influence of the solvent and the amount of catalyst in the cyclisation of **1a**. Thus, distilled dichloromethane, dichloroethane and nitromethane were used with only 1 mol% TfOH at different temperatures, as illustrated in Table 2. A good reproducibility was attained.

In refluxing dichloromethane, the conversion of **1a** was completed after 24 h, to afford **2a** quantitatively. After 9 h reaction, the conversion was of 53%, the reaction rate being lower than shown in Table 1, due to the lower catalyst ratio. In refluxing dichloroethane or nitromethane, reactions occurred much more rapidly; with nitromethane **2a** was quantitatively obtained after 15 min.

It's interesting to note that the cyclisation of **1a** could be effected in the absence of solvent with 1 mol% of TfOH and the reaction was completed after 2 h at 80 °C, to afford exclusively **2a** with an isolated yield of 80%. Moreover, in a reaction without solvent but with only 0.1 mol% of TfOH, the conversion of **2a** was 57% after 22 h. The cyclisation of *cis*-3-nonen-1-ol was also run without solvent (50 mol% of TfOH) and afforded a 78 : 22 mixture of 5- and 6-membered ring ethers with complete conversion after 1 h at 80 °C.

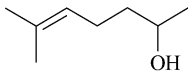
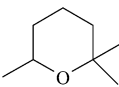
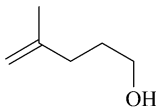
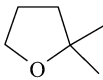
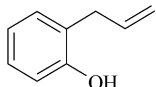
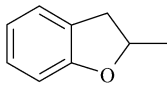
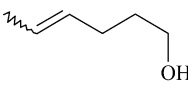
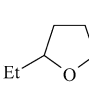
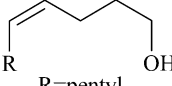
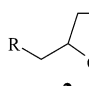
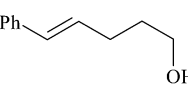
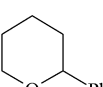
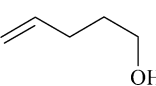
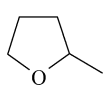
We then extended the cyclisation to other substrates by using catalytic amounts of TfOH (Table 3). All the conversions were quantitative. The reactivity of olefinic alcohols possessing a terminal disubstituted double bond such as in **1b** afforded exclusively the substituted tetrahydrofuran **2b** (entry 2). As previously observed for **1a**, the most stable carbocation was formed in the case **1b** to form the 5-membered ring ether. Terminal 2-allylphenol **1c** could also be quantitatively cyclised

**Table 2** Acid-catalysed cyclisation of **1a** in various solvents or in the absence of solvent with TfOH<sup>a</sup>

Entry	Solvent	Mol% of TfOH	Temp./ °C	Conversion of <b>1a</b>	Time/h	Yield <b>2a</b>
1	CH <sub>2</sub> Cl <sub>2</sub>	1 mol%	40	100%	24	100%
2	ClCH <sub>2</sub> CH <sub>2</sub> Cl	1 mol%	84	100%	1.5	100%
3	CH <sub>3</sub> NO <sub>2</sub>	1 mol%	101	100%	0.25	100%
4	—	1 mol%	80	100%	2	100%

<sup>a</sup> Yields were determined by GC analysis.

**Table 3** Cyclisation of unsaturated alcohols catalysed by TfOH<sup>a</sup>

Entry	Unsaturated alcohol	Conditions (mol% of TfOH)	Product(s) <sup>c</sup>	% GC yield (% isolated yield) <sup>b</sup> (Regioselectivity, %)
1	 <b>1a</b>	CH <sub>2</sub> Cl <sub>2</sub> reflux, 1.5 h (5 mol%)	 <b>2a</b>	100 (80)
2	 <b>1b</b>	CH <sub>2</sub> Cl <sub>2</sub> reflux, 2 h (5 mol%)	 <b>2b</b>	100 (69)
3	 <b>1c</b>	CH <sub>2</sub> Cl <sub>2</sub> reflux, 3 h (5 mol%)	 <b>2c</b>	100 (69)
4	 <b>1d</b>	CH <sub>3</sub> NO <sub>2</sub> reflux, 0.5 h (5 mol%)	 <b>2d</b>	100 (54) (92:8)
5	 <b>1e</b> R=pentyl	CH <sub>3</sub> NO <sub>2</sub> reflux, 1 h (5 mol%)	 <b>2e</b>	100 (100) (92:8)
6	 <b>1f</b>	CH <sub>3</sub> NO <sub>2</sub> reflux, 1 h (5 mol%)	 <b>2f</b>	100 (21)
7	 <b>1g</b>	CH <sub>3</sub> NO <sub>2</sub> reflux, 0.5 h (5 mol%)	 <b>2g</b>	100 (39)

<sup>a</sup> See ref. 11 for general cyclisation procedure. <sup>b</sup> Yields determined by GC analysis. Isolated yields were in the range of 40–80% due to the volatility of some of the products and to the isolation difficulties in low-scale reactions. <sup>c</sup> For characteristic <sup>1</sup>H-NMR data of products **2**, see ref. 12.

to 2-methyldihydrobenzofuran **2c** under the same catalytic conditions. The reaction was completely regioselective (entry 3).

No reaction occurred in CH<sub>2</sub>Cl<sub>2</sub> with alcohols having an internal disubstituted double bond such as compounds **1d** to **1f**. However, the cyclisation was efficient in refluxing CH<sub>3</sub>NO<sub>2</sub> affording a mixture of tetrahydrofuran and tetrahydropyran derivatives (entries 4 and 5). These cyclisations were highly regioselective and led to the tetrahydrofuran structures **2d** and **2e**, respectively, as the major isomers with 92% regioselectivity. Under the same conditions, the cyclisation of 5-phenyl-4-pentenol **1f** afforded exclusively the corresponding tetrahydropyran isomer **2f** after 1 h reaction, together with some polymers (entry 6).

A terminal monosubstituted olefin such as **1g** could also be cyclised (entry 7) and the 5-membered cyclic ether was the only product obtained in quantitative yield according to GC analysis. The isolation of this volatile compound after extraction and distillation gave an isolated yield of 40%. The isolation of the other ethers **2a–2e** was effected in 55–80% yields.

For a large scale reaction, the acid catalyst has been reported to be easily recovered and recycled.<sup>13</sup>

In conclusion, we report here a novel catalytic alternative for the cyclisation of unsaturated alcohols to the corresponding cyclic ethers in quantitative yields, using 0.1–5 mol% of commercial triflic acid in dichloromethane or nitromethane. Substituted tetrahydrofurans or tetrahydropyrans were selectively obtained from  $\gamma,\delta$ -unsaturated alcohols depending on the substitution. The cyclisation can also be run catalytically in the absence of solvent.

## Notes and references

- (a) T. L. B. Boivin, *Tetrahedron*, 1987, **43**, 3309; (b) G. Cradillo and M. Orena, *Tetrahedron*, 1990, **46**, 3321–3408; (c) H. Kotsubi, *Synlett*, 1992, 97; (d) P. A. Bartlett, *Tetrahedron*, 1980, **36**, 2.
- (a) A. F. Morris, E. Naef, S. Escher and A. Velluz, *U.S. Patent 5068362*, 1991; (b) A. R. Hochstetler, *U.S. Patent 4549029*, 1985; (c) P. D. Noire, *U.S. Patent 5510326*, 1996; (d) J. F. Vinals, R. Bank, J. Kiwala, D. E. Hrusa, J. B. Hall and M. H. Vock, *U.S. Patent*



- 4115406, 1978; (e) A. J. A. van der Weerd, R. Plomp and W. Apeldoorn, *U.S. Patent 4404127*, 1983.
- 3 A. P. S. Narula, *Perfum. Flavor.*, 2003, **28**, 62.
  - 4 (a) S. P. Chavan and A. K. Sharma, *Tetrahedron Lett.*, 2001, **42**, 4923; (b) S. P. Bew, J. M. Barks, D. W. Knight and R. J. Middleton, *Tetrahedron Lett.*, 2000, **41**, 4447; (c) S. B. Bedford, K. E. Bell, F. Bennett, C. J. Hayes, D. W. Knight and D. E. Shaw, *J. Chem. Soc., Perkin Trans. 1*, 1999, 2143; (d) S. H. Kang and S. B. Lee, *Tetrahedron*, 1993, **34**, 1955; (e) S. D. Rychnovsky and P. A. Bartlett, *J. Am. Chem. Soc.*, 1981, **103**, 3963.
  - 5 (a) M. Gruttadauria, C. Aprile, S. Riel and R. Noto, *Tetrahedron Lett.*, 2001, **42**, 2213; (b) B. Lipshutz and T. Gross, *J. Org. Chem.*, 1995, **60**, 3572; (c) K. C. Nicolaou, R. L. Magolda, W. J. Sipio, W. E. Barnette, Z. Lysenko and M. M. Joullie, *J. Am. Chem. Soc.*, 1980, **102**, 3784.
  - 6 (a) S. O. Kang, J. H. Lee and S. B. Lee, *Tetrahedron Lett.*, 1998, **39**, 59; (b) A. Garavelas, I. Mavropoulos, P. Perlmutter and G. Westman, *Tetrahedron Lett.*, 1995, **36**, 463; (c) P. Audin, A. Doutheau and J. Gore, *Bull. Soc. Chim. Fr.*, 1984, **7-8**, 297.
  - 7 (a) M. A. Arai, M. Kuraishi, T. Arai and H. Sasai, *J. Am. Chem. Soc.*, 2001, **123**, 2907; (b) I. Macsari and K. Szabo, *Tetrahedron Lett.*, 2000, 1119; (c) G. V. M. Sharma, A. S. Chander, K. Krishnu and P. R. Krishna, *Tetrahedron Lett.*, 1998, 6957.
  - 8 (a) M. L. J. Mihailovic and D. Marinkovic, *J. Serb. Chem. Soc.*, 1985, **50**, 5; (b) M. L. J. Mihailovic, N. Orbovic and D. Marinkovic, *Bull. Soc. Chim. Beograd*, 1979, **44**, 597; (c) R. Paul and H. Normant, *Bull. Soc. Chim. Fr.*, 1944, **11**, 365; (d) J. Colonge and A. Lagier, *Bull. Soc. Chim. Fr.*, 1949, **1**, 15; (e) O. Riobé, *Ann. Chim. (Paris)*, 1949, **12**, 632; (f) C. Crisan, *Ann. Chim. (Paris)*, 1956, **13**, 467.
  - 9 X. Franck, B. Figadère and A. Cavé, *Tetrahedron Lett.*, 1997, **38**, 1413.
  - 10 (a) K. Miura, S. Okajima, T. Hondo, T. Nakagawa, T. Takahashi and A. Hosomi, *J. Am. Chem. Soc.*, 2000, **122**, 11348; (b) K. Miura, T. Hondo, T. Takahashi and A. Hosomi, *Tetrahedron Lett.*, 2000, 2129.
  - 11 General acid-catalysed cyclisation procedure: a mixture of unsaturated alcohol (1 mmol) and TfOH (0.05 mmol) in distilled nitromethane or dichloromethane (5 ml) was stirred at reflux for 0.5 to 3 h. The progress of the reaction was monitored by GC analysis. The reaction mixture was quenched with HCl (1 M) and extracted with Et<sub>2</sub>O. The organic layer was washed with HCl (0.1 M), dried with MgSO<sub>4</sub> and the solvent was evaporated. The products were analysed by <sup>1</sup>H and <sup>13</sup>C-NMR and mass spectrometry.
  - 12 Characteristic <sup>1</sup>H-NMR data (200 MHz): **2a**: 3.7 (1 H, dqd, *J* = 12.3, 6.2, 2.0 Hz), 1.7–1.3 (6 H, m), 1.21 (3 H, s), 1.19 (3 H, s), 1.1 (3 H, d, *J* = 6.2 Hz); **2b**: 3.8 (2 H, t, *J* = 6.8 Hz), 1.9 (2 H, m), 1.7 (2 H, t, *J* = 7.7 Hz), 1.2 (6 H, s); **2c**: 7.2–7.0 (2 H, m), 6.8–6.6 (2 H, m), 4.8 (1 H, ddq, *J* = 8.8, 7.7, 6.3 Hz), 3.2 (1 H, dd, *J* = 15.4, 8.8 Hz), 2.7 (1 H, dd, *J* = 15.4, 7.7 Hz), 1.4 (3 H, d, *J* = 6.3 Hz); **2d**: 3.8–3.6 (3 H, m), 1.6–1.9 (4 H, m), 1.5 (2 H, m), (3 H, t, *J* = 7.4 Hz); **2e**: 3.9–3.6 (3 H, m), 1.9–1.7 (3 H, m), 1.5–1.1 (11 H, m), 0.8 (3 H, t, *J* = 6.8 Hz); **2e'**: 3.9–3.6 (3 H, m), 1.6–1.1 (14 H, m), 0.8 (3 H, t, *J* = 6.8 Hz); **2f**: 7.4–7.2 (5 H, m), 4.3 (1 H, m), 4.1 (1 H, m), 3.6 (1 H, m), 2.0–1.5 (6 H, m); **2g**: 4.0–3.8 (3 H, m), 3.7 (1 H, ddd, *J* = 8.1, 7.7, 6.4 Hz), 2.1–1.8 (3 H, m), 1.5–1.3 (1 H, m), 1.2 (3 H, d, *J* = 6.1 Hz).
  - 13 R. Effenberger, *J. Chem. Technol. Biotechnol.*, 1993, **58**, 129.



## Supercritical fluid extraction of mixed wastes

Kong-Hwa Chiu,<sup>\*a</sup> Hwa Kwang Yak,<sup>b</sup> Joanna Shaofen Wang<sup>c</sup> and Chien M. Wai<sup>c</sup>

<sup>a</sup> Department of Natural Sciences, National Science Council, Taipei, Taiwan, ROC

<sup>b</sup> Department of Chemistry, Chung Yuan Christian University, Chung-Li, Taiwan, ROC

<sup>c</sup> Department of Chemistry, University of Idaho, Moscow, Idaho 83844, USA

Received 25th March 2004, Accepted 1st July 2004

First published as an Advance Article on the web 24th September 2004

This study assesses the feasibility of extraction and separation of uranium and PCBs from contaminated soil samples using a sequential supercritical CO<sub>2</sub> extraction method. The contaminated soil was first extracted with neat supercritical CO<sub>2</sub> at 150 °C and 200 atm to remove PCBs. Subsequently, complexing agents, tri-*n*-butylphosphate (TBP) and thenoyltrifluoroacetylacetone (HTTA), were added to remove uranium from the contaminated soils. Using this method, nearly all PCBs were removed, and up to 75% of the uranium in the soil could be removed after multiple extractions. This sequential supercritical fluid extraction method may have a wide range of applications for treating various mixed wastes.

### Introduction

Supercritical fluid carbon dioxide (SF-CO<sub>2</sub>) has been generally accepted as a potential green solvent for chemical separations and reactions. Minimizing liquid waste generation, easy separation of solutes, and the ability to penetrate into small pores of solid materials are some of the advantages of the CO<sub>2</sub>-based supercritical fluid extraction (SFE) technology over conventional solvent extraction methods. Because CO<sub>2</sub> is not regulated by the US EPA as a volatile organic compound, CO<sub>2</sub>-based extraction processes are environmentally acceptable. The CO<sub>2</sub> used in SFE is produced by other industrial processes (e.g. fermentation processes), therefore the gas vented into the atmosphere from the SFE processes does not contribute to the “green house” effect.

Supercritical CO<sub>2</sub> extraction of organic pollutants including polychlorinated biphenyls (PCBs) and polyaromatic hydrocarbons (PAHs) from solid materials is a known technique for environmental analysis.<sup>1–5</sup> It is also known that metal species can be extracted by supercritical CO<sub>2</sub> using an *in situ* chelation method.<sup>6–8</sup> Real environmental wastes often contain toxic organic compounds and metal species. It is known that PCBs co-exist with uranium in certain types of nuclear wastes. New techniques for extraction and separation of mixed contaminants from solid materials are needed for analysis and for remediation of mixed wastes. According to the EPA's definition, mixed wastes contain both radioactive and chemically hazardous substances. Mixed waste composed of low-level radioactive waste (LLRW) and chemically hazardous substances are generated from industrial facilities, medical and academic institutes and nuclear power plants. The Department of Energy (DOE) will need to manage 1.5 million cubic metres of low-level waste (LLW) over the next 20 years.<sup>9</sup>

A number of methods are known for treatment of wastes containing radioactive materials.<sup>10</sup> Most of the known technologies often generate secondary wastes. While reducing solvent use is often considered a driving force behind SFE, greater selectivity, reduced time, quantitative yield, and lower cost are also important factors. Supercritical fluid extraction may provide a simpler and environmentally acceptable technique for treatment of mixed wastes. For a system containing both organic and metal contaminants, a sequential SFE procedure may be used to remove the organic and the metal contaminants separately, thus simplifying their final disposal requirements. Optimally, the chemicals and radioactive substances removed and isolated separately from mixed

wastes should be in small volumes so that their final disposal or storage would be economical.

There is no report available in the literature regarding the application of SFE to mixed wastes containing both organic pollutants and toxic metals. Extraction of uranyl ions from mine waters and from contaminated soil using HTTA and TBP as extractants in supercritical CO<sub>2</sub> has been reported.<sup>11</sup> We have experimentally evaluated the feasibility of removing uranium and PCBs from spiked soil samples separately using a sequential SFE process. The results are presented in this paper.

### Results and discussion

For this study, we prepared simulated mixed wastes by spiking different solid samples with PCB and uranium. The soils used in this study were characterized by the Soil Science Department, University of Idaho, USA. In order to achieve higher extraction efficiencies, several factors that may affect the SFE efficiency were investigated. Of these factors, temperature, matrix texture, ligands, and pressure were found to have the most significant influences on extraction results. For this study, typical standard deviations are around 4%.

#### Supercritical fluid extraction of PCB

A PCB congener, BZ#54, was used as a representative of PCBs in this study. A sea sand sample was spiked with the PCB for the initial SFE experiments because of sea sand's simple matrix composition. The percentage of extraction was determined by the amount of BZ#54 collected from the CO<sub>2</sub> phase after the extraction divided by the amount spiked onto the sand sample initially. The efficiency of extracting the spiked PCB from the sand depends on the temperature. According to this study, at 60 °C and 200 atm, about 80% of the spiked PCB could be removed (Table 1). When the temperature was raised to 100 °C, 98% of the spiked PCB could be removed from the sand sample under the same pressure. At 100 °C or above, virtually all of the spiked PCB in the sea sand could be removed. On the other hand, only 60% of the spiked PCB could be removed from the soil sample at this temperature. Essentially, with the same temperature, higher pressure will increase the density of SF-CO<sub>2</sub>, which induces a stronger solvation power and thus enhances the extraction efficiency.

When a soil sample was spiked with BZ#54, a higher temperature was required to remove the PCB from the solid matrix. At 200 atm, a temperature of 150 °C was needed to

**Table 1** Effect of temperature on extraction of PCB (BZ#54) sea sand and Santa soil using neat CO<sub>2</sub>. SFE conditions: pressure = 200 atm; 30 min each of static and dynamic extraction times (CO<sub>2</sub> flow rate  $\cong$  1.2 mL min<sup>-1</sup>); collection solvent = hexanes

T/°C	Collection efficiency (%)	
	Sea sand	Santa soil
	PCB(BZ#54)	PCB(BZ#54)
60	60	65
80	90	65
100	97	60
150	98	96

achieve a high SFE extraction efficiency for the PCB (Table 1). Extraction of the organic matter adsorbed on the solid phase in the presence of the supercritical fluid is controlled by the adsorption-desorption equilibrium. This means that once the supercritical fluid is introduced, a new equilibrium is established. The static extraction period in SFE allows enough time for this new equilibrium to establish. The subsequent dynamic extraction phase, on the other hand, perturbs this freshly established equilibrium by transporting the fraction dissolved out of the system, forcing a new equilibrium to establish. It is through this mechanism that extraction of targeted sorbates takes place.

Soil organic components usually have high surface areas and may contain various carbonaceous materials that behave like sorbents for trace contaminants such as PCBs. To reduce adsorption, a higher temperature should be favorable for removing the organic compound effectively from the soil matrix. Based on our experimental results, we chose 150 °C and 200 atm as the preferred experimental conditions for SFE of PCB from soil matrices. The higher temperature required for extraction of PCB from soil is most likely due to the interaction between the PCB molecules and the organic binding sites in the matrix.

### Supercritical fluid extraction of uranium

Uranyl ions (UO<sub>2</sub><sup>2+</sup>) are known to form stable complexes with fluorinated  $\beta$ -diketones in SF-CO<sub>2</sub>. Thenoyltrifluoroacetone (HTTA) was used in several previous SFE studies for extracting lanthanides and actinides because it is a solid at room temperature and is easy to handle experimentally.<sup>6</sup> For this study, we also used HTTA as an extractant in our initial uranium extraction experiments. The uranyl-TTA complex has a general formula of UO<sub>2</sub>(TTA)<sub>2</sub>·H<sub>2</sub>O, with one molecule of H<sub>2</sub>O coordinated with the complex. The solubility of water-containing complexes in SF-CO<sub>2</sub> is usually low because of the polar nature of H<sub>2</sub>O. If the coordinated water molecule is replaced by a stronger and CO<sub>2</sub>-soluble Lewis base such as tributylphosphate (TBP), the resulting complex UO<sub>2</sub>(TTA)<sub>2</sub>·TBP has a much higher solubility in SF-CO<sub>2</sub>. Thus a mixture of TBP and HTTA was used as the extractant for the spiked uranium in soil.<sup>12,13</sup>

The results of extracting spiked uranyl ions from the sea sand and a soil matrix (Santa soil) using HTTA and TBP at different temperatures are given in Table 2. The extraction process consisted of 30 min static extraction followed by 30 min dynamic flushing at a flow rate of 1.2 mL min<sup>-1</sup>. Under the

**Table 2** Collection efficiencies of uranium spiked onto sea sand and Santa soil as simulated mixed waste. SFE conditions for uranium: pressure = 200 atm; 30 minutes each of static and dynamic extraction times (CO<sub>2</sub> flow rate  $\cong$  1.2 mL min<sup>-1</sup>); collection solvent = chloroform; 200  $\mu$ L of TBP and 300 mg of HTTA were used in each extraction

T/°C	Collection efficiency (%)	
	Sea sand	Santa soil
	Uranium	Uranium
60	60	54
80	75	60
100	73	62
150	75	61

specified experimental conditions, the extraction efficiency for the spiked uranyl ions from soil was found to be almost constant at a temperature of 80 °C or above. Therefore, for SFE of uranium, we chose 80 °C and 200 atm as the standard temperature and pressure conditions for the mixed waste experiments.

The efficiency for a single-batch extraction of uranium from different soils ranges from 56 to 78% (Table 3). Several factors might be responsible for this result. Since the dominant species of uranium in soil, UO<sub>2</sub><sup>2+</sup>, is cationic and the polyelectrolyte soil matrix has abundant negative charges, UO<sub>2</sub><sup>2+</sup> in soil is strongly adsorbed.<sup>14</sup> The uranium extraction efficiency appears to decrease with increasing organic matter in the soil. The Santa soil with the highest organic content shows the lowest uranium extraction efficiency. It is known that in marine sedimentary environments, U(vi) can be reduced to U(IV) causing both precipitation and adsorption of uranium or complexation by organic matter.<sup>15</sup> Loss of uranium from water to sediment by adsorption is affected by sediment type and follows the order organic sediment, clay and sand.<sup>16</sup> All of these possibilities might be the reasons that quantitative extraction of uranium from soil could not be achieved.

### Sequential extraction of PCB and uranium from soil

The Santa soil sample was spiked with both BZ#54 (2,2,6,6-tetrachlorobiphenyl) and uranium as described in the experimental section for sequential extraction experiments. The soil was first extracted with neat CO<sub>2</sub> at 150 °C and 200 atm to remove the PCB. The extraction conditions were 30 min static followed by 30 min dynamic flush at a flow rate of 1.2 mL min<sup>-1</sup>. Under these conditions, the extraction of PCB could achieve 98% in both sea sand and soil samples (Table 3).

The trap solution, hexane, in the first neat CO<sub>2</sub> extraction, contained only BZ#54. The second ligand assisted extract contained uranium but no detectable amount of the PCB. The sequential extraction procedure described in this paper obviously can effectively extract the PCB and uranium in two separate fractions. The extraction efficiency of BZ#54 was satisfactory under the specified conditions, but the extraction of uranium was not quantitative. It is possible that a fraction of uranium in the matrix was not extractable by TBP-HTTA assisted SFE. Optimization of uranium extraction conditions

**Table 3** The properties of different soils and their corresponding sequential extraction efficiencies for PCB and uranium

Soil classification	pH <sup>a</sup>	Organic matter (%)	Extractable Fe <sup>b</sup> /mg g <sup>-1</sup>	PCB <sup>c</sup> Extracted (%)	Uranium <sup>d</sup> Extracted (%)
Santa (Fragiochrept)	6.1	20.0	2.9	98	56
Silver Valley	6.9	2.8	0.1	98	60
Lincoln County	5.2	0.2	0.4	98	78

Data from Analytical Sciences Lab., University of Idaho, Holm Research Center, Moscow, USA.<sup>a</sup> 1 : 1 (w/v) in distilled, deionized water. <sup>b</sup> Combustion method (CHN analyzer, LECO Corp., St. Joseph, MI). <sup>c</sup> One-cycle extraction at 150 °C and 200 atm (1st extraction). <sup>d</sup> One-cycle extraction at 80 °C and 200 atm with TBP and HTTA as described in Table 2 (2nd extraction).



**Table 4** Results of multiple-batch extractions of uranium from sand and soil. SFE conditions: 200 atm and 80 °C; flow rate of liquid CO<sub>2</sub> ≅ 1 mL min<sup>-1</sup>; 200 μL TBP and 300 mg HTTA

	Extracted (%)			Total
	1st	2nd	3rd	
Sea sand <sup>a</sup>	73	16	ND	89
Sea sand <sup>b</sup>	78	16	ND	94
Santa soil <sup>a</sup>	52	15	6	73
Santa soil <sup>b</sup>	57	13	5	75
Silver Val. soil	52	15	8	75

<sup>a</sup> Extraction conditions: 30 min each of static and dynamic extraction times. <sup>b</sup> Extraction conditions: 45 min each of static and dynamic extraction times. ND = not detectable.

and a search for other effective chelating agents are currently in progress. Based on the results given in Table 1–3, it is apparent that BZ#54 does not interfere with the extraction of uranium and *vice versa*.

### Multiple batch extraction of uranium

Table 4 shows repeated TBP–HTTA assisted extraction of uranium from different soils. Under the specified SFE conditions, the total extraction efficiency after 3 repeated extractions for the spiked uranyl ions was around 90% for sea sand and between 73–75% for the two soil samples. The results suggest that multiple batch extractions, or continuous ligand feeding, may be required to remove uranium from real soils. The first extraction probably removes most of the metal ions adsorbed on the soil surfaces. Subsequent extractions conducted on the same matrix probably extract the more stubbornly bound uranium ions in the soil. The amounts of uranium removed in the subsequent extractions are much lower compared with the first extraction. Repeated extractions under the same conditions resulted in an additional 13–15% extraction of uranium in the second time and 5–8% in the third time. For the spiked sea sand, after 2 extractions, virtually all spiked uranium was removed from the solid matrix. For the spiked soils, the percentage of uranium removed from the solid matrix varied from 73–75% after 3 repeated extractions. Some uranium species still trapped in the soil after three extractions probably partitioned into specific fractions that could not be extracted by TBP–HTTA complexation.

### Other factors affecting uranium extraction

Three other metal species, namely cadmium, lead and mercury were spiked with uranium (100 μg each) onto the sea sand and the Santa soil. According to our experiments, the SFE efficiency of uranium was not influenced by the other three metals using TBP–HTTA as the extractants at 80 °C and 200 atm. Other factors were also investigated for their possible relation with the SFE of uranium including extraction efficiency with different ligands and effects from other metal species. Table 5 summarizes the extraction efficiencies of uranium spiked on sea sand using different types of ligands. It is clear that dithiocarbamate salts such as bis(trifluorodiethylthiocarbamate, lithium salt (LiFDDC) and diethylthiocarbamate, sodium salt (NaDDC) are not capable of removing uranium from the sand matrix under these SFE conditions. Cyanex 302 showed some degree of complexing ability, but the metal–ligand complex was probably not soluble enough in the SF-CO<sub>2</sub> to be transported and collected. This precipitated fraction (39%) could be recovered by a solvent washing of the system. The major fraction of the uranium remained in the solid matrix as inorganic forms that could be recovered by nitric acid washing. TBP–HTTA appears to be a good mixture for SFE of uranium. However, about 16% of the uranium still remained in the

**Table 5** Recovery of uranium spiked on sea sand using various ligands. Initial quantity of uranium was 200 μg each. SFE conditions: *P* = 200 atm; *T* = 80 °C; flow rate of liquid CO<sub>2</sub> ≅ 1.2 mL min<sup>-1</sup>; static and dynamic times were 30 min each

Ligand	A (%) <sup>a</sup>	B (%) <sup>b</sup>	C (%) <sup>c</sup>	Total
LiFDDC	5	N/A	93	98
NaDDC	3	N/A	94	97
Cyanex 302	4	39	58	101
HTTA + TBP	73	16	6	97

<sup>a</sup> A: % uranium extracted and collected by SFE. <sup>b</sup> B: % uranium complexed by the ligand but not extracted by SFE; recovered by solvent extraction. <sup>c</sup> C: % uranium remaining in the matrix; recovered by 10% nitric acid wash.

extraction system which could be recovered by solvent washing. Another 6% of the uranium remained in the solid sample and could be recovered by 10% nitric acid washing. Other mixtures of complexing agents may further improve the SFE efficiency of uranium from soils. Research in this direction is currently in progress.

## Experimental

### Chemicals and reagents

PCB (polychlorinated biphenyl) congener (BZ#54, 2,2',6,6'-tetrachlorobiphenyl) was obtained from Ultra Scientific (North Kingstown, RI). Uranium standard solution was obtained from Aldrich Chemical, Inc. with a concentration of 960 ppm (in HNO<sub>3</sub>). Bis(2,4,4-trimethylpentyl) monophosphinic acid was obtained from Cytec Industrial Inc, Niagara Falls, Canada. TBP (tri-*n*-butylphosphate), HFA (hexafluoroacetylacetone, trihydrate), and FA (fluoranthene) were obtained from Aldrich (Milwaukee, WI). HTTA (Thenoyltrifluoroacetylacetone) was obtained from Fluorochem Limited, Derbyshire, UK. SFE/SFC grade liquid carbon dioxide were purchased from Air Products (Allentown, PA). Chloroform was purchased from EM Science (Gibbstown, NJ). The HPLC grade hexane and sea sand (S25–500) were obtained from Fisher Scientific (Fair Lawn, NJ). Santa soil (Typic Fragiocchrept) from Palouse, Idaho, and Silver Valley soil from Silver Valley, Idaho, were air-dried, crushed and sieved through 2-mm sieves.

### Instruments

An ISCO syringe pump, model 260D (ISCO, Lincoln, NB) with ISCO series D pump controller was used. A stainless steel extraction cell with an internal volume of 6.94 mL was obtained from Keystone Scientific Inc., Bellefonte, PA. 50 and 100 μm i.d. fused silica tubing (J & W Scientific, Folsom, CA) was used as pressure restrictor for the SFE extractions. The ICP-AES (Thermo Jarrel Ash, IRIS) was operated by the Department of Soil Science, University of Idaho, for uranium analysis with detection wavelength selected at 263.55 nm. The detection limit for uranium was around 1 ppm. A Hewlett-Packard 5890 GC-FID was used for the quantitative analysis of BZ#54. A DB-5 capillary column purchased from Alltech (Deerfield, IL) (30 m in length, 0.32 mm i.d. and 0.25 μm film thickness). The carrier gas was chromatographic grade N<sub>2</sub> (Oxarc, Spokane, WA). GC-FID conditions were: initial temperature 50 °C, final temperature 300 °C, rate 15 °C min<sup>-1</sup>, injector 250 °C, detector 300 °C. A typical chromatogram of a standard (Fig. 1) yields two peaks that correspond to the two compounds: BZ#54 and the internal standard (fluoranthene).

### Procedure

To investigate the feasibility of extraction of PCB and uranium from soils, extraction of these substances from sea sand was

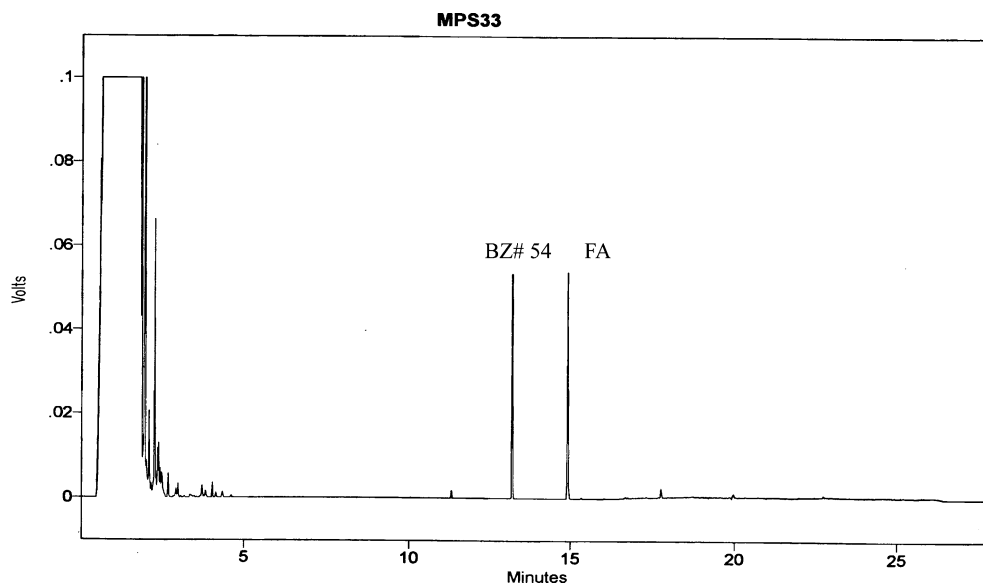


Fig. 1 GC Chromatogram of BZ# 54 and the internal standard fluoranthene (FA).

first studied since the characteristics of sea sand are much simpler than the soils. In general, spiked analytes are extracted more efficiently and rapidly than native analytes.<sup>17</sup> Many different combinations of various pressures and temperatures were tested to obtain an appropriate set of conditions for the extraction of PCB as well as uranium from the matrices. The ranges for pressure and temperature were 100 to 200 atm and 60 to 150 °C, respectively. The duration for static and dynamic extractions was 30 and 50 min, respectively.

### Sample preparation

A long piece of glass tubing with inner diameter 0.7 cm was cut into 4.5 cm segments, soaked in a 10% nitric acid bath for at least 24 hours, rinsed with distilled water, and then air-dried. Sea sand was used without any further treatment. Three soil samples were collected from different sources: (1) soil from Santa soil (Typic Fragiochrept), Palouse, Idaho, USA (2) soil from Silver valley soil, Idaho, USA and (3) soil from Lincoln County, Montana, USA. All these samples were air-dried and were ground to pass a 2 mm screen. The characteristics of these soils are briefly listed in Table 3.

A small piece of glass fiber (*ca.* 4 mm in length) was inserted into the bottom of a small glass tube to prevent the sand/soil from escaping. Enough sea sand/soil was transferred into the glass tubing. Sea sand or soils spiked with PCB and uranium were treated as mixed waste surrogates throughout this research. In a typical experiment, about 0.5 g of sea sand (or 1.2 g of soil) was delivered into the glass tubing. 100  $\mu\text{L}$  of 2 100 ppm BZ#54 solution dissolved in hexane was spiked onto the soil and allowed to air-dry for few minutes, followed by addition of 200  $\mu\text{L}$  of 960 ppm uranium solution. Another small piece of glass fiber was then used to cap the piece of glass tubing. Finally a small amount of deionized water was added to the matrix until it was wet but not dripping. The glass tubing was then placed in the extraction cell.

In another experimental design, the sand/soil was transferred directly into the extraction cell. Analyte loading to the matrix was identical to the aforementioned procedure.

### Supercritical fluid extraction

All extractions were performed with an ISCO 260D pump and ISCO series D pump controller. The flow rate was regulated by the use of high-pressure valves and the fused-silica restrictors.

Typical dynamic extraction flow rate is around 1.2 mL min<sup>-1</sup> of liquid CO<sub>2</sub>.

The set-up of the SFE apparatus is shown in Fig. 2. The extraction of mixed waste was divided into two steps. The first step was for PCB extraction, and the second for uranium extraction.

### PCB extraction and detection

The oven **E** was brought up to the desired temperature with both high-pressure valves **A** and **B** closed. Upon reaching the desired temperature, valve **A** was opened and CO<sub>2</sub> was allowed to flow through preheat loop **F**, where CO<sub>2</sub> was converted to supercritical state before reaching the extraction cell **G**. The entire system was then leak-checked. Timing of static (or no flow) extraction started when the temperature stabilized. After the desired amount of time had lapsed, valve **B** was opened very slowly and smoothly until the flow rate was maintained at about 1.2 mL min<sup>-1</sup> for dynamic extraction. A collection vial with about 20 mL of hexane was used for collecting the extractant. After the desired duration had lapsed, valve **A** was closed and the pressure of the circuit was allowed to release down to ambient pressure spontaneously.

The collected solvent was then sparged with nitrogen gas to about 8 mL, transferred into a 10-mL volumetric flask, 100  $\mu\text{L}$  of FA added (internal standard), and brought to volume. 1  $\mu\text{L}$  of this solution was taken for GC/FID analysis. Quantitation was based on conventional internal standard techniques. Peak areas of both the standard and sample solutions were normalized to the peak area of the internal standard after GC analyses. Collection efficiency is defined as the ratio of collected quantity to the spiked quantity.

### Uranium extraction and detection

After PCB extraction, the cell was disconnected from the circuit and the glass tube along with the soil sample was taken out from the vessel. 200  $\mu\text{L}$  of TBP, 300 mg of HTTA, and 100  $\mu\text{L}$  of methanol were added sequentially on top of the soil sample for chelation with uranium. The cell was reconnected to the circuit for uranium extraction. The SFE procedure was similar to that applied to the PCB extraction, except that chloroform was used as the collection solvent for the uranium-TTA·TBP complex. Two different modes of uranium extraction were conducted, one being single-batch extraction and the other multi-batch extraction. In the multi-batch extraction, three

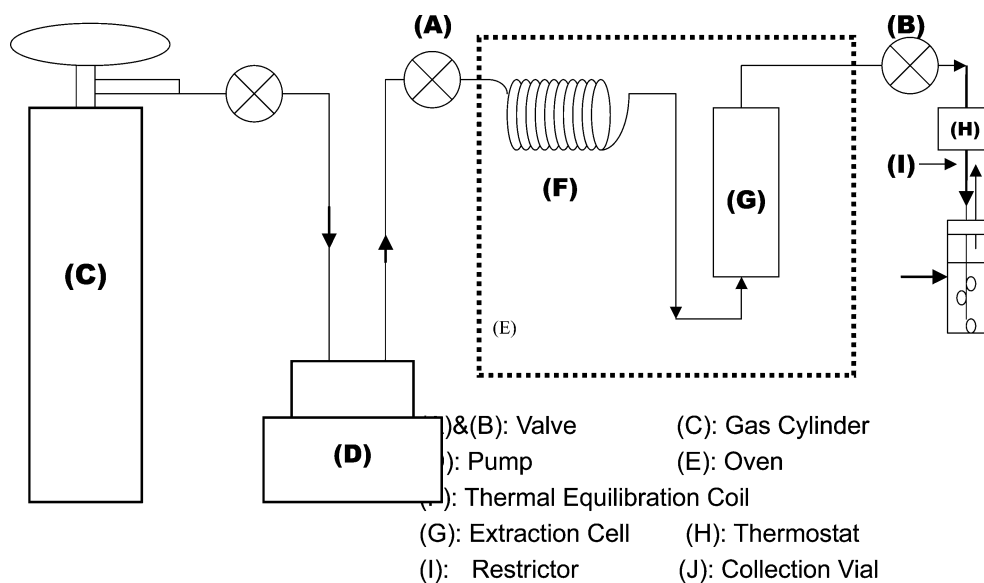


Fig. 2 Schematic diagram of supercritical fluid extraction.

consecutive and repeated extractions under the same conditions were applied to the same sample. The sum of these three individual extractions represented the total amount of uranium that could be removed.

Formation of the adduct of uranium  $\beta$ -diketonates with neutral donor, TBP can greatly improve SFE behavior. TBP was found to enhance the extraction of uranium with  $\beta$ -diketones in supercritical  $\text{CO}_2$ . X-Ray diffraction studies indicate that TBP is able to replace the water molecule coordinated with the uranyl- $\beta$ -diketonate complex thus making the adduct complex more soluble in supercritical  $\text{CO}_2$ .

For ICP-AES analysis of uranium, the uranyl-TTA complex has to be destroyed so that the uranyl ions "back extract" into the aqueous phase. Back extraction is performed by adding 2.0 mL of 50% nitric acid to the collected solution in the vial and shaking it by hand for about 3 min. The aqueous phase was then withdrawn and the organic phase washed twice with 1 mL each of deionized water. These three aliquots were combined into a clean glass vial and any trace amount of chloroform dissolved in the aqueous phase was removed by heating the solution in a hot bath kept at about 80 °C for 20 min. The final volume of the solution was then brought to 10 mL before sending for ICP-AES analysis.

## Conclusions

A sequential supercritical  $\text{CO}_2$  extraction process is described in this paper for removal of a PCB congener and uranium separately from sand and soil matrixes. Neat  $\text{CO}_2$  is used in the first extraction to remove the PCB congener at 150 °C and 200 atm. This is followed by a second extraction to remove uranium using a mixture of TBP and HTTA at 80 °C and 200 atm. The average recovery for the spiked PCB congener is around 98%, indicating that PCB can be effectively solubilized and extracted from a simulated mixed waste matrix. The average recoveries of uranium from sea sand and soil from based on a one-cycle extraction using TBP-HTTA as an extractant are 75% and 60%, respectively. These results imply that uranium extraction from soil is complicated due to many possible interactions between the uranyl cations and the matrix. The average recoveries of uranium from sea sand and soil based on repeated extractions are 94% and 75%, respectively.

The co-occurrence of heavy metals and organic compounds in mixed wastes often complicates their remediation options by conventional methods. This paper demonstrates that using a

sequential SFE procedure, PCBs and uranium can be removed separately from contaminated soils, thus greatly simplifying methods for their final disposal. The extraction efficiency of uranium decreases with increasing soil organic carbon content suggesting possible uranium-to-organic matter affinity.<sup>18</sup> Further work is needed to evaluate matrix effects on SFE efficiency for different soils. This environmentally benign supercritical fluid extraction method may provide a solution for treating mixed wastes with minimum secondary waste generation.

## Acknowledgements

This research was supported partly by a DOE-EMSP Program.

## References

- S. B. Hawthorne, *Anal. Chem.*, 1990, **62**, 633A.
- Q. Lang, F. Hunt and C. M. Wai, *J. Environ. Monit.*, 2000, **2**, 639.
- I. S. Dolezal, K. P. Segebarth, M. Zennegg and S. Wunderli, *Chemosphere*, 1995, **31**, 4013.
- J. R. Dean, *Analyst*, 1996, **121**, 85R.
- J. Hollender, J. Shneine, W. Dott, M. Heinzl, H. W. Hagemann and G. K. E. Goetz, *J. Chromatogr., A*, 1997, **776**, 233.
- C. M. Wai and S. Wang, *J. Chromatogr., A*, 1997, **785**, 369.
- K. E. Laintz, J. J. Yu and C. M. Wai, *Anal. Chem.*, 1992, **64**, 311.
- K. E. Laintz, G. M. Shieh and C. M. Wai, *J. Chromatogr. Sci.*, 1992, **30**, 120.
- Final Waste Management Programmatic Environmental Impact Statement For Managing Treatment, Storage, and Disposal of Radioactive and Hazardous Waste*, DOE/EIS-0200-F, US Department of Energy, Office of Environmental Management, US Government Printing Office, Washington, DC, USA, 1997.
- Hazardous and Radioactive Waste Treatment Technologies Handbook*, ed.-in-chief H. O. Chang, CRC Press, Boca Raton, FL, 2001.
- Y. Lin, C. M. Wai, F. M. Jean and R. D. Brauer, *Environ. Sci. Technol.*, 1994, **28**, 1190.
- K. Batzar, D. E. Goldberg and L. J. Newman, *Inorg. Nucl. Chem.*, 1967, **29**, 1511.
- Y. Lin, H. Wu, N. Smart and C. M. Wai, *J. Chromatogr., A*, 1998, **793**, 107.
- S. C. Sheppard and W. G. Evenden, *J. Environ. Radioact.*, 1988, **8**, 255.
- S. R. Anderson, *Geochim. Cosmochim. Acta*, 1982, **46**, 1293.
- G. A. Bird and W. G. Evenden, *J. Environ. Radioact.*, 1994, **22**, 219.
- J. J. Langenfeld, S. B. Hawthorne, D. J. Miller and J. Pawliszyn, *Anal. Chem.*, 1995, **67**, 1727.
- B. Brandy, C. Kao, K. Dooley and F. Knopf, *Ind. Eng. Chem. Res.*, 1987, **26**, 261.



# Highly efficient dehalogenation using hydroxyapatite-supported palladium nanocluster catalyst with molecular hydrogen

Takayoshi Hara, Kohsuke Mori, Michitaka Oshiba, Tomoo Mizugaki, Kohki Ebitani and Kiyotomi Kaneda\*

Department of Materials Engineering Science, Graduate School of Engineering Science, Osaka University, 1–3 Machikaneyama, Toyonaka, Osaka 560-8531, Japan.

E-mail: kaneda@cheng.es.osaka-u.ac.jp; Tel: +81-6-6850-6260; Fax: +81-6-6850-6260

Received 1st June 2004, Accepted 1st July 2004

First published as an Advance Article on the web 24th September 2004

A hydroxyapatite-supported Pd nanocluster (PdHAP) efficiently catalysed the dehalogenation of various organic halides in the presence of atmospheric molecular hydrogen; chlorobenzene gave benzene in an excellent TON of 10 000 for 10 h. Moreover, the dehalogenation of halophenols in aqueous conditions was also achieved.

The dehalogenation of organic halides is a significant process for the removal of halogenated organic pollutants as well as for the synthesis of fine chemicals.<sup>1</sup> Compared with oxidative methods,<sup>2</sup> reductive dehalogenation processes are advantageous in that no toxic by-products are formed. Various hydrogen donors such as metal alkoxides,<sup>3</sup> hydrosilanes,<sup>4</sup> Grignard reagents,<sup>5</sup> hydrazine hydrochloride,<sup>6</sup> and sodium formate<sup>7</sup> are generally available for this reductive transformation. These reagents, however, are often harmful and toxic, and required in considerable amounts. In view of the “greener” organic synthetic methodologies, much attention has been focused on the development of a highly efficient catalytic protocol using molecular hydrogen<sup>8</sup> in order to achieve the “cleaner” dehalogenation of organic halides.

Currently, we have been developing novel heterogeneous catalysts based on the unique properties of hydroxyapatite (HAP),  $\text{Ca}_{10}(\text{PO}_4)_6(\text{OH})_2$ , as a macroligand for the catalytically active species.<sup>9</sup> In particular, a monomeric  $\text{PdCl}_2$  species grafted on the HAP surface was readily transformed into Pd nanoclusters (PdHAP) with a narrow size distribution in the presence of reducing reagents, e.g. alcohols and molecular hydrogen. Such metallic Pd species showed extremely high catalytic activities for aerobic alcohol oxidation,<sup>10c</sup> deprotection of Z-groups with molecular hydrogen,<sup>10b</sup> and indoline dehydrogenation.<sup>10a</sup> Here, we report an efficient and convenient dehalogenation using molecular hydrogen catalysed by PdHAP. The present catalytic methodology possesses several attractive features: (1) high catalytic efficiency (turnover number up to 10 000), (2) use of atmospheric pressure molecular hydrogen, and (3) facile dehalogenation even in water. The above characteristics make it an ideal environmentally-benign chemical process in terms of a potential industrial application for disposing of halogenated wastes.

The hydroxyapatite-grafted palladium complex was synthesized according to the procedure described in the previous literature.<sup>10c</sup> Characterization by elemental analysis, XPS, EDX, and Pd–K edge XAFS revealed that a monomeric  $\text{PdCl}_2$  species was grafted by chemisorption on the HAP surface.

Initially, the reductions of chlorobenzene into benzene using various Pd catalysts under an atmospheric pressure of  $\text{H}_2$  were carried out (Table 1).

The PdHAP catalyst was found to be the most effective in methanol solvent (Table 1, entry 1). This catalytic activity was significantly higher than those of commercially available heterogeneous Pd catalysts (entries 7–11). Among the solvents

**Table 1** Dechlorination of chlorobenzene using various Pd catalysts<sup>a</sup>

Entry	Pd catalyst	Solvent	Convsn (%) <sup>b</sup>	Yield (%) <sup>b</sup>
1	PdHAP	MeOH	86	86
2		EtOH	85	84
3		2-PrOH	62	60
4		DMF	41	41
5		THF	13	13
6		Toluene	11	10
7 <sup>c</sup>	$\text{Pd}/\text{TiO}_2$ (5 wt%)	MeOH	38	36
8 <sup>c</sup>	$\text{Pd}/\text{SiO}_2$ (0.5 wt%)	MeOH	35	35
9 <sup>c</sup>	$\text{Pd}/\text{Al}_2\text{O}_3$ (5 wt%)	MeOH	34	33
10 <sup>d</sup>	$\text{Pd}/\text{Carbon}$ (5 wt%)	MeOH	25	23
11 <sup>d,e</sup>	$\text{Pd}/\text{AC}$ (10 wt%)	MeOH	18	17
12	$\text{PdCl}_2$	MeOH	Trace	Trace
13	$\text{Pd}(\text{OAc})_2$	MeOH	Trace	Trace
14	$\text{PdCl}_2(\text{PhCN})_2$	MeOH	Trace	Trace
15	$\text{Pd}_2(\text{dba})_3\text{CHCl}_3$	MeOH	Trace	Trace

<sup>a</sup> Chlorobenzene (1 mmol), Pd catalyst (Pd: 0.2 mol%), solvent (5 mL),  $\text{H}_2$  (1 atm), 60 °C, 2 h. <sup>b</sup> Determined by GC using an internal standard technique. <sup>c</sup> Purchased from N. E. Chemcat. <sup>d</sup> Purchased from WAKO Pure Chemical Ind, Inc. <sup>e</sup> AC: activated carbon.

examined, alcohol solvents yielded favorable results (entries 1–3),<sup>11</sup> whereas DMF, THF, and toluene were not effective (entries 4–6). The use of typical homogeneous Pd complexes resulted in low yields, accompanied with the formation of Pd black (entries 12–15).

Prior to use as a catalyst, the hydroxyapatite-grafted palladium complex was stirred in methanol under a  $\text{H}_2$  atmosphere. After this treatment, the catalyst color changed from yellow to light gray. Transmission electron microscopy (TEM) analysis for the isolated catalyst confirmed the formation of Pd nanoclusters with a mean diameter of 3 nm, showing that the monomeric Pd(II) species on HAP were transformed into Pd nanoclusters. The PdHAP was removed after 30% conversion of chlorobenzene, and the treatment of the filtrate at 60 °C for 1 h under a  $\text{H}_2$  atmosphere resulted in no dehalogenation. It can be said that *in situ* generated Pd nanoclusters on the HAP surface act as a catalytically active species for the dehalogenation. Notably, the quantitative conversion of chlorobenzene to benzene with excellent TON (10 000) and TOF ( $1000 \text{ h}^{-1}$ ) could be achieved using a low concentration of the PdHAP catalyst (Pd:  $1 \times 10^{-2}$  mol%). *These values are significantly higher than those previously reported for other catalytic systems, such as Ru(II) phosphine complex (TON = 40, TOF =  $40 \text{ h}^{-1}$ ),<sup>8c</sup>  $[(\text{C}_5\text{Me}_5)_2\text{RhCl}_2]_2$  catalyst (TON = 33, TOF =  $16.5 \text{ h}^{-1}$ ),<sup>8e</sup>*



**Table 2** Dehalogenation of various organic halides using PdHAP<sup>a</sup>

Entry	Substrate	Pd (mol%)	Time/h	Yield (%) <sup>b</sup>
1	R = H	0.2	3	>99
2	Br	0.2	2	95 <sup>c</sup>
3	CH <sub>3</sub>	0.2	3	98
4 <sup>d</sup>	C(O)CH <sub>3</sub>	0.2	1	>99 <sup>e</sup>
5 <sup>d</sup>	C(O)Ph	0.6	24	>99 <sup>f</sup>
6	CN	0.2	2	80
7	NH <sub>2</sub>	0.2	1	96
8	OH	0.2	3	>99
9		0.2	1	99
10		0.2	2	>99
11		0.2	2	>99
12		0.2	2	>99
13		0.6	3	>99
14		0.6	3	>99
15		0.6	1	>99

<sup>a</sup> Substrate (1 mmol), PdHAP (0.1–0.3 g), MeOH (5 mL), 60 °C, H<sub>2</sub> atmosphere. <sup>b</sup> Determined by GC and GC-MS using an internal standard technique. <sup>c</sup> Chlorobenzene yield. <sup>d</sup> KO<sup>t</sup>Bu (1.2 mmol) was added. <sup>e</sup> Acetophenone yield. <sup>f</sup> Benzophenone yield.

poly(*N*-vinyl-2-pyrrolidone) anchored Pd catalyst (TON = 1 000, TOF = 500 h<sup>-1</sup>),<sup>8d</sup> and Pd/carbon (TON = 130, TOF = 260 h<sup>-1</sup>).<sup>8f</sup>

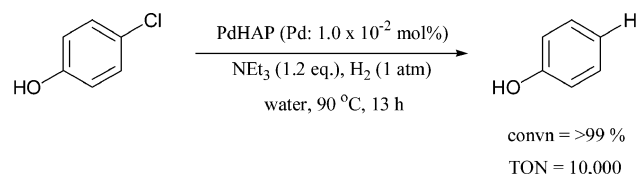
The PdHAP catalyst smoothly reduced various haloarenes to the corresponding arenes in the presence of molecular hydrogen (Table 2). The reactivity of bromoarenes was higher than that of the corresponding chloroarenes (entries 1, 3, vs. 9, 10). An intramolecular competitive dehalogenation of 4-bromochlorobenzene chemoselectively gave a 95% yield of chlorobenzene together with a 5% yield of benzene under the present conditions (entry 2). Interestingly, the reaction of iodoarenes hardly proceeded in the presence of the PdHAP.<sup>12</sup> In the case of 4-chloroacetophenone, addition of KO<sup>t</sup>Bu as a scavenger of HCl could efficiently suppress the reduction of carbonyl group to give acetophenone (entry 4). Without KO<sup>t</sup>Bu, the product selectivities of acetophenone, 4-chloro- $\alpha$ -methylbenzyl alcohol, and  $\alpha$ -methylbenzyl alcohol were 9, 11, and 80%, respectively. The PdHAP was also applicable to chlorinated substrates containing nitrogen or oxygen atoms (entries 12–15).

From the viewpoint of recent environmental consciousness, the use of water as a reaction solvent has received considerable attention.<sup>13</sup> Halogenated compounds are often detected in contaminated wastewater; therefore, achieving efficient dehalogenations in aqueous media is particularly important for practical applications. It is noteworthy that our PdHAP has proved to be an efficient heterogeneous catalyst in water under an atmospheric pressure of H<sub>2</sub>. As summarized in Table 3, various halophenols were converted into the corresponding phenols in quantitative yields (entries 1–6). Additionally, the

**Table 3** Dehalogenation in water catalysed by PdHAP<sup>a</sup>

Entry	Substrate	Pd (mol%)	Time/h	Yield (%) <sup>b</sup>
1		0.4	3	82
2		0.4	3	92
3		0.4	2	>99 (96)
4		0.4	3	90
5		0.4	3	98
6		0.4	3	>99
7		0.4	4	98
8		0.4	13	>99
9 <sup>c</sup>		0.4	13	>99 <sup>d</sup>
10		0.2	10	99
11		0.2	15	>99

<sup>a</sup> Substrate (1 mmol), PdHAP (0.1–0.2 g), water (5 mL), 60 °C, H<sub>2</sub> atmosphere. <sup>b</sup> Determined by GC and GC-MS using an internal standard technique. Value in parenthesis is an isolated yield. <sup>c</sup> NEt<sub>3</sub> (1.2 equiv. relative to Cl atom) was added. <sup>d</sup> Phenol yield.

**Scheme 1** Aqueous dechlorination by PdHAP catalyst.

dechlorination of polyhalogenated 2,4-dichlorophenol gave 99% of phenol in 13 h (entry 9). The reaction rates decreased slightly in water-insoluble substrates such as chlorobenzene and 4-chlorotoluene, as compared with those observed in the methanol solvent (entries 10 and 11).

In an effort to demonstrate the applicability of the present aqueous protocol, the reduction of 4-chlorophenol, a precursor to dioxins,<sup>14</sup> was achieved at a low concentration of the PdHAP catalyst (Scheme 1). This dechlorination proceeded completely within 13 h and the corresponding TON and TOF were 10 000 and 769 h<sup>-1</sup>, respectively. Contrastingly, previously reported catalyst systems in aqueous media required high hydrogen pressures and high catalyst concentrations in order to accomplish efficient dehalogenations.<sup>15</sup> The superior performance of the PdHAP catalyst is thought to be due to the high hydrophilic character of the hydroxyapatite,<sup>16</sup> which helps to overcome the problems related to diffusion limitations.

A possible catalytic cycle for this dehalogenation using the PdHAP was proposed as follows:<sup>17</sup> an oxidative addition of the C–X bond of haloarene to the active Pd<sup>0</sup> species on the surface of Pd nanoclusters affords a  $\sigma$ -aryl Pd species. Subsequently, this intermediate species undergoes attack by H<sub>2</sub> to give a H–Pd-aryl species together with the formation of HX,<sup>18</sup> followed by reductive elimination to afford the corresponding dehalogenation product and Pd<sup>0</sup> species.

In conclusion, the present PdHAP system serves as an efficient heterogeneous catalyst for the dehalogenation of



various organic halides. The present protocol based on the HAP as a catalyst support provides a possibility for the nano-scale design of functionalized catalysts for environmentally-friendly chemical processes.

## Experimental

### The synthesis of hydroxyapatite-grafted palladium complex

Hydroxyapatite (HAP),  $\text{Ca}_{10}(\text{PO}_4)_6(\text{OH})_2$  was synthesized from  $\text{Ca}(\text{NO}_3)_2 \cdot 4\text{H}_2\text{O}$  and  $(\text{NH}_4)_2\text{HPO}_4$  by the precipitation method according to the literature procedure.<sup>19</sup> HAP (2.0 g) was stirred in a  $\text{PdCl}_2(\text{PhCN})_2$  ( $2.67 \times 10^{-4}$  M) solution in acetone (150 mL) at room temperature for 3 h. The resulting slurry was filtered, washed with acetone and dried under vacuum, yielding the HAP-grafted Pd complex (2.01 g, Pd content:  $0.02 \text{ mmol g}^{-1}$ ) as a pale yellow powder.

### Typical procedure for dechlorination of chlorobenzene using the PdHAP catalyst

The HAP-grafted Pd complex (0.025 g, Pd:  $0.5 \mu\text{mol}$ ) was stirred in methanol (30 mL) at  $60^\circ\text{C}$  for 30 min under 1 atm of  $\text{H}_2$ . Chlorobenzene (0.563 g, 5 mmol) was added to this heterogeneous mixture and vigorously stirred. After 10 h, over 99% chlorobenzene was converted into benzene, determined by GC using the internal standard technique.

### General procedures for aqueous dechlorination of 4-chlorophenol using the PdHAP catalyst

The HAP-grafted Pd complex (0.2 g, Pd:  $4 \mu\text{mol}$ ) was stirred in water (5 mL) at  $60^\circ\text{C}$  for 30 min under a  $\text{H}_2$  atmosphere. 4-Chlorophenol (0.128 g, 1 mmol) was added to this heterogeneous mixture and vigorously stirred. The progress of the reaction was monitored by GC analysis. After complete conversion of the substrate (3 h), the reaction mixture was extracted three times with diethyl ether ( $3 \times 10 \text{ mL}$ ). The organic layer was dried over  $\text{MgSO}_4$  and the evaporation of the solvent afforded analytically pure phenol (0.090 g, 96%).

## Acknowledgements

This work is supported by a Grant-in-Aid for Scientific Research from Ministry of Education, Science, Sports and Culture of Japan. A part of the present experiments was carried out by using a facility in the Research Center for Ultrahigh Voltage Electron Microscopy, Osaka University. We are grateful to the Department of Chemical Science and Engineering, Graduate School of Engineering Science, Osaka University for scientific support via "Lend-Lease Laboratory System". T. H. and K. M. thank the JSPS Research Fellowships for Young Scientists.

## Notes and references

- (a) F. Alonso, I. P. Beletskaya and M. Yus, *Chem. Rev.*, 2002, **102**, 4009; (b) V. V. Grushin and H. Alper, *Chem. Rev.*, 1994, **94**, 1047; (c) A. R. Pinder, *Synthesis*, 1980, 425.
- One of the most general methodologies is thermal and/or chemical oxidations, but the complete decomposition of organic halides to  $\text{CO}_2$ ,  $\text{H}_2\text{O}$ , and  $\text{HCl}$  could not be achieved and the reactions are often accompanied with the formation of toxic halogenated chemicals such as dioxins, phosgene, and chlorine, see M. D. Erickson, S. E. Swanson, J. J. D. Flora Jr. and G. D. Hinshaw, *Environ. Sci. Technol.*, 1989, **23**, 462.
- (a) C. Desmarrets, S. Kuhl, R. Schneider and Y. Fort, *Organometallics*, 2002, **21**, 1554; (b) M. S. Viciu, G. A. Grasa and S. P. Nolan, *Organometallics*, 2001, **20**, 3607.
- (a) R. E. Maleczka Jr., R. J. Rahaim Jr. and R. R. Teixeira, *Tetrahedron Lett.*, 2002, **43**, 7087; (b) R. J. Rahaim Jr. and R. E. Maleczka Jr., *Tetrahedron Lett.*, 2002, **43**, 8823; (c) R. Boukherroub, C. Chatgililoglu and G. Manuel, *Organometallics*, 1996, **15**, 1508.
- R. Hara, K. Sato, W.-H. Sun and T. Takahashi, *Chem. Commun.*, 1999, 845.
- P. P. Cellier, J.-F. Spindler, M. Taillefer and H.-J. Cristau, *Tetrahedron Lett.*, 2003, **44**, 7191.
- (a) M. A. Atienza, M. A. Esteruelas, M. Fernández, J. Herrero and M. Oliván, *New J. Chem.*, 2001, **25**, 775; (b) I. Pri-Bar and O. Buchman, *J. Org. Chem.*, 1986, **51**, 734.
- (a) I. Yamanaka, K. Nishikawa, S. Takenaka and K. Otsuka, *Stud. Surf. Sci. Catal.*, 2003, **145**, 383; (b) N. Faucher, Y. Ambroise, J.-C. Cintrat, E. Doris, F. Pillon and B. Rousseau, *J. Org. Chem.*, 2002, **67**, 932; (c) M. E. Cucullu, S. P. Nolan, T. R. Belderrain and R. H. Grubbs, *Organometallics*, 1999, **18**, 1299; (d) Y. Zhang, S. Liao and Y. Xu, *Tetrahedron Lett.*, 1994, **35**, 4599; (e) D. T. Ferrughelli and I. T. Horváth, *J. Chem. Soc., Chem. Commun.*, 1992, 806; (f) C. A. Marques, M. Selva and P. Tundo, *J. Org. Chem.*, 1993, **58**, 5256; (g) J. B. Hoke, G. A. Gramiccioni and E. N. Balko, *Appl. Catal. B: Environ.*, 1992, **1**, 285.
- (a) K. Mori, T. Hara, T. Mizugaki, K. Ebitani and K. Kaneda, *J. Am. Chem. Soc.*, 2003, **125**, 11460; (b) K. Mori, M. Tano, T. Mizugaki, K. Ebitani and K. Kaneda, *New J. Chem.*, 2002, **26**, 1536; (c) K. Mori, K. Yamaguchi, T. Mizugaki, K. Ebitani and K. Kaneda, *Chem. Commun.*, 2001, 461; (d) K. Yamaguchi, K. Mori, T. Mizugaki, K. Ebitani and K. Kaneda, *J. Am. Chem. Soc.*, 2000, **122**, 7144.
- (a) T. Hara, K. Mori, T. Mizugaki, K. Ebitani and K. Kaneda, *Tetrahedron Lett.*, 2003, **44**, 6207; (b) M. Murata, T. Hara, K. Mori, M. Ooe, T. Mizugaki, K. Ebitani and K. Kaneda, *Tetrahedron Lett.*, 2003, **44**, 4981; (c) K. Mori, K. Yamaguchi, T. Hara, T. Mizugaki, K. Ebitani and K. Kaneda, *J. Am. Chem. Soc.*, 2002, **124**, 11572.
- In the dehalogenation of 4-chlorotoluene using  $\text{CD}_3\text{OD}$  as a solvent, the incorporation of deuterium atoms in toluene product could be observed by GC-MS and  $^1\text{H-NMR}$  spectra.
- Addition of 1 equiv. of iodobenzene significantly suppressed the dechlorination of chlorobenzene. This inhibition may be attributed to the strong coordination of  $\text{I}^-$  to the active Pd species.
- C.-J. Li and T.-H. Chan, *Organic Reactions in Aqueous Media*, Wiley, New York, 1997.
- K. A. Tuppurainen, P. H. Rrokojärvi, A. H. Asikainen, M. Aatamila and J. Ruuskanen, *Environ. Sci. Technol.*, 2000, **34**, 4958.
- (a) V. Felis, C. D. Bellefon, P. Fouilloux and D. Schweich, *Appl. Catal. B: Environ.*, 1999, **20**, 91; (b) C. Schuth and M. Reinhard, *Appl. Catal. B: Environ.*, 1998, **18**, 215.
- (a) J. C. Elliott, *Structure and Chemistry of the Apatites and Other Calcium Orthophosphates*, Elsevier, Amsterdam, 1994; (b) D. N. Misra, *J. Adhes. Sci. Technol.*, 1994, **8**, 87.
- Addition of a radical trap, 2,2',6,6'-tetramethylpiperidine *N*-oxyl (TEMPO), to the reaction medium hardly influenced the dehalogenation. This result indicates that the present dehalogenation does not proceed via the free radical pathway.
- Treatment of the reaction mixture with  $\text{AgNO}_3$  showed formation of an equimolar amount of  $\text{AgCl}$  relative to the consumed substrate.
- S. Sugiyama, T. Minami, H. Hayashi, M. Tanaka, N. Shigemoto and J. B. Moffat, *J. Chem. Soc., Faraday Trans.*, 1996, **92**, 293.



# Epoxidation of propylene with molecular oxygen in methanol over a peroxy-heteropoly compound immobilized on palladium exchanged HMS

Yanyong Liu,\* Kazuhisa Murata and Megumu Inaba

Research Institute for Green Technology, National Institute of Advanced Industrial Science and Technology, AIST Tsukuba Central 5, 1-1-1 Higashi, Tsukuba, Ibaraki 305-8565, Japan. E-mail: yy.ryuu@aist.go.jp; Fax: +81 29 861 4774

Received 13th May 2004, Accepted 10th August 2004

First published as an Advance Article on the web 4th October 2004

The peroxy-heteropoly compound  $\{HPO_4[W(O)(O_2)_2]_2\}$  was synthesized on the surface of HMS by reacting HMS-PrNH(PO<sub>3</sub>H<sub>2</sub>) with  $[W_2O_3(O_2)_4(H_2O)_2]^{2-}$  solution, and then palladium ions were exchanged into the channels of HMS to form a hybrid catalyst. The novel solid catalyst showed 34.1% propylene conversion and 83.2% selectivity for propylene oxide for the oxidation of propylene using molecular oxygen as an oxidant in methanol at 373 K for 6 h. Because  $\{HPO_4[W(O)(O_2)_2]_2\}$  was immobilized on the HMS surface by chemical bonds and palladium particles formed during the reaction were fixed in the HMS channels, the solid catalyst could be reused by a simple filtration method and the active components did not leach into the methanol medium after reaction. The selectivity for propylene oxide over the solid catalyst was similar to that over a homogeneous catalyst containing  $[(C_6H_{13})_4N]_2\{HPO_4[W(O)(O_2)_2]_2\}$  and Pd(OAc)<sub>2</sub>, but the propylene conversion over the solid catalyst was lower than that over the homogeneous catalyst. The highest yield of propylene oxide obtained over the solid catalyst by increasing catalyst amount was similar to the highest yield of propylene oxide over the homogeneous catalyst.

## Introduction

Propylene oxide (denoted by PO) is one of the most important chemical feedstocks for producing polyurethane, surfactants and other products. Its current worldwide production capacity is around 4.5 million metric tons per year. The two main conventional manufacturing methods of PO are the chlorohydrin process and the hydroperoxide process. Both of these are two-stage processes. The chlorohydrin process causes serious environmental pollution and the hydroperoxide process stoichiometrically produces co-products such as *t*-butyl alcohol and styrene. As a replacement for chlorine, environmentally benign oxidants, such as molecular oxygen and hydrogen peroxide, play an important role in green chemistry. Although it has been reported that a high selectivity for PO could be obtained from the oxidation of propylene over TS-1 and heteropolyacid using hydrogen peroxide as an oxidant,<sup>1</sup> hydrogen peroxide is currently too expensive to allow an economically viable process. Molecular oxygen is the best oxidant due to low cost and significant advantages for the environment. Using a mixed gas of oxygen and hydrogen, a high selectivity for PO (>90%) could be obtained at a low propylene conversion (<5%) over Au/TiO<sub>2</sub> and Pd/TS-1 catalysts, but a large amount of hydrogen is consumed to form water and a safety problem exists in processes using the hydrogen–oxygen mixed gas.<sup>2</sup> Alkene can be epoxidized by molecular oxygen in the presence of an organic reducing reagent.<sup>3</sup> Because the organic reducing reagents reported in the literature (such as 1-butanol, isobutyraldehyde, benzaldehyde, and so on) are co-oxidized to the corresponding organic acids, which are difficult to reuse as a reducing reagent, this process is complicated and needs heavy capital investment.<sup>4</sup> Although the oxidation of propylene to PO by molecular oxygen without any organic acid co-products would be important in industry, the direct catalytic epoxidation of propylene by molecular oxygen without any reducing reagents usually gives poor selectivity for

PO (<40%) because of the high activity of the allylic C–H bonds of propylene.<sup>5</sup>

Heteropoly acid catalysts are very attractive since they have both strong acidity and redox properties, and these two important properties for catalysis can be controlled though choosing appropriate constituent elements.<sup>6</sup> These merits make them potentially useful for the selective oxidation of hydrocarbons. Heteropoly acids H<sub>3</sub>PW<sub>12</sub>O<sub>40</sub> and H<sub>3</sub>PMo<sub>12</sub>O<sub>40</sub> are very effective catalysts for the epoxidation of alkene by hydrogen peroxide (so called Ishii–Venturello epoxidation).<sup>7</sup> The activity of these oxidant systems is due to the *in situ* formation of metal peroxy species, which are the real oxidants. Some of the metal peroxy species (peroxy-heteropoly compounds) have been isolated and showed excellent epoxidizing ability using hydrogen peroxide as an oxidant.<sup>8</sup> However, they cannot act as catalysts for the epoxidation of alkene using molecular oxygen as an oxidant. Recently, we have reported that a catalyst system consisting of palladium acetate and a peroxy-heteropoly compound in methanol effectively catalyzed the epoxidation of propylene by molecular oxygen.<sup>9</sup> Methanol is a safe and cheap medium. The catalyst system is promising for industrial manufacture of PO from propylene because it manufactures PO in high selectivity and the co-product CO<sub>x</sub> formed from methanol co-oxidation can be recycled for synthesizing methanol in industry. However, since the peroxy-heteropoly compound and palladium acetate are easily dissolved in methanol, the only possible method for reusing the homogeneous catalyst is the vacuum distillation of the mixture after reaction. From the view of green chemistry, heterogeneous catalysts are desirable in industry manufacture because of their versatility, their ease of separation, the lack of corrosion, the long lifetime and regenerability.<sup>10</sup>

The recent synthesis of silica based mesoporous materials, such as MCM-41 and HMS, has attracted great interest because of their high thermal stability, large surface and uniform-size pores. It was reported that a peroxy-heteropoly

compound could be immobilized on the surface of amine modified MCM-41.<sup>11</sup> We are focusing on HMS because HMS can be easily synthesized by a sol-gel reaction in the presence of primary alkylamine as template at room temperature and HMS possesses thicker framework walls, a small crystallite size of primary particles and complementary textural porosity.<sup>12</sup> These advantages mean that HMS materials are very interesting for catalysis and support.<sup>13</sup> Some metal ions, such as Pd<sup>2+</sup> and Fe<sup>3+</sup>, could be exchanged into the channels of HMS for preparing effective catalysts.<sup>14</sup> Moreover, aminopropyl-modified HMS has been synthesized using a one-pot synthesis,<sup>15</sup> and it has been used as a catalyst support by bonding the aminopropyl group with active catalysts.<sup>16</sup> Therefore, in this study, we designed a new type of solid hybrid catalyst through immobilizing a peroxy-heteropoly compound on the HMS surface and exchanging Pd<sup>2+</sup> ions into the HMS channels. The novel solid catalyst showed a high selectivity for PO in the oxidation of propylene by molecular oxygen in methanol and could be reused using a simple filtration method.

## Experimental

### Catalyst preparation

Peroxy-heteropoly compound [(C<sub>6</sub>H<sub>13</sub>)<sub>4</sub>N]<sub>2</sub>{HPO<sub>4</sub>[W(O)(O<sub>2</sub>)<sub>2</sub>]<sub>2</sub>} (denoted by THA-PW<sub>2</sub>) was prepared according to the method reported in the literature.<sup>8f</sup> Tungstic acid (2.5 g, 10 mmol) was added to 30% H<sub>2</sub>O<sub>2</sub> (7 ml, 69 mmol). After 40 min of stirring at 333 K, followed by centrifugation (15 min at 2000 rpm), 6 M H<sub>3</sub>PO<sub>4</sub> (0.85 ml, 5.1 mmol) was added to the supernatant. After stirring for 5 min, tetrahexylammonium chloride (7.8 g, 20 mmol) dissolved in 10 ml of water was added to the clear solution. After vigorously stirring at room temperature for 10 min, the solid product was filtered, washing with small amounts of water and diethyl ether, dried in air and stored in a vacuum desiccator.

Aminopropyl-modified HMS (denoted by HMS-PrNH<sub>2</sub>) was prepared according to the method reported by Macquarrie *et al.*<sup>15</sup> Tetraethoxysilane (TEOS, 18.5 g, 0.09 mol) and trimethoxy(3-aminopropyl)silane (AMPS, 1.79 g, 0.01 mol) were added, separately, to a stirred mixture of ethanol (41 g), distilled water (53 g) and n-dodecylamine (5.09 g) at room temperature. After 10 min the turbid solution became milky, and stirring was continued for 18 h, yielding a thick white suspension. The solid was filtered and n-dodecylamine was removed by heating the solid (*ca.* 10 g) at reflux in absolute ethanol (100 ml) for 3 h three times.

The method for preparing HMS-PrNH-PW<sub>2</sub> is similar to the method for preparing MCM-41-PrNH-PW<sub>2</sub>.<sup>11</sup> Thirty ml of a POCl<sub>3</sub> solution (50 mM in acetonitrile) and 30 ml of a 2,4,6-collidine solution (50 mM in acetonitrile) were consecutively added to 0.5 g of the dried HMS-PrNH<sub>2</sub>. The mixture was stirred for 24 h at room temperature, after which the resulting solid was washed with water to remove the chloride salts. The formed phosphoramidate-functionalized HMS (denoted by HMS-PrNH(PO<sub>3</sub>H<sub>2</sub>)) was subjected to an acidic washing with a dilute aqueous acid solution (0.1 N H<sub>3</sub>PO<sub>4</sub>) in order to have the phosphoramidate groups in fully hydrolyzed form. Ten mmol of tungstic acid were added to 7 ml of a 35% aqueous H<sub>2</sub>O<sub>2</sub> solution, and the mixture was heated for 60 min at 323 K to form [W<sub>2</sub>O<sub>3</sub>(O<sub>2</sub>)<sub>4</sub>(H<sub>2</sub>O)<sub>2</sub>]<sup>2-</sup> solution. Eight ml of acetone, 1 ml 35% H<sub>2</sub>O<sub>2</sub> and 0.25 g of HMS-PrNH(PO<sub>3</sub>H<sub>2</sub>) were added to 2.5 ml of the [W<sub>2</sub>O<sub>3</sub>(O<sub>2</sub>)<sub>4</sub>(H<sub>2</sub>O)<sub>2</sub>]<sup>2-</sup> solution. This mixture was stirred for 24 h at 293 K. The solid was isolated and washed six times with a 1 : 1 mixture of acetone-35% H<sub>2</sub>O<sub>2</sub>. Palladium was introduced into HMS-PrNH-PW<sub>2</sub> via ion-exchange from Pd(NH<sub>3</sub>)<sub>4</sub>Cl<sub>2</sub> aqueous solution.<sup>14</sup> 0.055 g Pd(NH<sub>3</sub>)<sub>4</sub>Cl<sub>2</sub> was dissolved in 40 ml water. One drop of aqueous NH<sub>3</sub> (10 wt%) was added reaching pH = 8. One gram dry HMS-PrNH-PW<sub>2</sub>

was added to the solution and the mixture was stirred vigorously at room temperature for 16 h. The resulting solid was filtered out, washed carefully with water and air-dried. The above synthetic process for the Pd-HMS-PrNH-PW<sub>2</sub> (Pd loading: 2.4 wt%) catalyst is described in Scheme 1.

### Instrumentation

Fourier transform infrared (FT-IR) spectra were recorded by a JASCO FT/IR-680plus spectrometer using KBr pellets under atmospheric conditions. Inductively coupled plasma (ICP) analysis was carried out using a Thermo Jarrell Ash IRIS/AP elemental analyzer. The powder X-ray diffraction (XRD) pattern was recorded using a MAC Science MX-Labo diffractometer equipped with Cu radiation operated at 40 kV and 50 mA. The N<sub>2</sub> adsorption isotherm was measured at 77 K using a Belsorp 28SA automatic adsorption instrument. The surface area was obtained from a BET plot, and the pore size distribution was performed by the BJH method. Pd particle size was measured by the CO pulse method at room temperature. Twenty mg of the catalyst was reduced in 100 ml min<sup>-1</sup> of H<sub>2</sub> at 673 K for 20 min and used for the measurement.

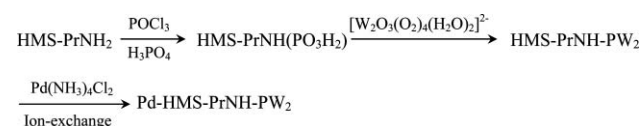
### Catalyst testing

The oxidation of propylene was carried out in a 50 ml stainless steel autoclave reactor, which was immersed into an oil-bath with temperature-control at the required temperatures. In the homogeneous system, 0.01 g of Pd(OAc)<sub>2</sub> and 0.2 g of THA-PW<sub>2</sub> (denoted by Pd+THA-PW<sub>2</sub>) were dissolved in 10 ml methanol and added into the autoclave. Thus the amount of Pd loading in Pd+THA-PW<sub>2</sub> was 2.4 wt%. In the heterogeneous system, 0.2 g of 2.4 wt% Pd-HMS-PrNH-PW<sub>2</sub> and 10 ml methanol were added into the autoclave. Then, 0.8 MPa propylene, 0.4 MPa molecular oxygen and 0.8 MPa Ar were charged to the autoclave at 298 K. After the mixture reacted at 373 K for 6 h with vigorous stirring, both the gas and the liquid were sampled and analyzed for the products by gas chromatography. Hydrocarbons and oxygenated compounds were detected by FID gas chromatography, the former with Porapak Q (1 m) at 473 K and the latter with 20 wt% FFAP on Chromosorb W (3 m) at 373 K. CO<sub>x</sub> and O<sub>2</sub> were detected by TCD gas chromatography, using a Shimadzu GC 14B equipped with Porapak Q (3 m) and molecular sieve MS-5A (3 m) columns kept at 343 K.

## Results and discussion

### Characterization of the catalysts

The IR spectra of various samples are shown in Fig. 1. HMS-PrNH<sub>2</sub> exhibits the symmetric stretching vibration bond at around 810 cm<sup>-1</sup> and the anti-symmetric vibration band at around 1090 cm<sup>-1</sup> of the tetrahedral SiO<sub>4</sub> units. The IR spectrum of HMS-PrNH(PO<sub>3</sub>H<sub>2</sub>) is similar to that of HMS-PrNH<sub>2</sub> but HMS-PrNH(PO<sub>3</sub>H<sub>2</sub>) showed a weak shoulder peak at 1060 cm<sup>-1</sup>. This peak may be assigned to stretching of the P-O bond although it is almost covered by the strong peak of Si-O vibration. As for THA-PW<sub>2</sub>, the peaks at 1075 cm<sup>-1</sup> and 1045 cm<sup>-1</sup> are assigned to the stretching vibration of P-O, the peak at 940 cm<sup>-1</sup> is assigned to the stretching vibration of W=O, and the peak at 840 cm<sup>-1</sup> is assigned to the stretching vibration of O-O. K<sub>2</sub>[W<sub>2</sub>O<sub>3</sub>(O<sub>2</sub>)<sub>4</sub>(H<sub>2</sub>O)<sub>2</sub>], which was obtained



Scheme 1 Synthesis route of Pd-HMS-PrNH-PW<sub>2</sub>.



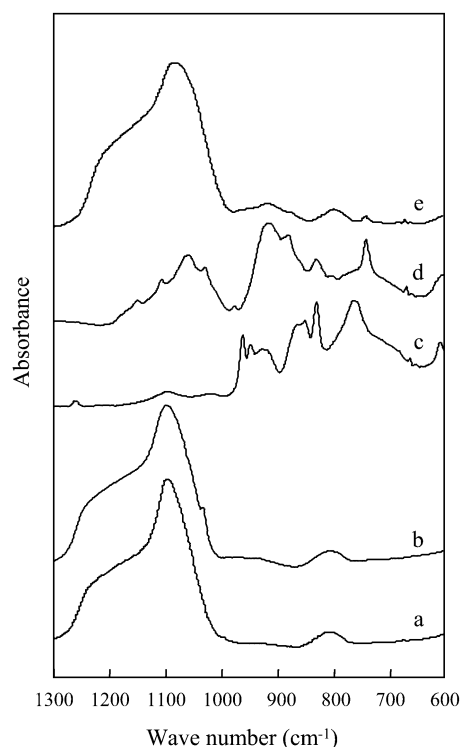


**Fig. 1** FT-IR spectra of various samples. (a) HMS-PrNH<sub>2</sub>; (b) HMS-PrNH(PO<sub>3</sub>H<sub>2</sub>); (c) K<sub>2</sub>[W<sub>2</sub>O<sub>3</sub>(O<sub>2</sub>)<sub>4</sub>(H<sub>2</sub>O)<sub>2</sub>]; (d) THA-PW<sub>2</sub>; (e) HMS-PrNH-PW<sub>2</sub>.

by adding KCl to the [W<sub>2</sub>O<sub>3</sub>(O<sub>2</sub>)<sub>4</sub>(H<sub>2</sub>O)<sub>2</sub>]<sup>2-</sup> solution, showed peaks at about 980, 960, 850, 835, 775 and 615 cm<sup>-1</sup>, which correlate with the data in the literature.<sup>3e</sup> Compared with the IR spectra of HMS-PrNH-PW<sub>2</sub>, THA-PW<sub>2</sub> and K<sub>2</sub>[W<sub>2</sub>O<sub>3</sub>(O<sub>2</sub>)<sub>4</sub>(H<sub>2</sub>O)<sub>2</sub>], HMS-PrNH-PW<sub>2</sub> clearly showed the peaks of PW<sub>2</sub> but did not show the peaks of K<sub>2</sub>[W<sub>2</sub>O<sub>3</sub>(O<sub>2</sub>)<sub>4</sub>(H<sub>2</sub>O)<sub>2</sub>] from 600 to 1000 cm<sup>-1</sup>. These results indicate that PW<sub>2</sub> had been synthesized on the HMS surface by reacting HMS-PrNH(PO<sub>3</sub>H<sub>2</sub>) with [W<sub>2</sub>O<sub>3</sub>(O<sub>2</sub>)<sub>4</sub>(H<sub>2</sub>O)<sub>2</sub>]<sup>2-</sup> solution.

The elemental analysis data for 2.4 wt% Pd-HMS-PrNH-PW<sub>2</sub> are shown in Table 1. The actual Pd loading measured by ICP analysis is almost consistent with the designed Pd loading. The molar ratio of W to P is nearly 2 in 2.4 wt% Pd-HMS-PrNH-PW<sub>2</sub>, which is evidence that PW<sub>2</sub> had been synthesized on the HMS surface.

**Table 1** Data of elemental analysis for Pd-HMS-PrNH-PW<sub>2</sub>

Pd-HMS-PrNH-PW <sub>2</sub>	Loading of Pd (%)	Loading of PW <sub>2</sub> (%)	Molar ratio of W/P
Designed	2.4	47.9 <sup>a</sup>	2.0
Found <sup>b</sup>	2.3	41.4	1.8

<sup>a</sup> Calculated from the amount of aminopropyl group designed in the sample. <sup>b</sup> Obtained by ICP measurement.

**Table 2** Oxidation of propylene by molecular oxygen over various catalysts in methanol at 373 K for 6 h<sup>a</sup>

Catalyst	Propylene conversion (%)	PO yield (%)	Selectivity (%)								O <sub>2</sub> conversion (%)
			PO	Acetone	Acrolein	PA <sup>b</sup>	Propane	HC <sup>c</sup>	ROP <sup>d</sup>	CO <sub>x</sub>	
Pd-HMS-PrNH-PW <sub>2</sub> <sup>e</sup>	34.1	28.4	83.2	2.8	3.0	1.6	5.4	1.2	2.7	0.1	47.1
Pd+PW <sub>2</sub> <sup>f</sup>	44.3	36.6	82.7	2.1	2.5	1.2	6.3	1.7	3.5	0.1	64.4
HMS-PrNH-PW <sub>2</sub> <sup>g</sup>	1.7	1.5	88.6	5.6	1.8	0.6	0.3	0.8	2.3	0	1.8
Pd-HMS-PrNH-PO <sub>3</sub> H <sub>2</sub> <sup>e</sup>	3.4	0.1	4.3	8.4	43.7	9.4	23.4	10.8	0	0	9.6
Pd-HMS-PrNH <sub>2</sub> <sup>e</sup>	2.9	0.1	5.1	25.6	11.3	12.5	30.4	15.1	0	0	10.3

<sup>a</sup> Autoclave: 50 ml; methanol: 10 ml; C<sub>3</sub>H<sub>6</sub>: 0.8 MPa; O<sub>2</sub>: 0.4 MPa; Ar: 0.8 MPa. <sup>b</sup> PA: propionaldehyde. <sup>c</sup> Hydrocarbons (HC = C<sub>4</sub> + C<sub>5</sub> + C<sub>6</sub>). <sup>d</sup> ROP: Ring opened by-products. <sup>e</sup> Catalyst: 0.2 g, Pd loading: 2.4 wt%. <sup>f</sup> THA-PW<sub>2</sub>: 0.2 g, Pd(OAc)<sub>2</sub>: 0.01 g. <sup>g</sup> Catalyst: 0.2 g.

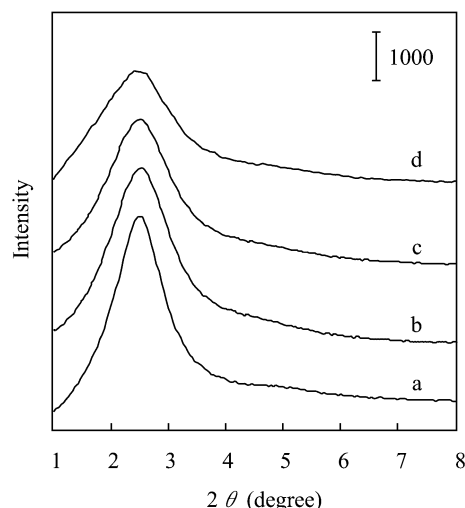


**Fig. 2** The XRD patterns of various samples. (a) HMS-PrNH<sub>2</sub>; (b) HMS-PrNH(PO<sub>3</sub>H<sub>2</sub>); (c) HMS-PrNH-PW<sub>2</sub>; (d) 2.4 wt% Pd-HMS-PrNH-PW<sub>2</sub>.

The low-angle powder XRD patterns of various samples are shown in Fig. 2. Each sample exhibits an intense reflection corresponding to the (100) plane at 2–3 degrees. These patterns are typical wormhole structures of HMS materials assembled from long alkyl chain neutral amines as surfactants. 2.4 wt% Pd-HMS-PrNH-PW<sub>2</sub> showed an intense reflection corresponding to the (100) plane although the intensity decreased and the reflection became broad compared with that of HMS-PrNH<sub>2</sub>, which indicates that the mesoporous structure of HMS-PrNH<sub>2</sub> remained after modification by PW<sub>2</sub> and Pd<sup>2+</sup> ions.

### Epoxidation of propylene with molecular oxygen in methanol

The propylene conversion and the selectivity for PO over various catalysts are shown in Table 2. The solid catalyst 2.4 wt% Pd-HMS-PrNH-PW<sub>2</sub> showed 34.1% propylene conversion and 83.2% selectivity for PO in the oxidation of propylene at 373 K for 6 h in methanol medium. The by-products observed were acetone, acrolein, propionaldehyde, propane, C<sub>4</sub>–C<sub>6</sub> hydrocarbons and ring-opened products. The homogenous catalyst 2.4 wt% Pd+THA-PW<sub>2</sub> showed 44.3% propylene conversion and 82.7% selectivity for PO for the propylene oxidation at 373 K for 6 h. HMS-PrNH-PW<sub>2</sub> showed a high selectivity for PO of 88.6% but the propylene conversion was only 1.7% for the propylene oxidation at 373 K for 6 h. Pd-HMS-PrNH(PO<sub>3</sub>H<sub>2</sub>) and Pd-HMS-PrNH<sub>2</sub> showed very low conversions and selectivities for PO in the oxidation of propylene by molecular oxygen. Thus the simultaneous existence of Pd and PW<sub>2</sub> in the catalyst system is very important for improving the yield of PO from the oxidation of propylene.

Molecular oxygen is consumed for both oxidizing propylene and oxidizing the solvent. The conversion of molecular oxygen

was higher than the conversion of propylene over Pd-HMS-PrNH-PW<sub>2</sub> in methanol at 373 K for 6 h (Table 2), which indicates that part of the methanol was co-oxidized during the propylene oxidation. Because the oxygenated compounds formed from methanol co-oxidation (such as formaldehyde and formic acid) were detected in very small amounts after reaction, the consumed methanol was almost oxidized to CO<sub>x</sub> and H<sub>2</sub>O during the reaction. We call the CO<sub>x</sub> formed from the propylene oxidation the by-product and the CO<sub>x</sub> formed from the methanol oxidation the co-product. The selectivity for CO<sub>x</sub> in the propylene oxidation (by-product) listed in Table 2 was calculated by subtracting the selectivity for every product formed from propylene oxidation except CO<sub>x</sub> from 100%. The amount of CO<sub>x</sub> detected by gas chromatography was much higher than the value of CO<sub>x</sub> listed in Table 2 due to the methanol co-oxidation over Pd-HMS-PrNH-PW<sub>2</sub>. The difference between the conversion of molecular oxygen and the conversion of propylene is the consumed molecular oxygen for the methanol co-oxidation. The conversion of molecular oxygen over Pd-HMS-PrNH-PW<sub>2</sub> for 6 h is 47.1%, in which 34.1% conversion of molecular oxygen is consumed for oxidizing propylene and the remaining 13% conversion of molecular oxygen is consumed for oxidizing methanol. The molar ratio and the mass ratio of the formed PO to the consumed methanol over Pd-HMS-PrNH-PW<sub>2</sub> for 6 h are nearly 2.2 and 4.0, respectively. Because the co-product CO<sub>x</sub> formed from the co-oxidation of methanol can be recycled for synthesizing methanol in industry, this catalyst system is promising for industrial manufacture of PO from propylene.

We discussed the reaction pathway for propylene oxidation in methanol by molecular oxygen over a catalyst system containing palladium and a peroxo-heteropoly compound in a previous report.<sup>9</sup> Pd<sup>2+</sup> species were reduced by methanol to form Pd<sup>0</sup> species, and the formed Pd<sup>0</sup> species activated the oxygen molecule resolved in the methanol medium. The activated oxygen molecule oxidized CH<sub>3</sub>OH to HCHO, and hydrated HCHO to form HCH(OH)<sub>2</sub>. Then a peroxy intermediate HOCH<sub>2</sub>OOH formed, like in other methanol-O<sub>2</sub> systems reported in the literature.<sup>17</sup> The peroxy intermediate HOCH<sub>2</sub>OOH probably plays a role in regenerating the peroxy O-O bonds of the peroxo-heteropoly compound for the epoxidation of propylene. Because the peroxy intermediate HOCH<sub>2</sub>OOH is not stable and finally decomposes to CO<sub>x</sub> and H<sub>2</sub>O, methanol is consumed during the propylene oxidation. Moreover, some other peroxy fragments would be formed during the decomposition of the intermediate HOCH<sub>2</sub>OOH, like in the Pd(OAc)<sub>2</sub>-Ti-Al-zeolite-CH<sub>3</sub>OH catalyst system.<sup>18</sup> Hydrogen peroxide is also probably formed *in situ* in this system *via* two routes and promotes the epoxidation of propylene. One route of the formation of hydrogen peroxide *in situ* is the decomposition of the peroxy intermediate HOCH<sub>2</sub>OOH. It has been reported that a small part of HOCH<sub>2</sub>OOH decomposes to HCHO and H<sub>2</sub>O<sub>2</sub>, while a large part of HOCH<sub>2</sub>OOH decomposes to HCOOH and H<sub>2</sub>O.<sup>17c</sup> Another route is similar to that in the Pd-CO-H<sub>2</sub>O-O<sub>2</sub> catalyst system.<sup>19</sup> The co-product CO reacts with the co-product H<sub>2</sub>O to form CO<sub>2</sub> and H<sub>2</sub>, then the formed H<sub>2</sub> reacts with O<sub>2</sub> to form H<sub>2</sub>O<sub>2</sub> over the palladium catalyst. The peroxo-heteropoly compound possesses high epoxidation ability even in the dilute hydrogen peroxide solution. Although it is difficult to confirm which peroxy intermediate is really responsible for regenerating the peroxy O-O bonds of the peroxo-heteropoly compound, palladium, peroxo-heteropoly compound and methanol are necessary for the production of PO in this study. Because the solid catalyst Pd-HMS-PrNH-PW<sub>2</sub> and the homogeneous catalyst Pd+THA-PW<sub>2</sub> simultaneously possess the factors described above in methanol medium, they showed high yields of PO for the propylene oxidation.

**Table 3** Reuse of 2.4 wt% Pd-HMS-PrNH-PW<sub>2</sub> for the oxidation of propylene in methanol at 373 K for 6 h by molecular oxygen<sup>a</sup>

Catalyst	Cycle No.	Conv. (%)	Select. for PO (%)
Fresh	1	34.1	83.2
Used <sup>b</sup>	2	35.3	83.5
	3	33.7	82.3
	4	34.3	81.8
	5	33.4	82.6

<sup>a</sup> Autoclave: 50 ml; methanol: 10 ml; C<sub>3</sub>H<sub>6</sub>: 0.8 MPa; O<sub>2</sub>: 0.4 MPa; Ar: 0.8 MPa; catalyst amount: 0.2 g. <sup>b</sup> Separated by filtrating the mixture after reaction.

The reusability of the solid catalyst 2.4 wt% Pd-HMS-PrNH-PW<sub>2</sub> for the oxidation of propylene in methanol by molecular oxygen is shown in Table 3. The used catalysts were obtained by filtrating the mixture after reaction. The conversion and the selectivity for PO did not decrease after being reused four times. Furthermore, we designed the following experiment to confirm the stability of the solid catalyst 2.4 wt% Pd-HMS-PrNH-PW<sub>2</sub> using the method reported in the literature.<sup>20</sup> As shown in Fig. 3, 0.2 g of 2.4 wt% Pd-HMS-PrNH-PW<sub>2</sub> was used to catalyze the propylene oxidation at 373 K for 6 h, then the solid catalyst was filtrated at 373 K and was put into another autoclave filled with the same reactants, and the reaction was also carried at 373 K for 6 h. The filtrated solution without the solid catalyst was charged with the reaction gases and allowed to react at 373 K for 6 h. For the solid catalyst that was being used for the second time, no reduction of the catalytic activity could be found compared to the first time. On the other hand, the filtrated solution that the solid catalyst was removed from did not show a further reaction at 373 K. The above operation was repeated 5 times, and we obtained the same results. The IR and XRD of 2.4 wt% Pd-HMS-PrNH-PW<sub>2</sub> after being reused 5 times did not change. These results indicate that the Pd-HMS-PrNH-PW<sub>2</sub> catalyst could be reused by a simple filtration method and the active components did not leach into the methanol medium after reaction for five times.

The model of the active catalyst Pd-HMS-PrNH-PW<sub>2</sub> is shown in Fig. 4. The Pd particle size of the Pd-HMS-PrNH-PW<sub>2</sub> catalyst after reaction, measured by the CO pulse method, is about 3 nm, which is very close to the size of HMS channels (2.9 nm) measured by the BJH method using the N<sub>2</sub> adsorption-desorption isotherms. The Pd<sup>2+</sup> species that exchanged into the channel of HMS were reduced by methanol to form Pd particles during reaction. The formed Pd particles were fixed in the channel of HMS in uniform size because the channels of HMS limited the growth of Pd particles. Moreover, the peroxo-heteropoly compound PW<sub>2</sub> was synthesized on the surface of HMS by reacting the NH(PO<sub>3</sub>H<sub>2</sub>) group on the HMS surface with the [W<sub>2</sub>O<sub>3</sub>(O<sub>2</sub>)<sub>4</sub>(H<sub>2</sub>O)<sub>2</sub>]<sup>2-</sup> solution. Therefore, Pd particles and peroxo-heteropoly compound did not leach from the Pd-HMS-PrNH-PW<sub>2</sub> catalyst during the oxidation of propylene in methanol.

#### Comparison of solid catalyst Pd-HMS-PrNH-PW<sub>2</sub> with homogeneous catalyst Pd+THA-PW<sub>2</sub>

Ten autoclave reactors were charged with the same gases and reacted in methanol at the same conditions using one catalyst. One autoclave reactor was analyzed every hour to obtain the propylene conversion and the selectivity for PO at that time. The dependences of the propylene conversion and the selectivity for PO on the reaction time over 2.4 wt% Pd-HMS-PrNH-PW<sub>2</sub> catalyst and 2.4 wt% Pd+THA-PW<sub>2</sub> catalyst are shown in Fig. 5. The propylene conversion increased with reaction time and the selectivity for PO decreased with reaction time over both catalysts. Because homogeneous catalyst



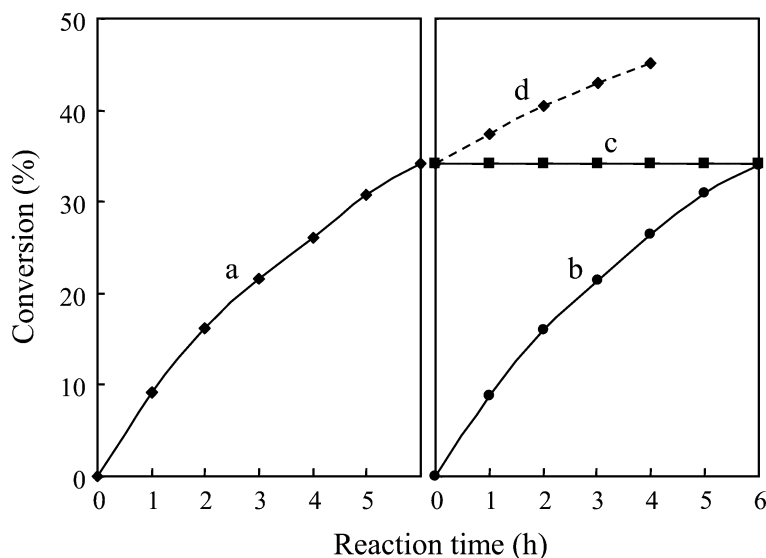


**Fig. 3** Stability of 2.4 wt% Pd-HMS-PrNH-PW<sub>2</sub> catalyst. (a) The catalyst used for the first run, (b) the catalyst used for the second run, (c) the reaction of the filtered solution after the first run without the solid catalyst, (d) the reaction of the filtered solution after the first run with the solid catalyst.

Pd+THA-PW<sub>2</sub> easily diffuses in the methanol medium, the peroxy intermediate HOCH<sub>2</sub>OOH or H<sub>2</sub>O<sub>2</sub> forms rapidly and regenerates peroxy O–O bonds of PW<sub>2</sub> with higher turnover frequency. Thus the homogeneous catalyst Pd+THA-PW<sub>2</sub>

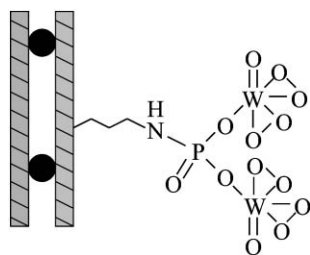


**Fig. 4** Model of the active catalyst Pd-HMS-PrNH-PW<sub>2</sub> after reaction.

showed higher conversion than that over the solid catalyst Pd-HMS-PrNH-PW<sub>2</sub>. On the other hand, because both the solid catalyst Pd-HMS-PrNH-PW<sub>2</sub> and the homogeneous catalyst Pd+THA-PW<sub>2</sub> possess the same active components and catalyze propylene oxidation *via* the same reaction mechanism, similar values of selectivity for PO were obtained over the two catalysts.

The plots of the yields of PO vs. the propylene conversions over the solid catalyst 2.4 wt% Pd-HMS-PrNH-PW<sub>2</sub> and the homogeneous catalyst 2.4 wt% Pd+THA-PW<sub>2</sub> for the propylene oxidation at 373 K for 6 h are shown in Fig. 6. Various PO yields and propylene conversions were obtained by changing the catalyst amount. With an increase of the catalyst amount, the propylene conversion increased but the selectivity for PO decreased because the side-reactions were promoted by the large amount of palladium. Both the heterogeneous catalyst and the homogeneous catalyst showed their highest PO yields

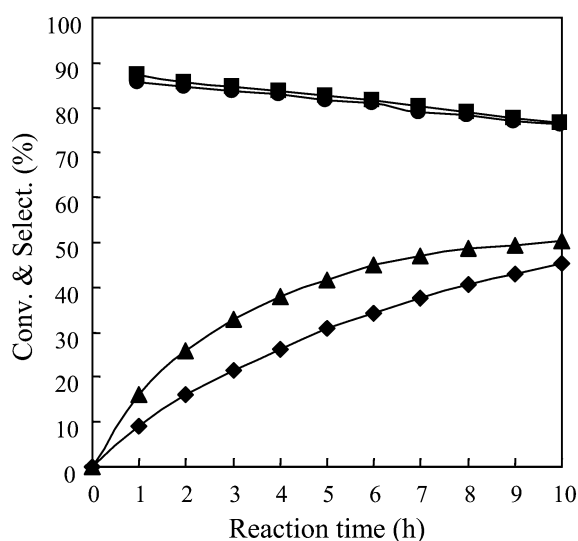


**Fig. 5** The dependences of the propylene conversion and the selectivity for PO on the reaction time for the propylene oxidation at 373 K. ◆: conversion over 2.4 wt% Pd-HMS-PrNH-PW<sub>2</sub>; ▲: conversion over 2.4 wt% Pd+THA-PW<sub>2</sub>; ■: selectivity for PO over 2.4 wt% Pd-HMS-PrNH-PW<sub>2</sub>; ●: selectivity for PO over 2.4 wt% Pd+THA-PW<sub>2</sub>. Catalyst amount: 0.2 g; autoclave: 50 ml; methanol: 10 ml; C<sub>3</sub>H<sub>6</sub>: 0.8 MPa; O<sub>2</sub>: 0.4 MPa; Ar: 0.8 MPa.

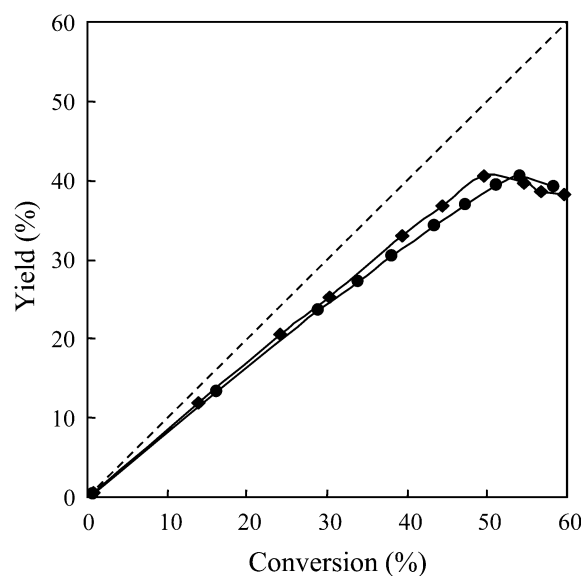


**Fig. 6** PO yields vs. propylene conversions over 2.4 wt% Pd-HMS-PrNH-PW<sub>2</sub> and 2.4 wt% Pd+THA-PW<sub>2</sub> in methanol for the propylene oxidation at 373 K for 6 h by molecular oxygen. ●: 2.4 wt% Pd-HMS-PrNH-PW<sub>2</sub>; ◆: 2.4 wt% Pd+THA-PW<sub>2</sub>. Autoclave: 50 ml; methanol: 10 ml; C<sub>3</sub>H<sub>6</sub>: 0.8 MPa; O<sub>2</sub>: 0.4 MPa; Ar: 0.8 MPa.

at about 42% at 373 K for 6 h. Therefore, a high yield of PO, which was similar to the highest PO yield obtained over the homogeneous catalyst Pd+THA-PW<sub>2</sub>, could be obtained over the solid catalyst Pd-HMS-PrNH-PW<sub>2</sub> by increasing catalyst amount.

## Acknowledgements

We gratefully acknowledge the financial support from the New Energy and Industrial Technology Development Organization.

## References

- (a) M. G. Clerici, G. Bellussi and U. Romano, *J. Catal.*, 1991, **129**, 159; (b) Z. Xi, N. Zhou, Y. Sun and K. Li, *Science*, 2001, **292**, 1139.
- (a) T. Hayashi, K. Tanaka and M. Haruta, *J. Catal.*, 1998, **178**, 566; (b) R. Meiers, U. Dingerdissen and W. F. Hölderich, *J. Catal.*, 1998, **176**, 376; (c) G. Jenzer, T. Mallat, M. Maciejewski, F. Eigenmann and A. Baiker, *Appl. Catal. A: Gen.*, 2001, **208**, 125; (d) E. J. Beckman, *Green Chem.*, 2003, **5**, 332.
- M. G. Clerici and P. Ingallina, *Catal. Today*, 1998, **41**, 351.
- (a) T. Iwahama, G. Hatta, S. Sakaguchi and Y. Ishii, *Chem. Commun.*, 2000, 163; (b) S. Murahashi, Y. Oda, T. Naota and N. Komiyama, *J. Chem. Soc., Chem. Commun.*, 1993, 139; (c) T. Mukaiyama, T. Takai, T. Yamada and O. Rhode, *Chem. Lett.*, 1990, 1661; (d) R. Ruiz, M. Triannidis, A. Aukauloo, Y. Journaux, I. Fernandez, J. R. Pedro, B. Cervera, I. Castro and M. C. Munoz, *Chem. Commun.*, 1997, 2283.
- (a) A. Palermo, A. Husain, M. S. Tikhov and R. M. Lambert, *J. Catal.*, 2002, **207**, 331; (b) F. W. Zemichael, A. Palermo, M. S. Tikhov and R. M. Lambert, *Catal. Lett.*, 2002, **80**, 93; (c) K. Murata and Y. Kiyozumi, *Chem. Commun.*, 2001, 1356; (d) Y. Liu, K. Murata, M. Inaba and N. Mimura, *Catal. Lett.*, 2003, **89**, 49.
- (a) T. Okuhara, N. Mizuno and M. Misono, *Adv. Catal.*, 1996, **41**, 113; (b) N. Mizuno and M. Misono, *Chem. Rev.*, 1998, **98**, 199; (c) C. L. Hill and C. M. Prosser-McCartha, *Coord. Chem. Rev.*, 1995, **143**, 407; (d) R. Neumann, *Prog. Inorg. Chem.*, 1998, **47**, 317.
- (a) Y. Ishii, K. Yamawaki, T. Yoshida, T. Ura and M. Ogawa, *J. Org. Chem.*, 1987, **52**, 1868; (b) Y. Ishii, K. Yamawaki, T. Ura, H. Yamada, T. Yoshida and M. Ogawa, *J. Org. Chem.*, 1988, **53**, 3587; (c) C. Venturello and M. Ricci, *J. Org. Chem.*, 1986, **51**, 1599; (d) C. Venturello and R. D'Aloiso, *J. Org. Chem.*, 1988, **53**, 1553.
- (a) C. Venturello, R. D'Aloiso, J. C. Bart and M. Ricci, *J. Mol. Catal.*, 1985, **32**, 107; (b) M. Hashimoto, K. Itoh, K. Y. Lee and M. Misono, *Top. Catal.*, 2001, **15**, 265; (c) D. C. Duncan, R. C. Chambers, E. Hecht and C. L. Hill, *J. Am. Chem. Soc.*, 1995, **117**, 681; (d) L. Salles, G. Aubry, R. Thouvenot, F. Robert, C. Doremieux-Morin, G. Chottard, H. Ledon, Y. Jeannin and J.-M. Bregeault, *Inorg. Chem.*, 1994, **33**, 871; (e) A. C. Dengel, W. P. Griffith and B. C. Parkin, *J. Chem. Soc., Dalton Trans.*, 1993, 2683; (f) C. Aubry, G. Chottard, N. Platzer, J.-M. Bregeault, R. Thouvenot, F. Chauveau, C. Huet and H. Ledon, *Inorg. Chem.*, 1991, **30**, 4409.
- Y. Liu, K. Murata and M. Inaba, *Chem. Commun.*, 2004, 582.
- W. F. Hoelderich and F. Kollmer, *Pure Appl. Chem.*, 2000, **72**, 1273.
- D. Hoegaerts, B. F. Sels, D. E. de Vos, F. Verpoort and P. A. Jacobs, *Catal. Today*, 2000, **60**, 209.
- (a) T. R. Pauly, Y. Liu, T. J. Pinnavaia, S. J. L. Billinge and T. P. Rieker, *J. Am. Chem. Soc.*, 1999, **121**, 8835; (b) W. Zhang, M. Froba, J. Wang, P. T. Tanev, J. Wong and T. J. Pinnavaia, *J. Am. Chem. Soc.*, 1996, **118**, 9164.
- (a) P. T. Tanev, M. Chibwe and T. J. Pinnavaia, *Nature*, 1994, **368**, 321; (b) Y. Liu, K. Suzuki, S. Hamakawa, T. Hayakawa, K. Murata, T. Ishii and M. Kumagai, *Catal. Lett.*, 2000, **66**, 205.
- (a) R. T. Yang, T. J. Pinnavaia, W. Li and W. Zhang, *J. Catal.*, 1997, **172**, 488; (b) I. Yuranov, P. Moeckli, E. Suvorova, P. Buffat, L. Kiwi-Minsker and A. Renken, *J. Mol. Catal. A: Chem.*, 2003, **192**, 239.
- (a) D. J. Macquarrie, *Green Chem.*, 1999, **1**, 195; (b) D. J. Macquarrie, *Chem. Commun.*, 1996, 1961; (c) D. J. Macquarrie and D. B. Jackson, *Chem. Commun.*, 1997, 1781.
- (a) S. Paul and J. H. Clark, *Green Chem.*, 2003, **5**, 635; (b) T. Pruss, D. J. Macquarrie and J. H. Clark, *J. Mol. Catal. A: Chem.*, 2004, **211**, 209.
- (a) Y.-H. Yeom, N. Ulagappan and H. Frei, *J. Phys. Chem. A*, 2002, **106**, 3350; (b) P. Jacob, B. Wehling, W. Hill and D. Klockow, *Appl. Spectrosc.*, 1997, **51**, 74; (c) S. Bauerl and G. K. Moortgat, *Chem. Phys. Lett.*, 1999, **309**, 43.
- (a) K. Murata, Y. Liu, N. Nomura and M. Inaba, *J. Catal.*, 2003, **220**, 513; (b) Y. Liu, K. Murata and M. Inaba, *Catal. Lett.*, 2004, **93**, 109.
- (a) M. Lin and A. Sen, *J. Am. Chem. Soc.*, 1992, **114**, 7307; (b) A. Pifer, T. Hogan, B. Snedeker, R. Simpson, M. Lin, C. Shen and A. Sen, *J. Am. Chem. Soc.*, 1999, **121**, 7485; (c) J. E. Remias and A. Sen, *J. Mol. Catal. A: Chem.*, 2002, **189**, 33.
- R. A. Sheldon, M. Wallau, I. W. C. E. Arends and U. Schuchardt, *Acc. Chem. Res.*, 1998, **31**, 485.



## Biocatalytic “green” synthesis of PEG-based aromatic polyesters: optimization of the substrate and reaction conditions†

Rajesh Kumar,<sup>a,b</sup> Rahul Tyagi,<sup>b,c</sup> Virinder S. Parmar,<sup>\*c</sup> Lynne A. Samuelson,<sup>d</sup> Jayant Kumar<sup>b</sup> and Arthur C. Watterson<sup>\*a</sup>

<sup>a</sup>Institute for Nano-Science Engineering and Technology, Department of Chemistry, University of Massachusetts Lowell, Lowell, MA-01854, USA. Fax: +1-978-458-9571; E-mail: Arthur\_Watterson@uml.edu

<sup>b</sup>Center for Advanced Materials, Departments of Chemistry and Physics, University of Massachusetts Lowell, MA-01854, USA

<sup>c</sup>Bioorganic Laboratory, Department of Chemistry, University of Delhi, Delhi-110 007, India

<sup>d</sup>US Army RDECOM, Natick Soldier Center, Kansas Street, Natick, MA 01760, USA

Received 20th May 2004, Accepted 30th July 2004

First published as an Advance Article on the web 29th September 2004

The condensation copolymerization of a variety of linker molecules with polyethylene glycols (PEGs) of varying molecular weights, catalyzed by lipases under solvent-less conditions is reported. Previously, we reported the lipase-catalyzed condensation polymerization of dimethyl 5-hydroxyisophthalate with polyethylene glycol. Herein we have used a number of linker molecules with hydroxyl, amino, carboxylic acid, alkoxy, amido and alkoxycarbonyl moieties. Also, studies were conducted on the effects of the reaction parameters on the polymerization reactions. The hydrophilic segment was also varied, *i.e.* polyethylene glycols with molecular weights 300, 600, 900 and 1500 have been used for copolymerization with dimethyl 5-hydroxyisophthalate. The molecular weight of the polyethylene glycol affected the polymer yield and molecular weight. In principle, the method developed is flexible so that it can be used to generate a wide array of functionalized amphiphilic copolymers. In the absence of biocatalytic transformation, such structural control is extremely difficult or currently impossible to obtain.

### Introduction

Over the past decade there has been an increased emphasis on the topic of “Green Chemistry and Green Chemical Processes”.<sup>1–5</sup> These efforts aim at the total elimination or at least the minimization of waste generation and the implementation of sustainable processes as discussed by Anastas and Warner.<sup>1</sup> Any attempt at meeting these goals must comprehensively address some of these principles in the design of a synthetic route, chemical analysis, or chemical process.<sup>1,3</sup> Utilization of non-toxic chemicals, environmentally benign solvents, and renewable materials are some of the key issues that merit important consideration in “green” synthetic strategies.

There has been growing interest in the use of enzymes to catalyze the condensation of diols and diacids believing, amongst other things, that such a protocol would be more efficient (being operable at lower temperatures) than the conventional acid-catalyzed procedures. More so, because many families of enzymes can be utilized for transformation of not only their natural substrates but a wide range of unnatural substrates to yield a variety of useful compounds.<sup>6–9</sup> The naturally occurring polymers are produced *by* enzymatic catalysis. The use of enzymes for the synthesis of useful polymers has been well-exploited,<sup>10–17</sup> most of which are otherwise very difficult to produce by conventional chemical catalysts as they require undesirable protection–deprotection steps. These features allow the generation of functional compounds for pharmaceutical and agro-chemical sectors employing non-toxic natural catalysts with “green appeal”; additional

advantages include catalyst recyclability and use in bulk reaction media avoiding organic solvents.<sup>18–22</sup>

Enzyme-catalyzed production of polyesters has been investigated in various laboratories. The use of enzymes in organic synthesis has several advantages also, such as superior catalytic power and high selectivity under mild conditions with regard to temperature, pressure and pH, promising substrate conversion efficiency, high diastereo-, enantio-, regio-, and chemoselectivities as well as regulating stereochemistry to provide development of new reactions and novel materials.<sup>10,11</sup>

Previous studies on biocatalytic polyesterifications using lipases have focused primarily on reactions between diols and activated diacids,<sup>23</sup> however diacid activation is expensive and limits the method’s potential technological impact. Although important progress has been made in lipase-catalyzed copolymerizations of acid and alcohol building blocks using non-activated free acids,<sup>24–28</sup> problems that must be overcome for practical use include long reaction times<sup>24,28</sup> and excessive quantities of lipase.<sup>24,26,28</sup>

Due to the considerable increase in interest in the area of enzyme-catalyzed organic reactions, we tried to carry out the synthesis of functionalized polymers using enzymes. We have earlier reported the chemical synthesis<sup>29</sup> of a series of unique polyethylene glycol-based amphiphilic copolymers. A more environmentally benign chemo-enzymatic synthesis of the same class of amphiphilic polymers has also been carried out by us.<sup>30–33</sup> The chemo-enzymatic methodology reported involves two steps, the first step is the enzyme-catalyzed copolymerization of dimethyl 5-hydroxyisophthalate with polyethylene glycol by using Novozyme-435 in bulk and the second step is the chemical modification of the polymers generated in the first step.<sup>30</sup> Herein we report rational, systematic investigations on

† Part of this work was presented at the 224<sup>th</sup> National Meeting of the American Chemical Society at Boston

the effects of the monomer structures on the lipase-catalyzed condensation reactions with a series of polyethylene glycols to develop a better understanding of this biocatalytic approach. We have also studied the influence of various reaction parameters on the copolymerization reactions under solvent-less conditions.

## Results and discussion

The three main steps in the preparation of copolymers that should be evaluated from a green chemistry perspective are the choice of the media of the reaction used for the synthesis, the choice of an environmentally benign reagent and the choice of non-toxic monomers or macromers for the synthesis of the polymers. Based on these considerations and our continued interest in the chemo-enzymatic synthesis of a unique class of amphiphilic copolymers, we have investigated the synthesis of amphiphilic copolymers in a single step starting from corresponding 5-alkoxyisophthalates and polyethylene glycols using an environmentally benign catalyst, and under solvent-less conditions to make the process "Green". A schematic representation of immobilized *Candida antarctica* lipase B (Novozyme 435)-catalyzed copolymerization of polyethylene glycol (**1**,  $M_n$  1500) and 5-alkoxyisophthalates **3–7** is shown in Scheme 1.

The monomers, 5-alkoxyisophthalates **3–7**, were prepared by the alkylation of dimethyl 5-hydroxyisophthalate (**2**) with corresponding alkyl bromides.<sup>29</sup> The 5-alkoxyisophthalates **3,6** and **7** were synthesized for the first time and characterized under their IR and <sup>1</sup>H NMR spectral data (cf. Experimental).

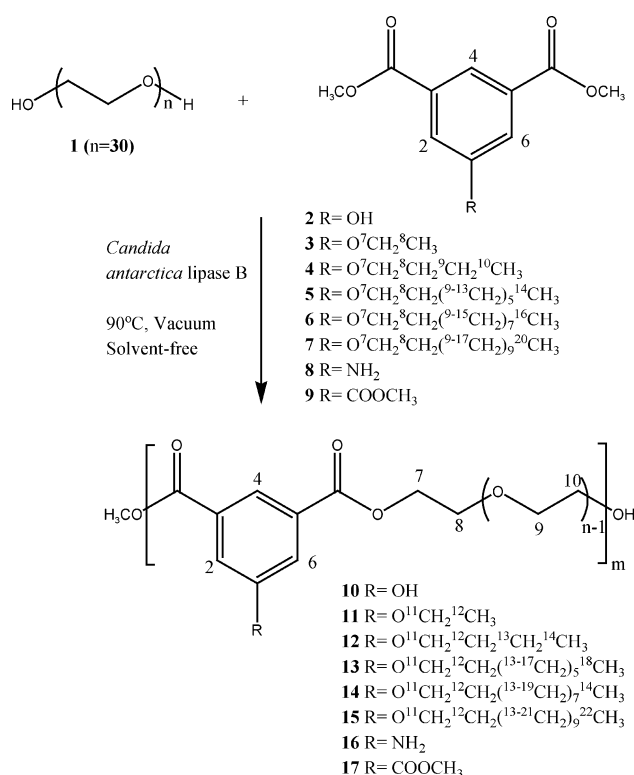
Novozyme-435-catalyzed condensation polymerization reactions of 5-alkoxyisophthalates **3–7** with polyethylene glycol (**1**,  $M_n$  1500) were performed at 90 °C in bulk (solvent-free conditions) under vacuum. No product formation in the reaction of PEG (**1**) with dimethyl 5-octanoyisophthalate (**5**), dimethyl 5-decanoyisophthalate (**6**) and dimethyl 5-dodecanoyisophthalate (**7**) having longer alkyl chains (with 8, 10 and

12 carbon atoms, respectively), was observed. Further during the reaction of **1** with dimethyl 5-ethoxyisophthalate (**3**) and dimethyl 5-butanoyisophthalate (**4**) having shorter alkyl chains (with 2 and 4 carbon atoms, respectively), only dimers and trimers were obtained. Moreover the percentage conversions with **3** and **4** to corresponding copolymers **11** and **12** were 38 and 17%, respectively (Fig. 1, determined from their <sup>1</sup>H NMR spectral data by comparing the ratio of the signal intensity at  $\delta$  4.50 due to ester formation for C–7H to the one at  $\delta$  7.75 for C–2H and C–6H) as compared to the reaction of PEG 1500 with dimethyl 5-hydroxyisophthalate (**2**), where high molecular weight copolymer **10** was obtained in almost quantitative yields and the reaction was highly chemoselective with no esterification observed involving the phenolic hydroxyl group. The extent of chemoselection was determined by quantitative derivatization of copolymer **10** by attaching the decane chain to the phenolic hydroxyl group (seen from the <sup>1</sup>H NMR spectrum).<sup>30</sup> These observations infer that with an increase in the size of the chain length attached to the phenolic hydroxyl group, both the % conversions and degrees of polymerization to products decrease.

This may be due to the increase in the hydrophobicity of the monomer with the increase in the size of the chain length, thus making it difficult for the hydroxyl of serine residue to form an activated complex with the monomers which results in a slow or no reaction depending upon the size of the alkyl chain (Fig. 2a). We have proposed a cartoon model pointing the alkoxy chain towards the active site based on the fact that the lipase active site is hydrophobic in nature and thus the hydrophobic part will enter the active site first. In the case of the diester **2**, which lacks any alkyl side chain, the free phenolic group is hydrophilic as compared to methoxycarbonyl units and thus these enter the enzyme cavity first making it easier for the hydroxyl of serine residue to form an activated complex as it is in close proximity to the methoxycarbonyl moieties of **2**, thereby causing high percentage conversion in this case. Consequently polymers of high molecular weights are formed (Fig. 2b).

To further understand the reaction mechanism, condensation polymerization reactions of PEG 1500 (**1**) with monomers having other functionalities at the C-5 position in dimethyl isophthalate, i.e. dimethyl 5-aminoisophthalate (**8**) and dimethyl 5-methoxycarbonylisophthalate (**9**) having an amino and ester functionality, respectively, were performed. The condensation polymerization reaction of **1** with **8** was highly chemoselective as no amide formation was observed and resulted in the formation of the amino functionalized polyester **16** with high molecular weight ( $M_n$  24000 and 80% conversion), however no reaction was observed with **9**, further suggesting the ease of activated complex formation in the case of **8** due to the right substrate orientation in the enzyme pocket.

In the lipase-catalyzed polymerizations of  $\alpha,\omega$ -alkylene diacids and diols, the methylene chain length strongly affected



Scheme 1 *Candida antarctica* lipase B-catalyzed polymerization.

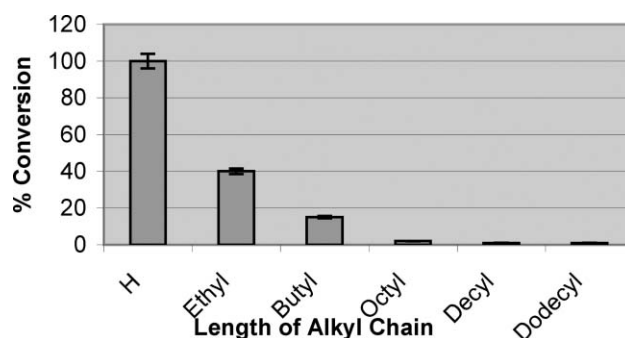
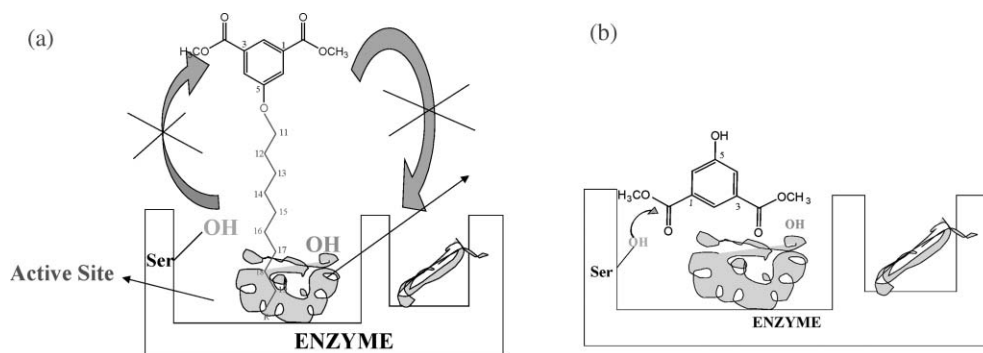


Fig. 1 Effect of alkyl carbon chain on the polymerization reaction.





**Fig. 2** Proposed cartoon model of (a) interaction of long alkyl chain containing monomers with enzyme cavity, (b) interaction of monomers without alkyl chains with the enzyme cavity.

the polymerization behavior. In the case of the dehydration polycondensation of dicarboxylic acids and glycol catalyzed by lipase PC in water, the polymerization behavior strongly depended on the hydrophobicity of the monomers.<sup>20</sup> We have carried out the reaction of dimethyl 5-hydroxyisophthalate with PEG of varying molecular weights (300, 600, 900 and 1500). It was observed that with an increase in the molecular weight of the macromer (PEG), the isolated yield and number average molecular weights of the copolymer increased. In the case of PEG 300, there was very small conversion to copolymer and the reaction produced only dimers and trimers. The low copolymer yield and number average molecular weight obtained in the case of low molecular weight polyethylene glycol units are perhaps due to the difficult solubilization of the diester monomer by PEGs of low molecular weights as these reactions are being done in solvent-free conditions. When we use one equivalent of high molecular weight PEGs, the amount of PEG used will be more than the case when one equivalent of low molecular weight PEG is used, *e.g.* if one uses one mmol of PEG 300 and 1 mmol of PEG 1500, then the corresponding amounts of PEG in terms of weights will be 300 mg and 1.5 g for the same amount of the monomer **2**. This implies that in the case of PEG 1500, the amount of the PEG used is 5 times more as compared to PEG 300. Therefore the solubilization of isophthalate-based monomer will be much better in PEG 1500 as compared to that in PEG 300, simply because it is present in larger amounts. We have repeated these experiments a few times without problem, and get consistent and reproducible results.

### Effects of reaction conditions

The effects of reaction time and temperature have been investigated in the copolymerization of PEG-1500 (**1**) and dimethyl 5-hydroxyisophthalate (**2**) using Novozyme-435 as catalyst. We have carried out the polymerization for different time periods as well as at different temperatures in order to find the optimum conditions with PEG-1500 (**1**) and dimethyl 5-hydroxyisophthalate (**2**). In a typical experiment, we have taken **1** and **2** in equimolar proportions along with the enzyme (10% w.r.t. the monomers) and allowed the reaction to proceed at different time intervals, *viz.* 2, 4, 12, 20 and 48 hours at 90 °C and under bulk conditions. Fig. 3 shows plots of the copolymer yield, and  $M_n$  versus reaction time. The copolymer yield and  $M_n$  increased rapidly to 22% and 37000 in 12 h. Further increase in copolymer yield with increased reaction time occurred gradually. Hence, by 48 h, the copolymer yield and  $M_n$  were 93% and 23000, respectively.

The number average molecular weight increased for reaction times up to 12 h and then decreased by 37% from 12 to 48 h. By 48 h, the conversion of monomers was quantitative. The molecular weight distribution increased up to 12 h and then

decreased with reaction time ( $M_w/M_n = 2.7$  and 1.8 for 12 and 48 h, respectively). Such decreases in molecular weight and molecular weight distributions at extended reaction times are in contrary with thermal depolymerization reactions starting from polymer ends. This further indicates that the enzyme starts cleaving the big chains and shows selectivity towards the formation of polymers of optimum lengths.

As regards to the effect of temperature on the rate of polymerization, we carried out the same polymerization reaction (of **1** and **2**) at different temperatures, *viz.* 40, 60, 70, 80 and 90 °C and allowed the reaction to proceed for 48 hours. After the usual work up, the product was isolated and the molecular weights determined. It was found that the molecular weight was independent of the temperature in the range 40–70 °C however after that it decreases and the polymer obtained had a number average molecular weight in the range of 12000–23000 Da. Interestingly, the copolymer isolated yield increased with the increase in temperature and was quantitative at 90 °C (Table 1).

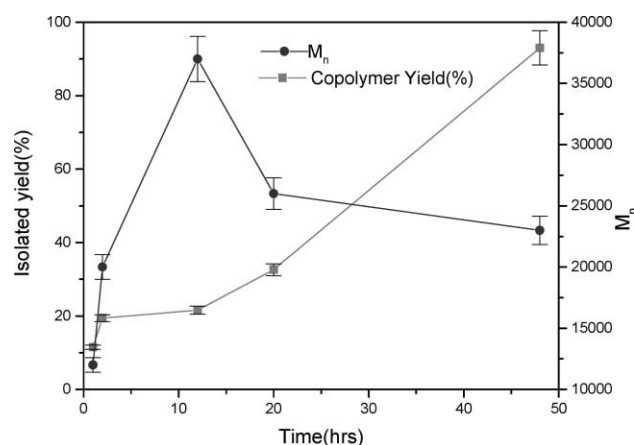


**Fig. 3** Time versus yield and molecular weight of the polymer in the copolymerization of PEG-1500 (**1**) and dimethyl 5-hydroxyisophthalate (**2**) using lipase (Novozyme-435) as catalyst in bulk.

**Table 1** Effect of temperature on isolated yield and number average molecular weight ( $M_n$ ) during the copolymerization of PEG 1500 (**1**) and dimethyl 5-hydroxy-isophthalate (**2**)

Entry	Temperature/°C	Isolated yield (%)	Molecular weight ( $M_n$ )
1.	40	37.4	12000
2.	60	43.7	13000
3.	70	46.7	12000
4.	80	65.5	15000
5.	90	93.5	23000



## Experimental

### Materials and methods

Novozyme-435, an immobilized enzyme, was a gift from Novozymes Inc., Denmark. All other chemicals and solvents were of analytical grade and were used as received unless otherwise noted.

### Characterization

Gel permeation chromatography (GPC) was used to determine the molecular weights and molecular weights distributions,  $M_w/M_n$  of polymer samples using polystyrene standards in tetrahydrofuran.  $^1\text{H}$  and  $^{13}\text{C}$  NMR spectra were recorded on a Bruker Instrument Inc. 250 MHz ARX spectrometer equipped with Silicone Graphics station. Infrared spectra were obtained on a Perkin-Elmer 1760 FTIR spectrometer, liquid films on a NaCl pellet and potassium bromide pellet were used in sample preparation.

### Synthesis of dimethyl 5-ethoxyisophthalate (3)

To a solution of dimethyl 5-hydroxyisophthalate (**2**, 5.0 g, 23.8 mmol) in dry acetone (50 ml) was added fused potassium carbonate (6.5 g, 47.2 mmol) and the contents stirred for 1 h at 50 °C under nitrogen atmosphere. To this mixture, a solution of ethyl bromide (23.8 mmol) in acetone (25 ml) was added and the mixture was allowed to stir for 6 h and the progress of the reaction was monitored by thin layer chromatography using a solvent system of ethyl acetate and hexane. After completion, the solvent was removed under reduced pressure on a vacuum rotavapor, followed by the addition of water. The product was extracted with  $\text{CH}_2\text{Cl}_2$ . The organic layer was collected and dried over anhydrous magnesium sulfate. The solvent was then removed to give a white solid powder, which recrystallized from methanol to give a white crystalline solid.

$^1\text{H}$ -NMR ( $\text{CDCl}_3$ ):  $\delta$  1.60 (3H, C-8H), 3.95 (6H, 2  $\times$   $\text{OCH}_3$ ), 4.13 (2H, C-7H), 7.76 (2H, C-2H and C-6H) and 8.20 (1H, C-4H).

IR ( $\text{cm}^{-1}$ ): 2928, 2857, 1729 (COO), 1595, 1456, 1435, 1340, 1314, 1241, 1118, 1104, 1049, 1006, 759.

### Dimethyl 5-decanoxyisophthalate (6)

This compound was also synthesized as a white solid as described above.

$^1\text{H}$ -NMR ( $\text{CDCl}_3$ ):  $\delta$  0.89 (3H, C-16H), 1.20–1.38 (14H, C-9H to C-15H), 1.80 (2H, C-8H), 3.95 (6H, 2  $\times$   $\text{OCH}_3$ ), 4.13 (2H, C-7H), 7.76 (2H, C-2H and C-6H) and 8.20 (1H, C-4H).

IR ( $\text{cm}^{-1}$ ): 2956, 2857, 1728 (COO), 1595, 1457, 1435, 1340, 1242, 1119, 1036, 758.

### Dimethyl 5-dodecanoxyisophthalate (7)

This compound was also synthesized as a white solid as described above.

$^1\text{H}$ -NMR ( $\text{CDCl}_3$ ):  $\delta$  0.87 (3H, C-18H), 1.15–1.140 (18H, C-9H to C-17H), 1.85 (2H, C-8H), 3.90 (6H, 2  $\times$   $\text{OCH}_3$ ), 4.10 (2H, C-7H), 7.70 (2H, C-2H and C-6H) and 8.25 (1H, C-4H).

IR ( $\text{cm}^{-1}$ ): 2868, 2859, 1722 (COO), 1592, 1463, 1429, 1333, 1241, 1113, 1039, 768.

### General method of polymerization

Equimolar amounts of the monomers **2–9** and polyethylene glycol ( $M_n$  300, 600, 900, or 1500) were placed in a round bottom flask. To this mixture was added the enzyme (10% by weight w.r.t. monomers) and the reaction flask was then placed in a constant temperature oil bath under vacuum. The reaction was allowed to proceed for a predetermined time period. Adding chloroform and filtering off the enzyme under vacuum

quenched the reaction. The organic solvent was then evaporated under vacuum to obtain the crude polymeric samples **10–17**, which were analyzed by NMR (Bruker 250 MHz). The molecular weights of the crude polymer products **10–17** were determined by GPC, using polystyrene standard samples. The polymers **10** and **16** were purified by dialysis (using membrane  $M_n$  CO 6000). After the completion of dialysis, the product polymers **10** and **16** were freeze-dried. Out of the prepared polymers **10–17**, the polymers **11** and **16** have been synthesized for the first time and characterized from their IR and  $^1\text{H}$  NMR spectrum.

### Poly[(poly(oxyethylene-1500)-oxy-5-ethoxyisophthaloyl) 11

$^1\text{H}$ -NMR ( $\text{CDCl}_3$ ):  $\delta$  1.65 (3H, C-12H), 3.6–3.79 (bs, C-9H & C-10H), 3.86 (t, 2H, C-8H), 3.96 (s,  $\text{COOCH}_3$  end group), 4.15 (2H, C-11H), 4.50 (t, 2H, C-7H), 7.75 (s, 2H, C-2H and C-6H) and 8.24 (s, 1H, C-4H).

IR ( $\text{cm}^{-1}$ ): 3495 (alc OH), 2872, 1724(COO), 1609, 1455, 1355, 1304, 1235, 1127, 937, 868, 732, 519.

### Poly[(poly(oxyethylene-1500)-oxy-5-aminoisophthaloyl) 16

$^1\text{H}$ -NMR ( $\text{CDCl}_3$ ):  $\delta$  3.6–3.79 (bs, methylene protons of PEG main chain), 3.86 (t, 2H, C-8H), 3.96 (s,  $\text{COOCH}_3$  end group), 4.50 (t, 2H, C-7H), 7.75 (s, 2H, C-2H and C-6H) and 8.24 (s, 1H, C-4H).

IR ( $\text{cm}^{-1}$ ): 3450 (alc.OH), 3360 (NH), 2872, 1720 (COO), 1637, 1605, 1455, 1348, 1244, 1104, 949, 844, 760.

## Conclusion

By engineering of monomer structures, it was established that *Candida antarctica* lipase efficiently catalyzed the polycondensation of dimethyl 5-hydroxy- and 5-amino- isophthalate and polyethylene glycols in a solvent-free system. It was established that the absence of a carbon alkyl chain at the C-5 position in dimethyl isophthalate is critical for the polymerization reaction, and at the same time the presence of polar groups such as hydroxyl or amino make reactions more efficient. The molecular weight of the polyethylene glycol unit strongly affected the copolymerization behavior. The polymer molecular weight increased under reduced pressure and at higher temperatures. The present reaction system affords a variety of biodegradable functionalized polymers *via* non-toxic enzyme catalysis under mild reaction conditions without the use of organic solvents. Therefore, it is environmentally benign and provides an example of "Green Polymer Chemistry".

## References

- P. T. Anastas and J. C. Warner, *Green Chemistry: Theory, and Practice*, Oxford University Press, Inc., New York, 1998.
- M. Poliakoff and P. T. Anastas, *Nature*, 2001, **413**, 257.
- A. S. Matlack, *Introduction to Green Chemistry*, Marcel Dekker, Inc., New York, 2001.
- J. M. DeSimone, *Science*, 2002, **297**, 799.
- R. S. Varma, *Pure Appl. Chem.*, 2001, **73**, 193.
- J. B. Jones, *Tetrahedron*, 1986, **42**, 3351.
- A. M. Klivanov, *Acc. Chem. Res.*, 1990, **23**, 114.
- E. Santaniello, P. Ferraboschi, P. Grisenti and A. Manzocchi, *Chem. Rev.*, 1992, **92**, 1071.
- C.-H. Wong and G. M. Whitesides, *Enzymes in Synthetic Organic Chemistry*, Pergamon, Oxford, 1994.
- A. K. Chaudhary, J. Lopez, E. J. Beckman and A. J. Russell, *Biotechnol. Prog.*, 1997, **13**, 318.
- B. J. Kline, E. J. Beckman and A. J. Russell, *J. Am. Chem. Soc.*, 1998, **120**, 9475.
- H. Uyama, S. Yaguchi and S. Kobayashi, *J. Polym. Sci., Polym. Chem. Ed.*, 1999, **37**, 2737.
- S. Kobayashi, S. Shoda and H. Uyama, *The Polymeric Materials*

- Encyclopedia*, ed. JC Salamone, CRC Press, Boca Raton, FL, 1996, p. 2102.
- 14 S. Kobayashi, S. Shoda and H. Uyama, *Catalysis in Precision Polymerization*, ed. S. Kobayashi, John Wiley & Sons, Chichester, 1997, ch. 8.
  - 15 H. Uyama, S. Yaguchi and S. Kobayashi, *Polymer*, 1999, **31**, 383.
  - 16 H. Uyama, K. Inada and S. Kobayashi, *Chem. Lett.*, 1998, p. 1285.
  - 17 R. A. Gross, D. L. Kaplan and G. Swift, *Enzymes in Polymer Synthesis*, *ACS Symp. Ser.*, 1998, 684.
  - 18 R. A. Gross, B. Kalra and A. Kumar, *Appl. Microbiol. Biotechnol.*, 2001, **55**, 655.
  - 19 R. A. Gross, A. Kumar and B. Kalra, *Chem. Rev.*, 2001, **101**, 2097.
  - 20 S. Kobayashi, H. Uyama and S. Kimura, *Chem. Rev.*, 2001, **101**, 3793.
  - 21 R. Kumar, F. Bruno, V. S. Parmar, J. Kumar, A. C. Watterson, K. G. Chittibabu and L. A. Samuelson, *Chem. Commun.*, 2004, 862.
  - 22 S. Soda, H. Uyama and S. Kobayashi, *Proc. Acad. Jpn.*, 1999, **75B**, 201.
  - 23 A. L. Magolin, J. Y. Creene and A. M. Klivanov, *Tetrahedron Lett.*, 1987, **28**, 1607.
  - 24 Y.-Y. Linko, Z.-L. Wang and J. Seppala, *J. Biotechnol.*, 1995, **40**, 133.
  - 25 Y.-Y. Linko, Z.-L. Wang and J. Seppala, *Enzymol. Microb. Technol.*, 1995, **17**, 506.
  - 26 A. Taylor and F. Binns, International patent WO 94/12652, 1994.
  - 27 H. Uyama, K. Inada and S. Kobayashi, *Polym. J.*, 2000, **32**, 440.
  - 28 F. Binns, P. Harffey, S. M. Roberts and A. Taylor, *J. Polym. Sci., Part A: Polym., Chem.*, 1998, **36**, 2069.
  - 29 K. Danprasert, R. Kumar, M. H. Cheng, P. Gupta, N. A. Shakil, A. K. Prasad, V. S. Parmar, J. Kumar, L. A. Samuelson and A. C. Watterson, *Eur. Polym. J.*, 2003, **39**, 1983.
  - 30 R. Kumar, N. A. Shakil, M. H. Chen, V. S. Parmar, L. A. Samuelson, J. Kumar and A. C. Watterson, *J. Macromol. Sci.-Pure Appl. Chem.*, 2002, **A39**, 1137.
  - 31 R. Kumar, R. Tyagi, V. S. Parmar, L. A. Samuelson, J. Kumar and A. C. Watterson, *Mol. Diversity*, 2003, **6**, 287.
  - 32 R. Kumar, R. Tyagi, V. S. Parmar, L. A. Samuelson, J. Kumar and A. C. Watterson, *J. Macromol. Sci., Pure Appl. Chem.*, 2003, **A40**, 1283.
  - 33 R. Kumar, M. H. Chen, V. S. Parmar, L. A. Samuelson, J. Kumar, R. Nicolosi, S. Yoganathan and A. C. Watterson, *J. Am. Chem. Soc.*, 2004, **126**, 10640.



# Continuous catalytic asymmetric hydrogenation in supercritical CO<sub>2</sub>

Phil Stephenson,<sup>a</sup> Peter Licence,<sup>\*a</sup> Stephen K. Ross<sup>b</sup> and Martyn Poliakoff<sup>\*a</sup>

<sup>a</sup>School of Chemistry, The University of Nottingham, University Park, Nottingham, UK NG7 2RD. E-mail: martyn.poliakoff@nottingham.ac.uk; Fax: +44 115 951 3058; Tel: +44 115 951 3386

<sup>b</sup>Thomas Swan & Co., Ltd., Crookhall, Consett, UK DH8 7ND.

E-mail: sross@thomas-swan.co.uk; Fax: +44 1207 590467; Tel: +44 1207 505131

Received 3rd August 2004, Accepted 4th August 2004

First published as an Advance Article on the web 24th September 2004

Continuous hydrogenation in supercritical fluids has been shown to be a technically viable alternative to traditional batch-wise methodologies. Clearly, the next stage of development of this technology is the application of immobilised enantioselective catalysis in the preparation of optically active products. Enantioselective hydrogenation has been successfully carried out in supercritical carbon dioxide using batch-type reactors but has yet to be efficiently carried out continuously. Here we examine an established method of catalyst immobilisation and demonstrate its suitability for application in continuous reactors using supercritical carbon dioxide as solvent.

## Introduction

Increased levels of environmental awareness now dictate that the application of traditional solvents and VOCs must be reduced to an absolute minimum. Supercritical fluids (SCFs) are becoming increasingly accepted as an alternative reaction medium in which a wide variety of synthetic reactions may be performed.<sup>1,2</sup> In particular supercritical carbon dioxide (scCO<sub>2</sub>) has been shown to be an excellent replacement solvent in the hydrogenation of organic compounds including oleochemical<sup>3</sup> and fine chemical precursors.<sup>4</sup> The enhanced solubility of hydrogen gas (H<sub>2</sub>) in SCFs and indeed expanded organic solutions<sup>5</sup> affords a greater degree of process control in terms of both selectivity and overall efficiency. The application of a heterogeneous catalyst in combination with SCFs allows reactions to be carried out under a continuous flow regime, which is often favoured by industry.<sup>6</sup> Indeed, flow reactors of this type, employing scCO<sub>2</sub> as the reaction solvent have recently been scaled up to commercial scale by Thomas Swan & Co. Ltd.<sup>3,7</sup>

Increasing demand for enantiopure materials has led to significant advances in the field of asymmetric hydrogenation. This field has been extensively reviewed, most recently by the publication of a thematic edition of the journal, *Advanced Synthesis and Catalysis*, that includes the Nobel Prize lectures of both Knowles<sup>8</sup> and Noyori.<sup>9</sup> However, there have been relatively few reported examples of asymmetric transformations of any type in SCFs. Jessop and Noyori report exceptional enantioselectivities, in excess of 95% ee, in both the addition of alkyl-zinc derivatives to aldehydes<sup>10</sup> and the cyclopropanation of prochiral olefins,<sup>11</sup> both of which were carried out in supercritical CHF<sub>3</sub>. Leitner and co-workers working with scCO<sub>2</sub> report the successful application of homogeneous catalysis, often in association with ionic liquids, in a variety of reaction systems including hydrogenation<sup>12</sup> and hydroformylation.<sup>13</sup>

All these examples were carried out under batch conditions. However, scale-up of SCF processes usually demands that reactions be carried out continuously. To date, there are very few examples of what appear to be continuous enantioselective reaction in SCFs. Indeed, Leitner and co-workers, in a recent paper give details of the continuous hydrovinylolation of styrene

derivatives over a Ni catalyst immobilised in an ionic liquid,<sup>1,14</sup> encouraging ee values up to 92% and conversions in excess of 95% are reported. Baiker *et al.* have employed a chinchonidine-modified Pt in the continuous hydrogenation of ethyl pyruvate in both scCO<sub>2</sub> and supercritical propane (scPropane),<sup>15,16</sup> with ee values as high as 75% (with conversion ≤ 80%). However, the authors drew attention to a marked increase in the rate of reaction in scPropane compared to scCO<sub>2</sub>, possibly because of decomposition of CO<sub>2</sub> to CO over the Pt catalyst.

The reliable immobilisation of a homogeneous catalyst to a suitable support is a very tricky task. A number of criteria have to be satisfied before any such immobilisation may be considered successful. For instance, the support must be robust enough to withstand the particular reaction conditions, but it must be flexible enough to allow the reactants access to the catalytic centre. Similarly, the interaction between the support and the catalytic centre must be strong enough to hold the catalyst in place but not so strong as to disrupt the arrangement of the ligand system. This is a very delicate “balancing act” because, if the interaction is too strong, catalysis is suppressed. On the other hand, if the interaction was too weak, the metal centre could become dislodged from the support. In batch processes this is not a fatal problem because the catalyst and support can re-associate when the reaction is complete. In a continuous regime, however, constant attachment between the support and catalyst is essential. If the association is broken even for an instant, the “free” catalyst will be swept away in the reactant flow with consequent leaching of the catalyst and product contamination. In addition, any immobilisation system should be versatile so that a range of ligands can easily be screened for a specific reaction. Finally, the smaller the reactor, the more economically viable the SCF reaction will be; this means that the reaction needs to be carried out at the highest possible temperature to maximise the productivity of the reactor but, thereby, placing additional demands on the performance of the catalyst.

## Experimental

Recently we described custom-built flow reactor systems that are capable of producing hydrogenated products on a small to

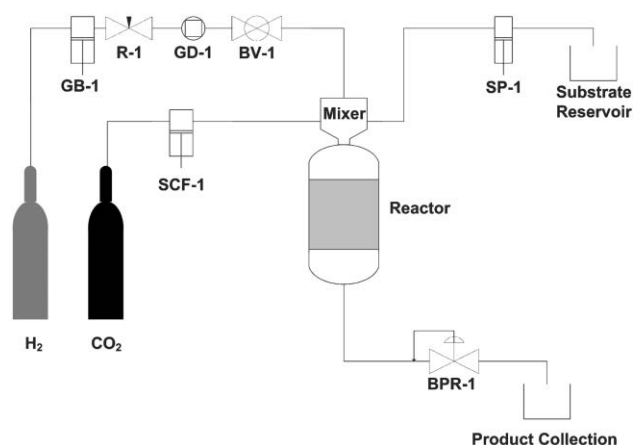


**Fig. 1** Schematic diagram of the SCF "midi" reaction system. The SCF is pressurised and delivered by a Peltier cooled pump running in constant flow mode, SCF-1 [Jasco PU-1580-CO<sub>2</sub>]. Hydrogen gas is pressurised to a constant pressure using a gas booster, GB-1 [NWA CU-105] and regulator, R-1, before being dosed quantitatively into the reactor by a switchable gas dosage unit, GD-1 [Rheodyne 7000L], the supply is isolable using the ball valve (BV-1). Organic substrates are delivered at a constant rate *via* a standard HPLC pump, SP-1 [Jasco PU-980]. All feed streams are mixed in a heated, static mixer before being passed through a packed catalyst bed (0.5 cm<sup>-3</sup> in volume). Products are collected after a single stage depressurisation of the fluid mixture by an electronic backpressure regulator, BPR-1 [Jasco BP-1580-81], depressurised gases are vented at this point.<sup>†</sup>

medium scale.<sup>4</sup> This system is well suited to reactions carried out over commercially available catalysts; however, the volume of the catalyst bed in such reactors renders it unsuitable for application with small amounts of expensive, experimental catalysts. Herein we report a modified reactor system that contains a significantly smaller reactor bed that is entirely composed of commercially available components, Fig. 1.

The catalyst employed here was prepared by supporting a traditional enantioselective hydrogenation catalyst [Rh(S,S-Skewphos)(nbd)]<sup>+</sup>(BF<sub>4</sub>)<sup>-</sup> onto an inorganic support with a phosphotungstic acid (PTA) linker,<sup>17,18</sup> see Fig. 2.

This catalytic "composite" system has been shown to have a high activity and modest ee when employed in more traditional solvent systems.<sup>19</sup> Control experiments, conducted in EtOH with our catalyst ([Rh(S,S-Skewphos)(nbd)]<sup>+</sup>(BF<sub>4</sub>)<sup>-</sup>-PTA-alumina) yielded an ee of around 65–70% in the hydrogenation of dimethyl itaconate, DMIT (1), which is often used as a model reaction for the asymmetric reduction of prochiral starting materials (Scheme 1).

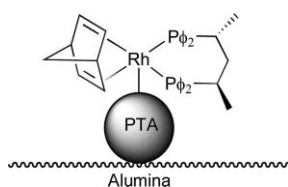
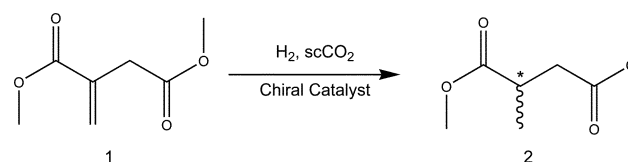


**Fig. 2** Generalised structure of the catalytically active composite system. PTA = phosphotungstic acid [H<sub>3</sub>O<sub>40</sub>PW<sub>12</sub>], φ = C<sub>6</sub>H<sub>5</sub>.<sup>18</sup>

<sup>†</sup> **Safety note:** The experiments described in this paper involve the use of relatively high pressures and require equipment with the appropriate pressure rating. It is the responsibility of individual researchers to verify that their particular apparatus meets the necessary safety requirements. The individual components that we describe work well, but they are not necessarily the only equipment of this type available nor the most suitable for the purpose.



**Scheme 1** Model reaction, hydrogenation of dimethyl itaconate, DMIT (1), to dimethyl 2-methylsuccinate (2).

## Results

A series of experiments was conducted exploring the effect of both temperature and pressure on the hydrogenation of DMIT in scCO<sub>2</sub> to establish whether the reaction could indeed be carried out enantioselectively at the elevated temperatures typically employed for SCF reaction chemistry. Selected results are collected in Table 1.

**Table 1** The effect of temperature and pressure on the ee and conversion of DMIT<sup>a</sup> in scCO<sub>2</sub> using the immobilised chiral catalyst shown in Fig. 2

Entry	Temp./°C	Press./MPa	Conv. (%) <sup>b</sup>	ee (%) <sup>c</sup>
1	40	10	10	5
2	60	6	50	27
3	60	8	65	40
4	60	10	66	63
5	60	12	46	50
6	80	10	63	42
7	100	10	61	32

<sup>a</sup> CO<sub>2</sub> flow rate (liquefied at -10 °C) 1.0 mL min<sup>-1</sup>, substrate flow rate 0.25 mL min<sup>-1</sup> (2.5 M solution in IPA), hydrogen to substrate ratio 4 : 1 dosed at 5 MPa overpressure. <sup>b</sup> Starting material conversion was determined by GC: column RTX-5, 30 m, 0.25 mm od, 0.25 μm df; 40 °C (2 min), 10 °C min<sup>-1</sup>, 200 °C (5 min). <sup>c</sup> ee values were determined by chiral HPLC: column Daicel OD-H, eluting with a pre-prepared solution of IPA (8%) in hexane, isothermal at 25 °C, 1 mL min<sup>-1</sup>. The retention time of the major (R) enantiomer, Rt<sub>R</sub> = 5.9 min, was comparable to that of a commercially available standard; the retention time of the minor (S) enantiomer was Rt<sub>S</sub> = 8.8 min.

It is clear from these results that: (a) enantioselective hydrogenation is indeed possible at temperatures up to 100 °C, see Fig. 3. (b) The best ee is similar to that observed with this catalyst in conventional solvents; therefore scCO<sub>2</sub> is not impairing the selectivity of the catalyst. (c) Most interestingly, high ee values are not observed at lower reaction temperatures; indeed, significant enantioselectivity is only observed at temperatures in excess of 40 °C. Possibly, this change in reactivity may coincide with a change in the phase composition of the reactant mixture.

Above 100 °C there is an unsurprising loss of enantioselectivity which is compounded by more surprising losses of both

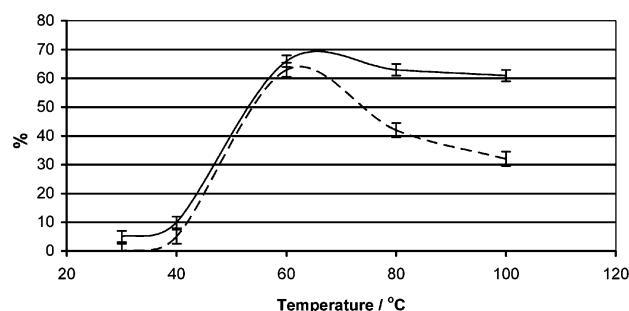


**Fig. 3** Plot showing the effect of increasing temperature on both the conversion (solid line) and ee (dashed line) in the hydrogenation of DMIT over [Rh(S,S-Skewphos)(nbd)]<sup>+</sup>(BF<sub>4</sub>)<sup>-</sup>-PTA-alumina.



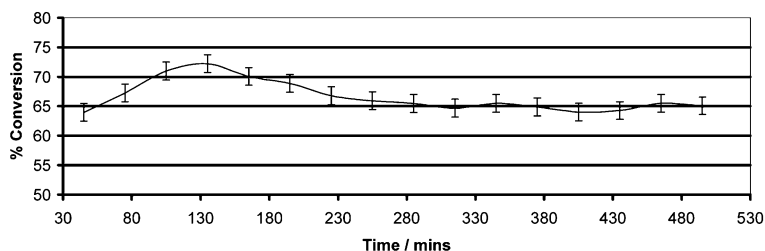


Fig. 4 Variation in conversion of DMIT over a period of 8 hours, demonstrating the essentially constant performance of the catalyst.

regio- and chemo-selectivity. The conversion of DMIT was found to be relatively unaffected by changes in the total system pressure. However a maximum in enantioselectivity was observed at pressures *ca.* 10 MPa; the reason for this is not yet clear, but a similar pressure maximum in reaction selectivity was noted by Rayner *et al.* in the diastereoselective sulfoxidation of cysteine derivatives.<sup>20</sup> Further studies on both the solubility and indeed the phase behaviour of the DMIT-IPA system are in progress to see whether this might be the origin of this effect.

A catalyst stability study was carried out at the "optimum" reaction conditions (see Table 1, entry 4) see Fig. 4. The catalyst was found to be stable under these reaction conditions, with minimal degradation of performance over a period of 8 h. Metal analysis of the product stream by ICP-MS showed levels of leached total metals <1 ppm. When a similar analysis was conducted on the products from a reaction at high temperature (110 °C), Rh (7.16 ppm) and 1 ppm W were observed, indicating a disruption of the immobilisation.

In conclusion, this study has demonstrated the viability and stability of this immobilisation technique for applications in continuous SCF reactions. We have shown that ee values similar to those in batch reactions in conventional solvents can be achieved in continuous reactors employing scCO<sub>2</sub>, even when working at temperatures considerably higher than ambient. Further studies on the hydrogenation of DMIT involving other chiral ligands are in progress at Nottingham. Initial results are promising; incorporating the Josiphos ligand into the system has yielded an improvement in enantioselectivity to 70% ee.

## Acknowledgements

We would like to thank our colleagues in the Clean Technology Group at The University of Nottingham, in particular to Messrs M. Guyler, M. Dellar, P. Fields, R. Wilson and D. Litchfield of the Chemistry Workshops for their invaluable technical assistance. We are grateful to Drs J. R. Hyde and R. Amandi and Mr B. Walsh for helpful discussions. We thank Thomas Swan & Co. Ltd., the CRYSTAL Faraday Partnership and the EPSRC (Grant No. GR/R02863) for financial support. We would also like to acknowledge the

support of Drs J. Rouzaud, E. Rowsell, and S. Stevenson and the catalyst development group at The Technology Centre, Johnson Matthey Plc., particularly for their generous provision of precious metal catalysts and analytical support (ICP-MS). This immobilisation system is now available under licence from Johnson Matthey Plc. (CATAXA<sup>®</sup>).

## References

- 1 W. Leitner, *Pure Appl. Chem.*, 2004, **76**, 635–644.
- 2 E. J. Beckman, *J. Supercrit. Fluids*, 2004, **28**, 121–191.
- 3 M. Härröd, S. Van der Hark and A. Holmqvist, *Chem. Eng. Trans.*, 2002, **2**, 537–543.
- 4 M. G. Hitzler, F. R. Smail, S. K. Ross and M. Poliakoff, *Org. Process Res. Dev.*, 1998, **2**, 137–146.
- 5 B. Kerler, R. E. Robinson, A. S. Borovik and B. Subramaniam, *Appl. Catal., B: Environ.*, 2004, **49**, 91–98.
- 6 J. R. Hyde, P. Licence, D. Carter and M. Poliakoff, *Appl. Catal., A: Gen.*, 2001, **222**, 119–131.
- 7 P. Licence, J. Ke, M. Sokolova, S. K. Ross and M. Poliakoff, *Green Chem.*, 2003, **5**, 99–104.
- 8 W. S. Knowles, *Adv. Synth. Catal.*, 2003, **345**, 3–13.
- 9 R. Noyori, *Adv. Synth. Catal.*, 2003, **345**, 15–32.
- 10 P. G. Jessop, R. A. Brown, M. Yamakawa, J. L. Xiao, T. Ikariya, M. Kitamura, S. C. Tucker and R. Noyori, *J. Supercrit. Fluids*, 2002, **24**, 161–172.
- 11 D. C. Wynne, M. M. Olmstead and P. G. Jessop, *J. Am. Chem. Soc.*, 2000, **122**, 7638–7647.
- 12 G. Francio, K. Wittmann and W. Leitner, *J. Organomet. Chem.*, 2001, **621**, 130–142.
- 13 G. Francio, F. Faraone and W. Leitner, *Angew. Chem., Int. Ed.*, 2000, **39**, 1428–1430.
- 14 G. Francio, F. Faraone and W. Leitner, *J. Am. Chem. Soc.*, 2002, **124**, 736–737.
- 15 R. Wandeler, N. Kunzle, M. S. Schneider, T. Mallat and A. Baiker, *J. Catal.*, 2001, **200**, 377–388.
- 16 R. Wandeler, N. Kunzle, M. S. Schneider, T. Mallat and A. Baiker, *Chem. Commun.*, 2001, 673–674.
- 17 R. Augustine, S. Tanielyan, S. Anderson and H. Yang, *Chem. Commun.*, 1999, 1257–1258.
- 18 R. L. Augustine, S. K. Tanielyan, N. Mahata, Y. Gao, A. Zsigmond and H. Yang, *Appl. Catal., A: Gen.*, 2003, **256**, 69–76.
- 19 R. L. Augustine, P. Goel, N. Mahata, C. Reyes and S. K. Tanielyan, *J. Mol. Catal., A: Chem.*, 2004, **216**, 189–197.
- 20 R. S. Oakes, A. A. Clifford, K. D. Bartle, M. T. Petti and C. M. Rayner, *Chem. Commun.*, 1999, 247–248.





# Nickel-catalyzed dehydrative transformation of CO<sub>2</sub> to urethanes

Mahmut Abla, Jun-Chul Choi and Toshiyasu Sakakura\*

National Institute of Advanced Industrial Science and Technology (AIST), Higashi, AIST Central 5, Tsukuba, Ibaraki 305-8565, Japan. E-mail: t-sakakura@aist.go.jp; Fax: +81-298-61-4719; Tel: +81-298-61-4719

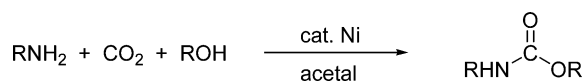
Received 3rd June 2004, Accepted 14th July 2004

First published as an Advance Article on the web 24th September 2004

Ni(OAc)<sub>2</sub>-bipyridine or phenanthroline complexes catalyze the environmentally benign synthesis of urethane from amine, alcohol, and CO<sub>2</sub> without toxic and corrosive phosgene; electron-donating and rigid ligands on Ni promote the reaction.

## Introduction

Current commercial processes for producing polyurethane are based on isocyanate which is synthesized from a primary amine and phosgene. This procedure has the major drawbacks of using highly toxic and corrosive phosgene, and the liberation of hydrogen chloride as a co-product. Replacing phosgene with CO<sub>2</sub> is very attractive because CO<sub>2</sub> is renewable, non-toxic, non-corrosive, and economical.<sup>1</sup> CO<sub>2</sub> as a phosgene substitute is also promising since there are similarities in the oxidation states between CO<sub>2</sub> and carbonic acid derivatives. In addition, the only by-product using CO<sub>2</sub> is water. Previously, we reported the direct transformation of CO<sub>2</sub> to aliphatic carbonates and urethanes catalyzed by dialkyltin derivatives in the presence of organic dehydrating agents such as acetals.<sup>2</sup> However, the space time yield of the tin system is unsatisfactory by industrial standards and the toxicity of organotin compounds is an environmental concern. Hence, developing less toxic and more active catalysts based on metals other than Sn is desirable. Dimethyl carbonate was recently synthesized from carbon dioxide using ZrO<sub>2</sub> and Ni(OAc)<sub>2</sub>.<sup>3,4</sup> However, the turnover numbers of the metals were very low in both cases. Herein we report novel Ni-based catalytic systems for dehydrative urethane formation from carbon dioxide, amine, and alcohol (Scheme 1).



Scheme 1

## Results and discussion

Initially, the catalytic activities of various metal acetates or halides for the urethane synthesis were surveyed without additional ligands and in the presence of acetal (2,2-dimethoxypropane). Other than Sn, first row transition metals such as Co(OAc)<sub>2</sub> and Ni(OAc)<sub>2</sub> exhibited low activities for the reaction of *t*-BuNH<sub>2</sub> with MeOH, but the amount of urethane was impractical; less than 2% yield under the typical reaction conditions (see Experimental).

Interestingly, adding nitrogen-based bidentate ligands such as bipyridine efficiently improved the catalytic activity of Ni(OAc)<sub>2</sub>-based catalysts (Table 1). The activity of the unsubstituted-bipyridine system (37% conversion) is as high as that of Bu<sub>2</sub>Sn(OMe)<sub>2</sub> (35% conversion). Adding PPh<sub>3</sub> or

diimine (**1**) to Ni(OAc)<sub>2</sub> was much less effective compared with bipyridine; the yields were merely 7 and 4%, respectively.

Table 1 summarizes the effects of various bipyridine or phenanthroline ligands. The coordinating power of the ligands is essential for promoting catalysis. Indeed, bipyridines with electron-withdrawing groups such as CF<sub>3</sub> and NO<sub>2</sub> resulted in poor yields. The very low catalytic activity of the system with 6,6'-dimethylbipyridine is also reasonable since steric hindrance causes weak coordination. On the other hand, introducing electron-donating substituents to the bipyridine backbone enhances the catalytic activity. Hence, 4,4'-bis(dimethylamino)-bipyridine is much more effective than unsubstituted or 4,4'-dimethylbipyridine. In addition, the phenanthroline structure is more effective than bipyridine as the ligand. Unsubstituted phenanthroline is as effective as 4,4'-bis(dimethylamino)-bipyridine.

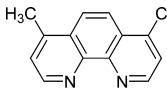
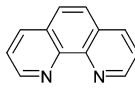
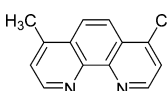
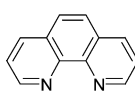
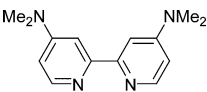
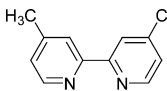
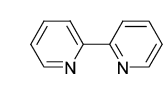
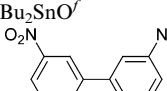
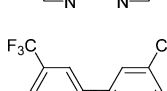
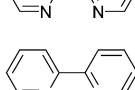
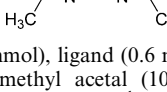
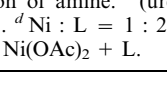
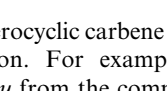
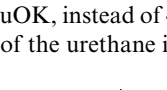
It is noteworthy that the catalytic activity of the Ni(OAc)<sub>2</sub>-(4,4'-dimethylbipyridine) system is highly dependent on the ligand/metal ratio. Increasing the ligand/metal ratio from one to two increased the conversion and selectivity. A ligand/metal ratio of three is necessary for the highest catalytic activity, but further increasing the ratio did not promote the reaction much.

The choice of anionic ligands on Ni(II) is also important. The yields increased in the order of F (2%), I (2%) < Br (4%) < Cl (10%) < NO<sub>3</sub> (29%) < OAc (38%) combined with 4,4'-dimethylbipyridine as the ligands. Higher CO<sub>2</sub> pressures also effectively promoted the reaction. Using the Ni(OAc)<sub>2</sub>-(4,4'-dimethylbipyridine) system, the yields obtained under 10, 20, and 30 MPa were 14, 23, and 38%, respectively.

Using noble metal complexes like Pd(OAc)<sub>2</sub> instead of Ni(OAc)<sub>2</sub> did not afford the desired product, but resulted in metal deposition, presumably due to reduction by methanol under the reaction conditions. Using cyclohexylamine in place of *t*-BuNH<sub>2</sub> afforded the highest yield (67%); the major side reaction was imine formation from acetone along with a little methylation of amines by methanol.

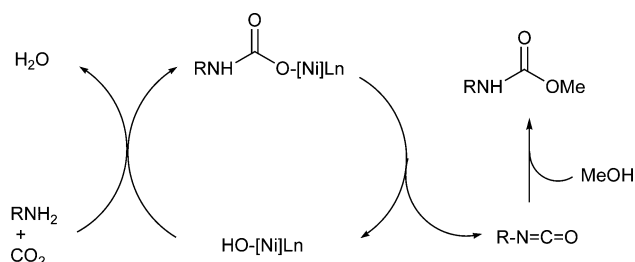
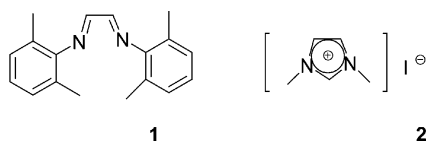
The mechanism of Ni-catalyzed urethane synthesis is currently unclear. It is presumed that the Ni-complex promotes the formation of isocyanate as an intermediate as shown in Scheme 2. The inactivity of secondary amines such as Et<sub>2</sub>NH and Bu<sub>2</sub>NH is consistent with this mechanism. A role as a Lewis acid<sup>5</sup> in promoting esterification of carbamic acid also seems possible. The acceleration of the urethane synthesis by excess ligand (L/Ni = 3) may be related to the formation of cationic complexes, which may work as a Lewis acid,<sup>6</sup> although the favourable effect of electron-donating ligands is contradictory to the role as a Lewis acid.

**Table 1** Ni-catalyzed urethane synthesis from CO<sub>2</sub>

$\text{RNH}_2 + \text{MeOH} + \text{CO}_2 \xrightarrow[\text{Me}_2\text{C}(\text{OMe})_2]{\text{cat. Ni}(\text{OAc})_2, \text{L (3 eq)}} \text{RHN}-\text{C}(\text{O})-\text{OMe}$			
Amine	Ligand	Conv. <sup>a</sup> (%)	Sel. <sup>b</sup> (%)
CyNH <sub>2</sub>		83	81
		81	61
<i>t</i> -BuNH <sub>2</sub>		49	98
		44	98
		49	94
		18	34 <sup>c</sup>
		24	98 <sup>d</sup>
		39	97
		41	100 <sup>e</sup>
		37	92
<i>n</i> -Bu <sub>2</sub> SnO <sup>f</sup>		35	95
		33	36
		19	17
		8	26

Ni(OAc)<sub>2</sub> (0.2 mmol), ligand (0.6 mmol), amine (10 mmol), methanol (100 mmol), dimethyl acetal (10 mmol), CO<sub>2</sub> 30 MPa, 200 °C, 24 h.<sup>a</sup> Conversion of amine. <sup>b</sup> (urethane)/(consumed amine) × 100. <sup>c</sup> Ni : L = 1 : 1. <sup>d</sup> Ni : L = 1 : 2. <sup>e</sup> Ni : L = 1 : 5. <sup>f</sup> *n*-Bu<sub>2</sub>SnO was used in place of Ni(OAc)<sub>2</sub> + L.

Finally, heterocyclic carbene ligands are also effective for the present reaction. For example, using the carbene ligand, prepared *in situ* from the commercially available imidazolium salt (**2**) and *t*-BuOK, instead of 4,4'-dimethylbipyridine resulted in a 63% yield of the urethane in the reaction of *t*-BuNH<sub>2</sub> with MeOH.

**Scheme 2**

In summary, we have developed new Ni-based catalytic systems for CO<sub>2</sub> conversion to urethanes. Bipyridines and phenanthrolines with strong coordinating abilities (low steric hindrance and high electron densities) were preferable for obtaining urethanes in high yields. It is noteworthy that the Ni-phenanthroline system is more active and less toxic than [Bu<sub>2</sub>SnO]<sub>n</sub> under the same reaction conditions. Further improvement of the catalytic activity as well as the recycling of the homogeneous catalyst will be the future directions of this study.

## Experimental

**Typical procedure.** All manipulations were conducted under purified argon. In a stainless steel autoclave (20 cm<sup>3</sup> inner volume), carbon dioxide (liquid, 6.5 MPa) was added to a mixture of *t*-butylamine (10 mmol), Ni(OAc)<sub>2</sub> (0.2 mmol), nitrogen-ligand (0.6 mmol), methanol (100 mmol), and biphenyl (50 mg, internal standard for GC analysis) at room temperature. The initial pressure was adjusted to 30 MPa at 200 °C and the autoclave was heated at that temperature for 24 h. The mixture was agitated by magnetic stirrer and was homogeneous during the reaction. After cooling, product yield was determined by GC and the products were further identified using GC-MS by comparing the retention times and fragmentation patterns with authentic samples. The yields were reproducible to within ± 3%.

## References

- (a) M. Aresta and E. Quaranta, *CHEMTECH*, 1997, **27**, 32; (b) H. Arakawa, M. Aresta, J. N. Armor, M. A. Barteau, E. J. Beckman, A. T. Bell, J. E. Bercaw, C. Creutz, E. Dinjus, D. A. Dixon, K. Domen, D. L. DuBois, J. Eckert, E. Fujita, D. H. Gibson, W. A. Goddard, D. W. Goodman, J. Keller, G. J. Kubas, H. H. Kung, J. E. Lyons, L. E. Manzer, T. J. Marks, K. Morokuma, K. M. Nicholas, R. Periana, L. Que, J. Rostrup-Nielsen, W. M. H. Sachtler, L. D. Schmidt, A. Sen, G. A. Somorjai, P. C. Stair, B. R. Stults and W. Tumas, *Chem. Rev.*, 2001, **101**, 953
- (a) J.-C. Choi, L.-N. He, H. Yasuda and T. Sakakura, *Green Chem.*, 2002, **4**, 230; (b) M. Abila, J.-C. Choi and T. Sakakura, *Chem. Commun.*, 2001, 2238; (c) T. Sakakura, J.-C. Choi, Y. Saito and T. Sako, *Polyhedron*, 2000, **19**, 573; (d) J.-C. Choi, T. Sakakura and T. Sako, *J. Am. Chem. Soc.*, 1999, **121**, 3793; (e) T. Sakakura, J.-C. Choi, Y. Saito, T. Masuda, T. Sako and T. Oriyama, *J. Org. Chem.*, 1999, **64**, 4506; (f) T. Sakakura, Y. Saito, M. Okano, J.-C. Choi and T. Sako, *J. Org. Chem.*, 1998, **63**, 7095.
- (a) K. Tomishige and K. Kunimori, *Appl. Catal. A*, 2002, **237**, 103; (b) K. T. Jung and A. T. Bell, *Top. Catal.*, 2002, **20**, 97.
- T. Zhao, Y. Han and Y. Sun, *Fuel Process. Technol.*, 2000, **62**, 187.
- (a) K. Pignat, J. Vallotto, F. Pinna and G. Strukul, *Organometallics*, 2000, **19**, 5160; (b) S. Otto and J. B. F. N. Engberts, *J. Am. Chem. Soc.*, 1999, **121**, 6798; (c) S. Otto and J. B. F. N. Engberts, *Tetrahedron Lett.*, 1995, **36**, 2645.
- A. Vavasori and L. Toniolo, *J. Mol. Catal. A*, 2000, **151**, 37.



# A facile method for catalyst immobilisation on silica: nickel-catalysed Kumada reactions in mini-continuous flow and batch reactors

Nam T. S. Phan,<sup>a</sup> David H. Brown<sup>a,b</sup> and Peter Styring<sup>\*a</sup>

<sup>a</sup>Department of Chemical and Process Engineering, The University of Sheffield, Mappin Street, Sheffield, UK S1 3JD. E-mail: p.styring@sheffield.ac.uk; Fax: +44 (0) 114 222 7501; Tel: +44 (0) 114 222 7571

<sup>b</sup>School of Biomedical and Chemical Sciences, The University of Western Australia, 35 Stirling Hwy, Crawley, 6009, Australia

Received 6th April 2004, Accepted 15th July 2004

First published as an Advance Article on the web 7th October 2004

An unsymmetrical salen-type nickel(II) complex was readily immobilised onto functionalised silica using a convenient tethering method. The supported complex was an effective recyclable heterogeneous catalyst in a room temperature cross-coupling reaction between 4-bromoanisole and phenylmagnesium chloride. Leaching of the metal into solution from the supported catalyst proved almost negligible. The silica-supported catalyst was ideal for use in a mini-continuous flow reactor since it did not exhibit swelling which is common and a problem for organic polymer resin supports.

## Introduction

Metal-catalysed cross-coupling reactions have gained popularity over the past thirty years, in particular as convenient techniques for the formation of carbon–carbon bonds.<sup>1</sup> Numerous reactions have been developed to achieve cross-coupling, of which the Kumada reaction is a particular type involving the coupling of a Grignard reagent with an aryl halide.<sup>2</sup> The reaction can be carried out over a wide range of temperatures from sub-ambient to elevated temperatures (refluxing solvents), however for commercial efficiency a reaction at ambient temperature is preferable.<sup>3</sup> Catalysts used in the reaction are generally based on either homogeneous nickel- or palladium-phosphine complexes.<sup>4–6</sup> However, the use of homogeneous catalysts suffers from the problem of catalyst separation.<sup>7</sup> Moreover, phosphine ligands are expensive, toxic; and in large-scale applications the phosphines may be a more serious economical burden than the metal itself.<sup>8</sup> The majority of industrial processes are therefore carried out using heterogeneous catalysts since catalyst recovery and recycling is more amenable. A potential solution to this problem is through the use of immobilised homogeneous catalysts. While formally heterogeneous, supported homogeneous catalysts can offer the catalyst selectivity of homogeneous catalysts and the practicalities of heterogeneous catalysts. One of the most common catalyst supports reported in the literature is polymeric supports and this is evident in the review by Leadbeater and Marco.<sup>9</sup> However, in recent years the use of silica supports has become of interest.<sup>10–18</sup> These supports exhibit features, such as robustness, that would make them much more suited to commercial use than polymeric supports.

Reactor miniaturisation, for example micro reactors—in which microlitre quantities of reagents are manipulated, has been shown to confer many advantages over conventional scale chemical apparatus.<sup>19–21</sup> Heat transfer is improved and mixing times reduced by orders of magnitude as a result of the decrease in linear dimensions.<sup>22</sup> Whilst the size of an individual reactor may seem to preclude large-scale synthesis, it is possible to use multiple copies of the reactor in parallel ('scaling-out') to bypass the process development stage of 'scaling-up', creating a

high throughput system while maintaining the control and selectivity of the original system. Using micro reactors, products can be generated on demand, at the point of use, so reducing the need to store and transport hazardous chemicals.<sup>23</sup> Furthermore, micro reactors offer a particularly suitable technology for performing reactions that involve highly reactive reagents because of the small inventory of reagents in the reaction vessel, thus increasing operational safety.<sup>24</sup> To date the scope of liquid phase synthesis in micro reactors has, in the majority, been limited to non-metal-catalysed reactions, with the exception of a few examples of heterogeneous catalysis.<sup>23,25</sup> There are only a couple of reports of supported homogenous catalysts being used in miniaturised continuous-flow reactors.<sup>26,27</sup>

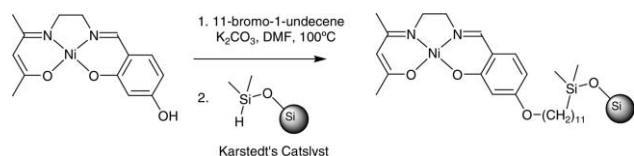
Recently we reported the synthesis and characterisation of an unsymmetrical salen-type nickel(II) complex and its immobilisation onto a polystyrene–divinylbenzene cross-linked Merrifield resin.<sup>28,29</sup> The supported catalyst was air- and moisture-stable, and could be reused several times without a significant degradation in catalytic activity in the Kumada reaction of 4-bromobenzene and phenylmagnesium bromide at room temperature. In this paper we report for the first time, to our best knowledge, the immobilisation of a homogeneous nickel complex onto a silicon hydride functionalised silica and its catalytic activity in the room temperature Kumada reaction, without any added phosphine. This immobilisation method has not been reported previously. Immobilisation onto silica provides a material in which the catalyst is tethered to the support by strong covalent bonds. This material possesses an active catalytic centre that is essentially in the homogeneous phase because of the extended hydrocarbon chain tether, yet as the support remains heterogeneous with respect to the reactant solution, it displays the beneficial properties of both. Therefore, we have termed these materials androgynous catalysts, being indistinguishable as either purely homo- or heterogeneous. We will show using kinetic analysis of reactions, using different forms of the catalyst complex, that this is in fact the case. The silica support also provides the material with the added advantages of robustness and solvent-independent behaviour, unlike organic polymeric supports that lack the mechanical

strength of silica and show solvent-dependent swelling. The silica-supported catalyst's lack of swelling in solvents is crucial for its use in a mini-continuous flow reactor system. Performing a Kumada reaction in this flow-system is also reported: reasonable conversions can be achieved in a matter of minutes, compared to conversions obtained after 24 hours in a batch reaction, albeit on a much smaller scale.

## Results and discussion

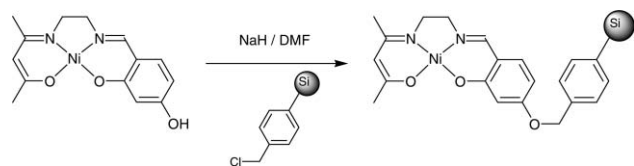
### Catalyst immobilisation

The unsymmetrical salen-type nickel complex was covalently immobilised onto a hydrosilyxy-silica using a two-step procedure (Scheme 1). The first step is an etherification reaction



**Scheme 1** Catalyst immobilisation onto hydrosilyxy-silica (catalyst 1).

which appends an anchoring tether to the complex. The resulting alkenyl species can be readily purified by column chromatography and then recrystallisation. The second step is a platinum-catalysed hydrosilylation reaction (addition of a silicon hydride 'Si-H' across a C=C double bond). In this case the silicon hydride moiety is covalently bound to the silica support. Finally the silica is thoroughly washed to remove any of the unreacted nickel complex since any residual species would affect the results of catalytic studies. Inductively coupled plasma-atomic emission (ICP-AE) analysis of the silica-bound catalyst showed there to be *ca.* 1.5% (wt/wt) nickel on the silica, corresponding to a complex loading of 0.25 mmol nickel g<sup>-1</sup> silica (catalyst 1). The unsymmetrical salen-type nickel complex was also immobilised onto 4-benzyl chloride-functionalised silica, which is analogous to Merrifield resin in terms of the functional group, using the previously reported procedure (Scheme 2).<sup>28,29</sup> ICP-AE measurement showed there to be *ca.*

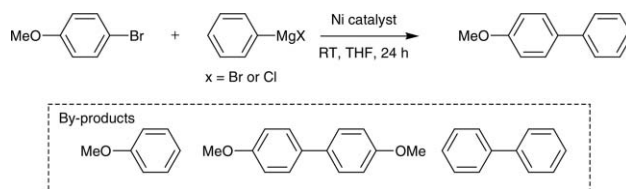


**Scheme 2** Catalyst immobilisation onto 4-benzyl chloride-functionalised silica (catalyst 2).

1% (wt/wt) nickel on the silica, corresponding to a catalyst loading of 0.15 mmol nickel g<sup>-1</sup> silica (catalyst 2). The intractable nature of the silica made it difficult to obtain meaningful data from infrared analysis. Therefore, proof that the nickel complex is covalently immobilised on the silica comes from the ICP-AE analysis of the silica and the crude reaction solutions, which showed very little, if any, leaching of the metal into the reaction solution.

### Batch reactions—conventional apparatus

The unsymmetrical salen-type nickel complex (starting material in Scheme 1) supported on Merrifield resin has previously been shown to be effective in the Kumada reaction,<sup>28,29</sup> a carbon-carbon coupling reaction between a Grignard reagent and an organohalide (Scheme 3). It had been found that the nickel resin could be recovered and reused several times in the



**Scheme 3** The Kumada reaction of 4-bromoanisole and a phenylmagnesium halide.

reaction of phenylmagnesium bromide and 4-bromoanisole at room temperature, with 4-methoxybiphenyl being formed in a conversion of 66% (Scheme 3, X = Br). The nickel complex on hydrosilyxy-silica (catalyst 1) can also effectively catalyse the reaction. Initial tests indicated that the silica-supported nickel catalyst was slightly less active with 52% conversion. However, it was noticed that in the reaction MgBr<sub>2</sub> precipitated from solution and presumably the MgBr<sub>2</sub> also deposited on the surface pores of the silica, making the active catalytic sites less accessible to the reagents. By changing the Grignard reagent, from the bromide to the chloride (PhMgCl instead of PhMgBr), the activity was increased to a 67% conversion (Scheme 3, X = Cl; Table 1, Run 1), *without* any precipitate being observed during the reaction. This activity is the same as the organic resin-supported nickel catalyst. As with the nickel resin catalyst system, by-products are formed in the reaction (Scheme 3): 4-bromoanisole was also converted to 4,4'-dimethoxybiphenyl and anisole. These were not reported in the original paper<sup>29</sup> because the GC method used could not detect anisole and the homocoupled product had a retention time above the upper limit of the conditions used on the particular column. However, their formation was reported in detail, in a more recent publication.<sup>28</sup> Biphenyl was also formed through sacrifice of some of the Grignard reagent in the first step of the catalytic cycle.<sup>28,29</sup> The absence of any precipitate using the PhMgCl method is critical for use in a micro flow reactor since any precipitation would cause blockages in the reactor.

Active lifetimes for heterogeneous and homogeneous catalysts is an important characteristic of catalysts, particularly for industrial and pharmaceutical applications of cross-coupling reactions.<sup>30</sup> Therefore, the silica-supported catalyst was tested for recyclability. After each run, the original nickel silica was filtered off, washed several times with THF and water to remove any excess reagents, dried under vacuum at room temperature and reused under the same reaction conditions as for the initial run without any regeneration. Results in Table 1

**Table 1** Study of catalyst recycling in the Kumada reaction using 0.5 mol% nickel catalyst 1, 1 equiv. 4-bromoanisole and 1 equiv. phenylmagnesium chloride in THF at room temperature for 24 hours under a nitrogen atmosphere (figures as a mol% of the final mixture based on conversion from 4-bromoanisole). All data are from GC studies

Run	4-Methoxy-biphenyl	4-Bromoanisole	Anisole	4,4'-Dimethoxy-biphenyl
1	67%	0%	18%	15%
2	66%	0%	17%	17%
3	64%	6%	12%	18%

show that the nickel silica catalyst 1 can be recovered and reused in further reactions without a significant degradation of activity. The leaching of active species from heterogeneous catalysts into solution is also a crucial question. In order to determine the absolute amount of nickel species dissolved into solution by leaching the crude reaction mixtures were evaporated to dryness and analysed using ICP-AE, after



removal of the catalyst by filtration. It was shown that less than 1% of the total amount of the original nickel species was lost into solution during the course of a reaction. This almost negligible leaching level accounts for the recoverability and reusability of the nickel silica.

Catalyst **2** was found to be less active than catalyst **1**, as shown in Table 2. Reactions were carried out using different

**Table 2** Comparison of catalyst **1** and catalyst **2** in the Kumada reaction using 1 equiv. 4-bromoanisole and 1 equiv. phenylmagnesium chloride in THF at room temperature for 24 hours under a nitrogen atmosphere (figures as a mol% of the final mixture based on conversion from 4-bromoanisole). All data are from GC studies

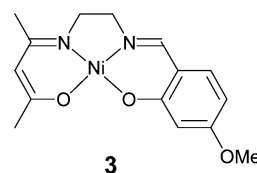
Mol% Ni catalyst	4-Methoxy-biphenyl	4,4'-Dimethoxy-biphenyl	Anisole	4-Bromoanisole
0.05	38%	3%	19%	40%
0.1	59%	13%	13%	15%
0.3	68%	20%	12%	0%
0.5	67%	15%	18%	0%
1.0	67%	11%	22%	0%

Mol% Ni catalyst	4-Methoxy-biphenyl	4,4'-Dimethoxy-biphenyl	Anisole	4-Bromoanisole
0.05	19%	0%	8%	73%
0.1	23%	1%	12%	64%
0.3	46%	12%	9%	33%
0.5	49%	16%	7%	28%
1.0	51%	13%	12%	24%

concentrations of catalyst **1** and catalyst **2**. In all cases, the concentration of the solutions was  $0.5 \text{ mol L}^{-1}$  with respect to each of the starting materials. For the reaction using catalyst **1**, the best conversion to 67–68% 4-methoxybiphenyl was observed for 0.3 mol% nickel (12 mg) or greater with all the 4-bromoanisole starting material being consumed. Catalyst content below 0.3 mol% nickel resulted in incomplete consumption of 4-bromoanisole. In all cases the ratio of product to combined by-products was 2 : 1. The useful catalyst loadings found in this study were comparable to those of previously publicised works, in which the concentration of nickel-phosphine complexes normally used as catalysts for the related Kumada cross-coupling reaction is in the range of 0.1–1.0 mol%.<sup>3</sup> Therefore, it was decided to use 0.3 mol% of the supported nickel complex in subsequent reactions. For the given concentration, this requires 12 mg of catalyst **1**. However, reaction using 0.3 mol% nickel of catalyst **2** (20 mg) yielded only 46% conversion of 4-methoxybiphenyl with up to 33% unreacted starting material. Increasing the nickel loading of catalyst **2** to 1 mol% still afforded only 51% conversion. This means that although the catalytically active sites remain the same in the two catalysts, the nature of the supports as well as the immobilisation method have to be taken into account. Reactive sites have to be made accessible to the reactants during the course of the reaction. Despite the fact that the silica possesses high surface areas, its rigid structure may prevent the availability of active sites. Catalyst **1** possesses an active centre that is essentially removed from the silica surface because of the extended hydrocarbon chain tether; catalyst **2** contains a shorter tether.

If the tethered catalyst **1** is behaving as an androgynous catalyst, possessing properties of both the homogeneous catalyst and the heterogeneous catalyst (**2**) then this should be reflected in the kinetics, with a rate constant intermediate between the two extremes. In order to test this further we carried out kinetic studies of the reaction using 0.3 mol% nickel of catalyst **1**, catalyst **2**, and their homogeneous methoxy-terminated analogue **3**, respectively. The synthesis, purification



and characterisation of the homogeneous nickel catalyst has been published previously.<sup>28</sup> The concentration of each starting material was  $0.5 \text{ mol L}^{-1}$ , with 1 mmol of each reagent being present in the solutions studied. Aliquots were withdrawn at different time intervals over a 12 hour period to measure the corresponding conversion of 4-bromoanisole to 4-methoxybiphenyl (Fig. 1). The data were analysed using the first order

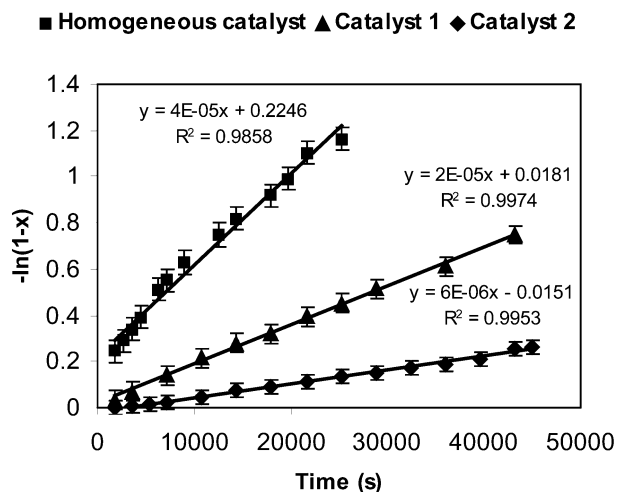
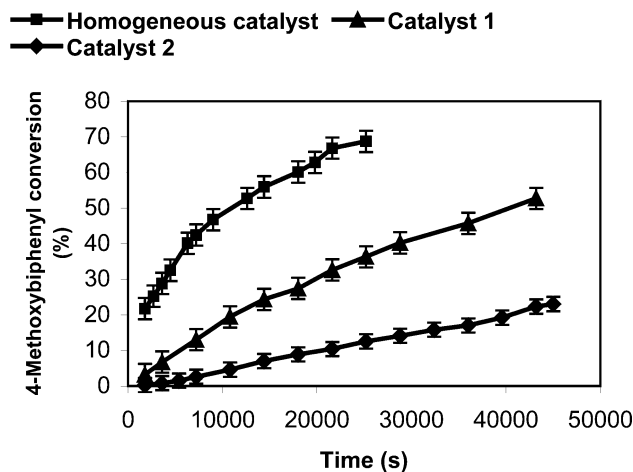


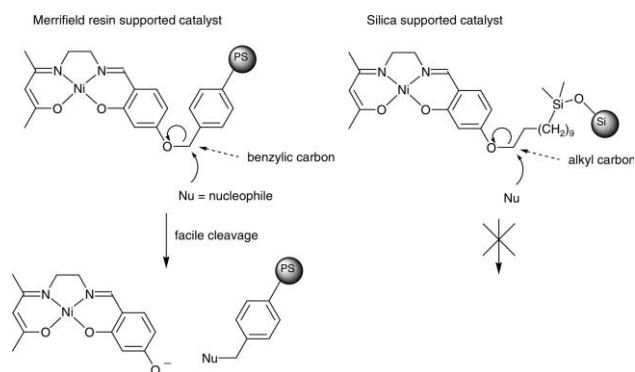
**Fig. 1** Kinetic data of the Kumada reaction using catalyst **1** (triangles), catalyst **2** (diamonds), and the corresponding homogeneous catalyst (squares), showing observed rate constants of  $2 \times 10^{-5} \text{ s}^{-1}$  (catalyst **1**),  $6 \times 10^{-6} \text{ s}^{-1}$  (catalyst **2**), and  $4 \times 10^{-5} \text{ s}^{-1}$  (homogeneous catalyst).

reaction design equation (eqn 1), where  $x$  is the mole fraction of 4-methoxybiphenyl produced and  $t$  is the corresponding reaction time (Fig. 1). The mechanism of the overall reaction, and hence the order of the individual elementary reactions in the catalytic cycle is complex and still remains to be elucidated.<sup>28</sup> However, the cross-coupling reaction to form 4-methoxybiphenyl was shown to be *pseudo* first order with respect to the starting bromide giving an observed overall rate constant of  $2 \times 10^{-5} \text{ s}^{-1}$  for catalyst **1**, which is comparable to that determined for the nickel complex immobilised on the

Merrifield resin.<sup>29</sup> As expected, the reaction using the directly linked catalyst **2** proceeded more slowly with an observed overall rate constant of  $6 \times 10^{-6} \text{ s}^{-1}$ . In the case of the homogeneously catalysed reaction an observed overall rate constant of  $4 \times 10^{-5} \text{ s}^{-1}$  was observed. Therefore, catalyst **1** can be classified as an androgynous catalyst, being indistinguishable as either purely homo- or hetero- geneous. Furthermore, the effect of the tether to decouple the catalyst from the solid support can be clearly seen as its performance is closer to that of the homogeneous catalyst than the heterogeneous form. It is interesting here to consider the turnover frequencies (mol product produced per mol catalyst per hour) for each of the catalysts. The turnover frequency for the tethered catalyst **1** was determined as  $14.6 \text{ h}^{-1}$ , for the directly linked catalyst **2** it was found to be  $6.1 \text{ h}^{-1}$  and for the homogeneous catalyst  $32.7 \text{ h}^{-1}$ .

$$k_{\text{obs}} = -[\ln(1 - x)] \times 1/t \quad (1)$$

Our experience with both resin and silica supports indicates that the silica-supported system offers a number of advantages over the Merrifield resin supports. The silica system is much more robust than the resin system in which mechanical failure (breakage) of the resin can be a major problem. Resin breakage or fracture can arise from mechanical stresses (caused by stirring the solution) as well as stresses on the polymer caused by solvent induced swelling. Stirring and heating of catalyst-supported resins proved extremely detrimental to the bulk structure of the resin particles and in some cases the Merrifield resin beads were broken into a fine powder. Another advantage of the immobilisation method reported in this paper is that the nickel complex is bound to the silica by strong covalent bonds. In comparison, the nickel complex supported on Merrifield resin,<sup>28,29</sup> contains the much more labile (and thus cleavable) phenolic benzylic ether linkage connecting the complex to the resin support (Scheme 4) as opposed to the stronger phenolic alkyl ether linkage. While not a problem in this reaction, it could be significant in other systems.



Scheme 4 Possible catalyst cleavage mechanism.

### Micro flow reactions

In this study, the reaction of 4-bromoanisole and phenylmagnesium chloride in THF was carried out in a pressure driven micro flow reactor constructed from Omnifit glassware (Fig. 2). A syringe pump was connected to the fixed bed reactor (bed size = 25 mm  $\times$  3 mm), a glass-walled tube, using PTFE tubing and standard HPLC connectors. The reactor was filled with the silica-immobilised nickel catalyst. The Omnifit reactor is a low pressure liquid chromatography column which is packed with the catalyst particles; these are held in place by 25  $\mu\text{m}$  pore size stainless steel frits integrated into the screw caps that connect the column to the fluidic system, at the

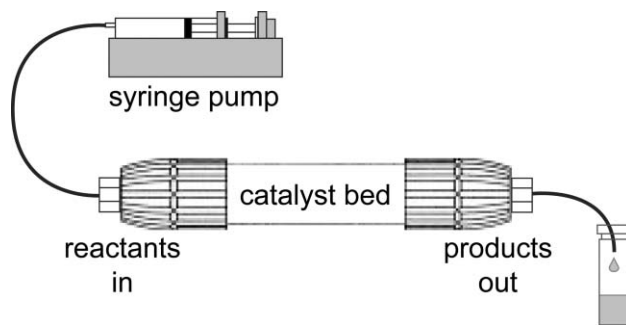


Fig. 2 Mini-flow reactor setup (catalyst bed dimensions 25 mm  $\times$  3 mm).

reactor entrance and exit. The design of the reactor system makes catalyst filling and removal an extremely easy and quick process. A syringe pump (RAZAL A-99) was used to drive a pre-determined volume of a solution containing equimolar amounts ( $0.5 \text{ mol L}^{-1}$ ) of the reagents in THF through the reactor at the different flow rates for 1 hour. The results of conversion dependence on flow rates are shown in Table 3. The

Table 3 Study of the conversion dependence on flow rates in the continuous Kumada reaction using 1 equiv. 4-bromoanisole and 1 equiv. phenylmagnesium chloride in THF at room temperature (figures as a mol% of the final mixture based on conversion from 4-bromoanisole). All data are from GC studies

Flow rates/ $\mu\text{l min}^{-1}$	4-Methoxy- biphenyl	4-Bromoanisole	Anisole	4,4'-Dimethoxy- biphenyl
6	64%	5%	23%	8%
13	64%	6%	20%	10%
20	59%	11%	23%	7%
33	54%	17%	23%	6%

best result was achieved using a flow rate of  $13 \mu\text{l min}^{-1}$  with 64% conversion to 4-methoxybiphenyl being achieved, which is comparable to conversion observed in the batch reaction. Decreasing the flow rate to less than  $13 \mu\text{l min}^{-1}$  was found to be unnecessary as the conversion to the principal product did not increase any further. Increasing the flow rate resulted in a drop in conversion. Since reaction conditions such as concentration, ratio of phenylmagnesium chloride to 4-bromoanisole, solvent and temperature remained unchanged in all cases, the observed increase in conversion, when decreasing the flow rate of the system, was due to an effective increase in residence time within the continuous reactor and hence an increase in reaction time.

The common prejudice against micro reactors is the possibility of blockage.<sup>31</sup> The immobilisation of the salen-type nickel complex onto Merrifield resin gave a good polymer-supported catalyst in terms of activity.<sup>27-29</sup> However, when performing the Kumada reaction in a micro reactor, the swelling of the resin in THF caused a significant pressure drop and reactor blockage when fully packed. When only pure THF was driven through the reactor filled with the nickel resin the reactor blocked after a few minutes because of swelling. As a result, the amount of resin catalyst had to be reduced in order to avoid blockage, leading to a drop in conversion. Therefore, if under-packing of the reactor is used then the exact swelling characteristics of the resin must be known in order to avoid a reduction in performance. However, this is not trivial due to the range of particle sizes used for the resin and so non-uniform swelling could lead to inconsistencies in reactor performance. Furthermore, we found the organic polymer resin catalysts to be unusable in small dimension micro channels etched in glass which became blocked on each occasion. Using other common

solvents for the Kumada reactions such as diethyl ether in which the resin has little or no swelling could solve the problem of blockage. However, in low cross-linked polymer supports most of the active sites are located inside the beads not on the outer surface, and thus swelling makes these sites accessible to the reagents. Therefore, poor swelling of polymer supports in diethyl ether results in loss of activity of the catalyst.<sup>32</sup> These problems could be simply solved by using the nickel catalyst supported on silica, with high surface areas and no swelling in THF.

The continuous reactor was filled with catalyst **1** (100 mg, 25  $\mu\text{mol}$  Ni) and run for 5 hours at a flow rate of 13  $\mu\text{L min}^{-1}$  with product samples being collected every hour. The results are shown in Table 4. Unexpectedly, the continuous flow

**Table 4** Study of the conversion against reactor run time in the continuous flow Kumada reaction using 1 equiv. 4-bromoanisole and 1 equiv. phenylmagnesium chloride in THF at room temperature (figures as a mol% of the final mixture based on conversion from 4-bromoanisole). All data are from GC studies

Reaction time/h	4-Methoxybiphenyl	4,4'-Dimethoxybiphenyl	Anisole	4-Bromoanisole
1	62%	7%	25%	6%
2	60%	5%	24%	11%
3	49%	3%	20%	28%
4	41%	3%	16%	40%
5	30%	1%	11%	58%

reactor system showed a gradual degradation in performance with a conversion of only 30% being achieved after 5 hours. As many of the reactions reported to occur in micro reactors are only allowed to proceed for short time periods, we believed it was important to look at the longevity of the system over continuous use. As mentioned earlier in the batch experiment, the nickel catalyst can be recovered and reused in further reaction without a significant degradation in activity. Therefore, we decided to test the activity of the catalyst after being used for 5 hours in the micro flow reactor. The catalyst was filtered off, washed several times with THF and water to remove any excess reagents, dried under vacuum at room temperature and reused under the same conditions for a typical batch reaction. It was shown that a conversion of 65% was still achieved. Moreover, in the continuous reactor this recovered nickel catalyst was found to afford a conversion of 53%. This means that although no precipitate was visually observed, deposition of salts ( $\text{MgBrCl}$ ,  $\text{MgBr}_2$ ) on the surface of the catalyst still occurred, making active sites less accessible to reactants. The problem of deposition, which is negligible in the batch reaction due to rapid stirring, still remains to be solved for the continuous reactor. Optimisation of the solvents (*i.e.* using diethyl ether, in which the salts are more soluble) may provide a solution. Studies are now being carried out to perform the catalyst wash in-line, without the need to remove the catalyst from the reactor.

The micro flow reaction system still offers advantages over the conventional batch reaction. Yields obtained after 24 hours in a batch reaction could be realised in a matter of minutes using the micro flow reactor system, albeit on a much smaller scale. This can be rationalised in terms of the effective ratio of catalyst to substrate. The volume of an unpacked reactor is 177  $\mu\text{L}$ , however in our case we have a packed bed. The catalyst particles are spherical and so a reactor voidage of 40% can be assumed. This gives a reactor volume available for solution flow of *ca.* 70  $\mu\text{L}$  and a calculated reactor residence time of 5.5 minutes. Therefore, at any given time there is *ca.* 35  $\mu\text{mol}$  of substrate in the reactor and 25  $\mu\text{mol}$  of catalyst. This gives an effective ratio of 70 mol% of the nickel catalyst. Therefore, by

comparison with the batch reactions there is a small amount of substrate which is forced into intimate contact with a large amount of catalyst in the flow reactor. With the current system, using a flow rate of 13  $\mu\text{L min}^{-1}$ , *ca.* 0.96 mmol (177 mg) of 4-methoxybiphenyl was produced in 5 hours. By scaling out the system, it can be envisaged that yields of synthetic value could be readily achieved (*e.g.* 10 reactors in parallel would produce more than 1.7 g of the target material in the same time interval). Moreover, the Kumada reaction could be carried out in the flow reactor without the need for a nitrogen atmosphere as rigorously required for the conventional batch reaction. A series of batch reactions exposed to air formed less than 2% of the 4-methoxybiphenyl with the Grignard reagent reacting with THF to yield 1-phenyl-1,4-butanediol in the presence of air.<sup>28</sup> It was found that this by-product was formed by the reaction of the Grignard reagent, THF and the oxygen from the headspace in the batch reaction. No diol was detected when oxygen was rigorously excluded. The fact that 4-methoxybiphenyl could be produced using the continuous reactor without the need for a nitrogen atmosphere, as the system does not contain a headspace, is therefore an advantage.

We decided to investigate the observed rate constant of the continuous flow reaction, compared with that of the batch reaction. It is noted that in a continuous flow reactor, the mean residence time is also the reaction time and that the residence time in the mini-flow reactor is much shorter than in the batch process. The reaction is also assumed to be *pseudo* first order because the mechanism in batch and flow modes are the same, so comparisons were made using this assumption. The residence time of the solution within the catalyst bed was measured according to the procedure previously reported,<sup>33</sup> giving a period of 5.2 minutes at a flow rate of 13  $\mu\text{L min}^{-1}$ . This means that the observed rate constant of the coupling reaction was considerably faster, with  $k_{\text{obs}} = 3.3 \times 10^{-3} \text{ s}^{-1}$  using the continuous mini-flow reactor. This represents an enhancement of the reaction rate of 160 times as compared to the batch reaction. However, in this reaction this can be attributed entirely to the increased catalyst concentration in the reactor element. It is therefore worth considering the turnover frequency in the flow reactor. This was determined as 10.7  $\text{h}^{-1}$ , which is similar within experimental error to the TOF of the same catalyst in the stirred batch reactor (14.6  $\text{h}^{-1}$ ).

The micro flow system did not show any increased yield or selectivity over the batch process. The maximum product yield was found to be 64% with the flow rates used. Performing a mass balance on products and by-products shows a 2 : 1 distribution, which is identical to that achieved in the batch process. However, the by-product distribution is different in the flow reactor when compared to the batch system. While the amount of 4,4'-dimethoxybiphenyl produced is less in the flow reactor, more anisole is formed. Both of these by-products are formed by metal-catalysed processes as discussed previously<sup>28</sup> therefore while the selectivity of the product remains unchanged, by-product formation is different in batch and continuous systems. This was also shown to be independent of flow rate and hence residence time, with less starting material being consumed as the residence time decreased (Table 3).

## Conclusions

The nickel silica catalyst (**1**) exhibits high activity towards the Kumada cross-coupling reaction of 4-bromoanisole and phenylmagnesium chloride at room temperature without any added phosphine ligands. The catalyst can be easily separated from the reaction mixture by simple filtration and reused after washing without a significant degradation in activity. The concentration of nickel leaching into solution from the catalyst during the course of the reaction is very low. This has



advantages in the clean processing of the reaction solution. Using the mini-flow reactor system, reasonable conversions can be achieved in a matter of minutes. Although simple in design and concept, with easily replaceable catalyst beds and interchangeable reagent premixes, the mini-flow reactor system provides a powerful tool in catalyst screening and a route to high throughput synthesis. This is the case because although the TOF is unaffected by moving to the mini-flow system, 64% completion can be achieved in a matter of minutes whereas 24 hours are required in batch. Therefore, the mini-flow system is ideal for the rapid production of small inventories of reagents and for the rapid screening of solid catalysts due to their ease of addition to and removal from the reactor.

## Experimental

Chemicals were obtained from Aldrich and Fisher and used as received. Karstedt's catalyst [platinum divinyltetramethyl-disiloxane complex in xylene (2–3%)] from Fluorochem was used as received. The unsymmetrical salen-type nickel complex was synthesised according to previously published methods.<sup>28,29</sup> NMR spectra were recorded using a Bruker AC250 spectrometer (<sup>1</sup>H, 250.1 MHz; <sup>13</sup>C, 62.9 MHz) or a Bruker AMX 400 spectrometer (<sup>1</sup>H, 400.1 MHz; <sup>13</sup>C, 100.6 MHz). <sup>1</sup>H and <sup>13</sup>C chemical shifts were referenced to solvent resonances. Microanalyses were performed by Alan Jones, Mass Spectra (EI mode) were recorded by Jane Stanbra and Simon Thorpe, ICP-AE analyses were performed on a Spectro Ciros<sup>CD</sup> instrument (Spectro Analytical, UK) by Alan Cox and Ian Staton from the Department of Chemistry, The University of Sheffield. GC-MS analyses were performed using a Perkin Elmer GC-MS with a 30 m × 0.25 mm × 0.25 μm Phenomenex-2B5 column. The temperature program was 60–260 °C at 10 °C min<sup>-1</sup> with a final temperature isothermal hold for 10 min. The MS mass limit was set between 50 and 450 Da.

### [9-(2'-Hydroxy-4'-undec-10''-enyloxyphenyl)-5,8-diaza-4-methyl-non-2,4,8-trienato](-2) nickel(II)

A mixture of [9-(2',4'-dihydroxyphenyl)-5,8-diaza-4-methyl-non-2,4,8-trienato](-2) nickel(II) (0.39 g, 1.2 mmol), 11-bromo-1-undecene (0.35 g, 1.4 mmol) and potassium carbonate (0.43 g, 3.1 mmol) in DMF (10 ml) was stirred for 3 days and then was heated at ca. 100 °C overnight. The resulting mixture was extracted with ether (100 ml). The organic phase was washed with water (4 × 50 ml), dried (MgSO<sub>4</sub>) and concentrated *in vacuo*. The residue was triturated with hot light petroleum (ca. 50 ml, with a small amount of DCM ca. 1 ml). After cooling the solid was collected and dried yielding a red-brown powder. The powder was then purified by column chromatography (silica, ether and then ether-DCM 1 : 1) and then recrystallisation from methanol to yield a red-brown powder (0.20 g, 35%). <sup>1</sup>H NMR (CDCl<sub>3</sub>; 250 MHz): 1.19–1.43 (12 H, m, -(CH<sub>2</sub>)<sub>6</sub>CH<sub>2</sub>CH=CH<sub>2</sub>), 1.69 (2 H, m, -OCH<sub>2</sub>CH<sub>2</sub>-), 1.86 (3 H, s, -(CH<sub>3</sub>)=N-), 1.90 (3 H, s, 3 × H1), 2.01 (2H, m, -CH<sub>2</sub>CH=CH<sub>2</sub>), 3.03 (2 H, apparent t, splitting 6.6 Hz, 2 × H6), 3.27 (2 H, apparent t, splitting 6.6 Hz, 2 × H7), 3.84 (2 H, t, *J* = 6.8 Hz), 4.86–5.00 (2 H, m, -CH=CH<sub>2</sub>), 4.92 (1 H, s, H3), 5.78 (1H, m, -CH=CH<sub>2</sub>), 6.10 (1 H, dd, *J*(H3'H5') = 2.3 Hz, *J*(H5'H6') = 8.8 Hz, H5'), 6.38 (1 H, d, H3'), 6.90 (1 H, d, H6'), 7.23 (1 H, s, -N=CH-). <sup>13</sup>C NMR (CDCl<sub>3</sub>; 62.9 MHz): 21.3 (C1), 24.5 (-C(CH<sub>3</sub>)=N-), 26.0, 28.9, 29.0, 29.1, 29.3, 29.4, 29.5 33.8 (-(CH<sub>2</sub>)<sub>8</sub>CH=CH<sub>2</sub>), 51.7 (C6), 59.6 (C7), 68.1 (-OCH<sub>2</sub>-), 99.7 (C3), 103.3 (C5'), 106.7 (C3'), 114.1 (-CH=CH<sub>2</sub>), 114.2 (C1'), 132.7 (C6'), 139.2 (-CH=CH<sub>2</sub>), 159.8 (C9), 163.9, 165.0, 166.8 (C2', C4', C4) and 177.3 (C2). Mass Spec. (EI): 470 (M<sup>+</sup>; 100%), 318, 169. HRMS (EI<sup>+</sup>): *m/z* 470.2096 (M) (requires 470.2079) Microanalysis:

found C, 63.70; H, 7.76; N, 6.06. C<sub>26</sub>H<sub>36</sub>N<sub>2</sub>O<sub>3</sub>Ni requires C, 63.72; H, 7.70; N, 5.94%.

### Immobilisation of alkenyl-substituted nickel complex onto hydrosiloxo-silica

A mixture of the [9-(2'-hydroxy-4'-undec-10''-enyloxyphenyl)-5,8-diaza-4-methyl-non-2,4,8-trienato](-2) nickel(II) (0.98 g, 2.0 mmol), dimethylsiloxy silica (Aldrich, 1.5 mmol g<sup>-1</sup>; 1.02 g, 1.53 mmol) and Karstedt's catalyst (20 μL, 2–3% solution) in toluene (20 ml) was stirred at 90 °C for 3 days. The mixture was cooled down to room temperature and the silica triturated several times for a total of 12 hours with toluene (3 × 20 ml), DCM (3 × 20 ml), THF (3 × 20 ml) and diethyl ether (20 ml) to remove physically adsorbed nickel complex, and was then dried to yield a red-orange powder (1.10 g). ICP-AE analysis showed there to be ca. 1.5% Ni (wt/wt) supported on the silica, corresponding to a catalyst loading of 0.25 mmol nickel g<sup>-1</sup> silica (catalyst 1).

### Immobilisation of nickel complex onto 4-benzyl chloride-functionalised silica

A deep red solution of the [9-(2'-hydroxy-4'-undec-10''-enyloxyphenyl)-5,8-diaza-4-methyl-non-2,4,8-trienato](-2) nickel(II) (0.41 g, 1.28 mmol) in dry DMF (20 ml) and THF (10 ml) was added dropwise at room temperature to a dispersion of excess 60% sodium hydride in mineral oil (0.09 g, 1.3 mmol) and the resulting mixture stirred for 10 minutes. A suspension of 4-benzyl chloride-functionalised silica (0.95 g, 1.3 mmol-Cl g<sup>-1</sup>, 1.23 mmol) in DMF (20 ml) was then added and the mixture stirred gently at room temperature overnight. The initially white silica became deep red. The solid was filtered off, washed several times with water (3 × 20 ml), soaked in DMF (50 ml) overnight, triturated with THF (3 × 20 ml) and air-dried to yield yellow solid (0.25 g). ICP-AE analysis showed there to be ca. 1% (wt/wt) nickel on the silica, corresponding to a catalyst loading of 0.15 mmol nickel g<sup>-1</sup> silica (catalyst 2).

### ICP Analysis of the supported catalysts

Calibration against nickel standards and a blank was linear, using 2% nitric acid solutions containing 0, 1, 5 and 10 ppm nickel made from a 1000 ppm stock solution (Aristar). Weighed samples (20.0 mg) of immobilised nickel catalysts were placed in glass tubes and digested at 180 °C in a mixture of concentrated nitric acid (5 cm<sup>3</sup>, Aristar) and concentrated perchloric acid (0.5 cm<sup>3</sup>, Aristar). For each catalyst, 3 parallel samples were digested in 2, 4 and 6 hours, respectively. The deep red nickel catalysts became white residues after digestion. The digest was then diluted to 50 cm<sup>3</sup> with water. Analysis showed that all the metal was removed from the support within 2 hours as increasing the digestion time to 4 hours and 6 hours achieved no increase in the amount of the metal in the digest.

### Catalysis studies

**Batch reactions.** Unless otherwise stated, a solution of 4-bromoanisole (0.187 g, 1 mmol) in dry THF (1.5 ml) was added to a Radley's Carousel reaction tube containing the required amount of catalyst silica. The Grignard reagent, phenylmagnesium chloride (2 M, 0.5 ml, 1 mmol) in THF was transferred *via* syringe under a nitrogen atmosphere and added directly into the solution of the organobromide. The mixture was stirred at room temperature for 24 hours under a nitrogen atmosphere. To work-up the reaction, saturated aqueous sodium chloride solution (2 ml) was added. The organic components were extracted into diethyl ether (2 × 2 ml) which was



then dried over anhydrous  $\text{MgSO}_4$  and the resulting solution analysed by GC and GC-MS with reference to standard solutions of 4-methoxybiphenyl, anisole and 4,4'-dimethoxybiphenyl.

**Micro flow reactions.** The Kumada coupling reaction of 4-bromoanisole and phenylmagnesium chloride in THF was carried out in a pressure driven micro flow reactor (length = 25 mm; I.D. = 3 mm) build up from Omnifit glassware containing the silica-supported nickel catalyst (100 mg). Standard HPLC connectors allowed one end of the reactor to be connected to a disposable solvent-resistant syringe, while the other end was attached to a syringe needle leading to a quenching vessel containing diethyl ether and saturated aqueous sodium chloride. A syringe pump (Razel, A-99) was used to drive a pre-determined volume of a mixture of equimolar solutions of 4-bromoanisole and phenylmagnesium chloride in THF (concentration of each component was 0.5 M) through the reactor at known flow rates. The organic components were extracted into diethyl ether and analysed by GC as described above.

## References

- 1 E. Negishi, F. Liu, A. Suzuki, S. Brase, and A. D. Meijere, in *Metal-catalysed Cross-coupling Reactions*, ed. F. Diederich and P. J. Stang, Wiley-VCH, Weinheim, 1998, p. 1.
- 2 K. Tamao, K. Sumitani and M. Kumada, *J. Am. Chem. Soc.*, 1972, **94**, 4374.
- 3 M. Kumada, *Pure Appl. Chem.*, 1980, **52**, 669.
- 4 K. Tamao, K. Sumitani, Y. Kiso, M. Zembayashi, A. Fujioka, S. Komada, I. Nakajima, A. Minato and M. Kumada, *Bull. Chem. Soc. Jpn.*, 1976, **7**, 1957.
- 5 A. Sekiya and N. Ishikawa, *J. Organomet. Chem.*, 1976, **118**, 349.
- 6 A. Sekiya and N. Ishikawa, *J. Organomet. Chem.*, 1977, **125**, 281.
- 7 K. Shimizu, E. Hayashi, T. Inokuchi, T. Kodama, H. Hagiwara and Y. Kitayama, *Tetrahedron Lett.*, 2002, **43**, 5653.
- 8 I. P. Beletskaya and A. V. Cheprakov, *Chem. Rev.*, 2000, **100**, 3009.
- 9 N. E. Leadbeater and M. Marco, *Chem. Rev.*, 2002, **102**, 3217.
- 10 E. B. Mubofu, J. H. Clark and D. J. Macquarrie, *Green Chem.*, 2001, **3**, 23.
- 11 O. Hemminger, A. Marteel, M. R. Mason, J. A. Davies, A. R. Tadd and M. A. Abraham, *Green Chem.*, 2002, **4**, 507.
- 12 D. J. Macquarrie, *Chem. Commun.*, 1997, 601.
- 13 B. Gotov, S. Toma and D. J. Macquarrie, *New J. Chem.*, 2000, **24**, 597.
- 14 N. J. Meehan, A. J. Sandee, J. N. H. Reek, P. C. J. Kamer, P. W. N. M. van Leeuwen and M. Poliakoff, *Chem. Commun.*, 2000, 1497.
- 15 B. F. G. Johnson, S. A. Raynor, D. S. Shephard, T. Mashmeyer, J. M. Thomas, G. Sankar, S. Bromley, R. Oldroyd, L. Gladden and M. D. Mantle, *Chem. Commun.*, 1999, 1167.
- 16 J. S. Kingsbury, S. B. Garber, J. M. Giftos, B. L. Gray, M. M. Okamoto, R. A. Farrer, J. T. Fourkas and A. H. Hoveyda, *Angew. Chem., Int. Ed.*, 2001, **40**, 4251.
- 17 H. Gao and R. J. Angelici, *Organometallics*, 1999, **18**, 989.
- 18 H. Yang, H. Gao and R. J. Angelici, *Organometallics*, 2000, **19**, 622.
- 19 S. J. Haswell, R. J. Middleton, B. O'Sullivan, V. Skelton, P. Watts and P. Styring, *Chem. Commun.*, 2001, 391.
- 20 K. Jähnisch, V. Hessel, H. Löwe and M. Baerns, *Angew. Chem., Int. Ed.*, 2004, **43**, 406.
- 21 P. D. I. Fletcher, S. J. Haswell, E. Pombo-Villar, B. H. Warrington, P. Watts, S. Y. F. Wong and X. Zhang, *Tetrahedron*, 2002, **58**, 4735.
- 22 X. Ouyang and R. S. Besser, *Catal. Today*, 2003, **84**, 33.
- 23 S. J. Haswell and P. Watts, *Green Chem.*, 2003, **5**, 240 and references therein.
- 24 R. D. Chambers, D. Holling, A. J. Rees and G. Sandford, *J. Fluorine Chem.*, 2003, **119**, 81.
- 25 M. Ueno, H. Hisamoto, T. Kitamori and S. Kobayashi, *Chem. Commun.*, 2003, 936.
- 26 M. Mayr, B. Mayr and M. R. Buchmeiser, *Angew. Chem., Int. Ed.*, 2001, **40**, 3839.
- 27 S. J. Haswell, B. O'Sullivan and P. Styring, *Lab Chip*, 2001, **1**, 164.
- 28 N. T. S. Phan, D. H. Brown, H. Adams, S. E. Spey and P. Styring, *Dalton Trans.*, 2004, 1348.
- 29 P. Styring, C. Grindon and C. M. Fisher, *Catal. Lett.*, 2001, **77**, 219.
- 30 L. Djakovitch and K. Koehler, *J. Mol. Catal. A: Chem.*, 1999, **142**, 275.
- 31 O. Wörz, P. Jäckel, T. Richter and A. Wolf, *Chem. Eng. Sci.*, 2001, **56**, 1029.
- 32 W. E. Rapp, in *Combinatorial Chemistry*, ed. S. R. Wilson and A. W. Czarnik, John Wiley & Sons, New York, 1997, p. 66.
- 33 P. He, S. J. Haswell and P. D. I. Fletcher, *Lab Chip*, 2004, **4**, 38.



## Rearrangement of $\alpha$ -pinene oxide using a surface catalysed spinning disc reactor (SDR)

M. Vicevic,<sup>a</sup> R. J. J. Jachuck,<sup>\*a†</sup> K. Scott,<sup>a</sup> J. H. Clark<sup>b</sup> and K. Wilson<sup>b</sup>

<sup>a</sup> School of Chemical Engineering and Advanced Materials, University of Newcastle, Newcastle upon Tyne, UK NE1 7RU. E-mail: rjachuck@clarkson.edu

<sup>b</sup> Clean Technology Centre, Department of Chemistry, University of York, York O10 5DD

Received 19th March 2004, Accepted 1st July 2004

First published as an Advance Article on the web 7th October 2004

Isomerisation of  $\alpha$ -pinene oxide to campholenic aldehyde was performed by immobilising zinc triflate based catalysts on the surface of a spinning disc reactor (SDR). Two types of catalyst have been studied and the influence of operating parameters such as rotational speed, feed flow rate and reaction temperature on conversion and selectivity towards campholenic aldehyde has been investigated in considerable detail. The findings of the study suggest that immobilising the catalyst on the reactor surface and performing the reaction in continuous mode has potential for achieving benefits of Green Chemical Technology (GCT).

### Introduction

Campholenic aldehyde is an important intermediate used by the fragrance industry in the synthesis of santalol, which is the principle component of sandalwood oil, and is currently prepared by Lewis acid catalysed rearrangement of  $\alpha$ -pinene oxide.<sup>1</sup> Commercially used homogeneous catalysts for this reaction are  $ZnCl_2$  and  $ZnBr_2$  and extraction of these catalysts from the reaction media is difficult and involves the use of energy intensive separation processes. This provides scope for development and use of heterogeneous catalysts, which can be separated by using filtration techniques. However if the heterogeneous catalyst can be fixed onto the reactor surface then it may be possible to eliminate the use of downstream separation modules required for recovering the catalyst from the product mixture. This approach can have significant influence not only on the energy efficiency of the process but also on the catalyst activity as shear between the fluid and the catalyst fixed on the reactor wall will be high. The Green Chemistry Group at the University of York and the Process Intensification team at Newcastle University have carried out a detailed study by using supported Lewis acid catalyst fixed on the surface of a spinning disc reactor and performing the rearrangement of  $\alpha$ -pinene oxide. The characterisation of the catalyst used in this study has been presented in detail by Wilson *et al.*<sup>2</sup> A new solid acid catalyst based on silica supported zinc triflate has been used as it was reported to be active and reasonably selective in the rearrangement of pinene oxide to campholenic aldehyde.<sup>2</sup> In this paper experimental results together with detailed analysis of the catalyst activity, batch reactions which were used for bench marking purposes and SDR results are presented.

### Spinning disc reactor technology

The spinning disc technology uses centrifugal accelerations to create thin highly sheared films on rotating surfaces (Fig. 1), of the order of 25–200  $\mu\text{m}$ . These reactors have the following characteristics: high heat and mass transfer,<sup>3</sup> controlled residence time, provide an intense mixing environment and have a high surface area to volume ratio. The SDR has been

successfully used for performing polymerisation (both free radical<sup>4,5</sup> and condensation<sup>6</sup>) reactions, precipitation of particles with controlled size and shape<sup>7</sup> and for performing fast reactions.

A review of literature has shown that this study is the first of its kind which has investigated the use of immobilised catalyst on the surface of a SDR. Preliminary findings of this study, using a 0.05 mmol  $\text{g}^{-1}$  zinc triflate– $\text{SiO}_2$  catalyst for performing the rearrangement reaction of  $\alpha$ -pinene oxide to campholenic aldehyde, have been reported in ref. 8. It was concluded that it is possible to achieve complete conversion of  $\alpha$ -pinene oxide on the disc as long as the residence time on the reactor surface was greater than 2 seconds. Complete conversion was achieved at the expense of selectivity as it was found that for a given rotational speed, higher feed flow rates enhanced selectivity towards aldehyde to a maximum of 62% but with lower conversion of 75% (flow rate of 6cc  $\text{s}^{-1}$ ). When the SDR experiments were compared with batch reactor results it was obvious that the low selectivity achieved on the disc was due to the sensitive nature of the product, which has a similar reactivity to  $\alpha$ -pinene oxide and the high mixing intensity of the spinning disc accelerated this reaction. In this paper experimental findings of tests carried out by using 0.05 mmol  $\text{g}^{-1}$   $Zn(OTf)_3$ – $HMS_{24}$  catalyst are presented.

### Experimental programme

#### Batch process

In order to compare the results achieved on the catalysed spinning disc reactor, the rearrangement reaction was carried



Fig. 1 Waves formed on the surface of the SDR.

<sup>†</sup> Current address: Process Intensification and Clean Technology (PICT) Group Department of Chemical Engineering, Clarkson University Potsdam, Box 5705, NY – 13699, USA.

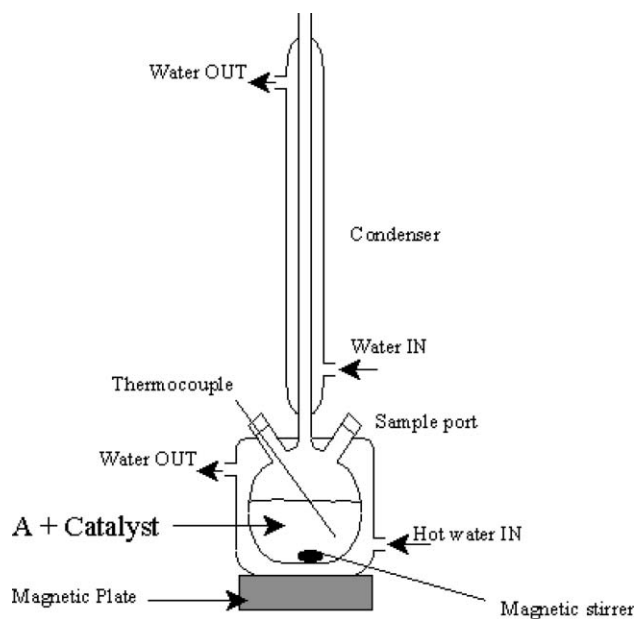


**Fig. 2** Schematic diagram of the batch reactor used for the rearrangement reaction of  $\alpha$ -pinene oxide (A).

out in a batch reactor, which is schematically shown in Fig. 2. The reactor consisted of a jacketed glass vessel for controlling the reactor temperature. The temperature of the reaction mixture was maintained at 45 °C and monitored by a thermocouple immersed in the reactant–product mixture. The stirrer speed was set at 800 rpm in order to achieve a uniform distribution of the catalyst within the reaction mixture. Product samples were taken every minute during the reaction and analysed using gas chromatography. After the reaction had proceeded to completeness, samples were withdrawn and analysed every five minutes to investigate product stability. The results of the batch experiments are presented in Fig. 3.

### Spinning disc reactor experiments

Tests were carried out by supporting the catalyst on the surface of a spinning disc reactor and a range of process conditions studied. A 200 mm diameter smooth disc, shown in Fig. 4, was used to perform the isomerisation reaction. A schematic diagram of the catalytic SDR can be seen in Fig. 5. The reactor

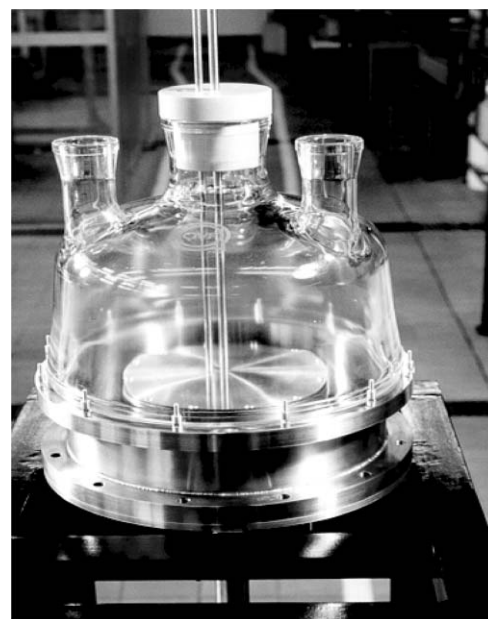


**Fig. 4** Spinning disc reactor.

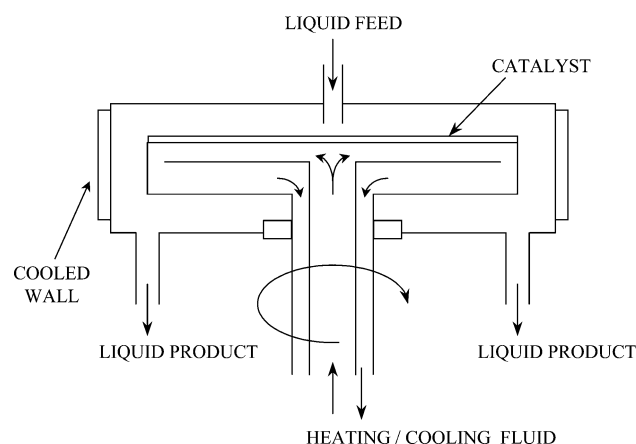


**Fig. 5** Schematic of internally heated spinning disc reactor (SDR).

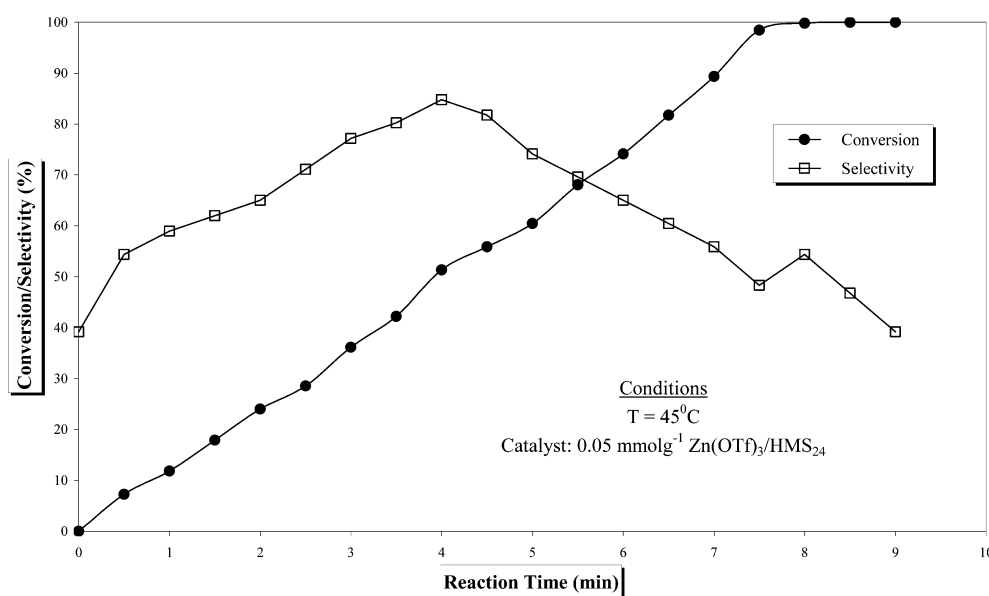


**Fig. 3** Conversion and selectivity data in a batch reactor.

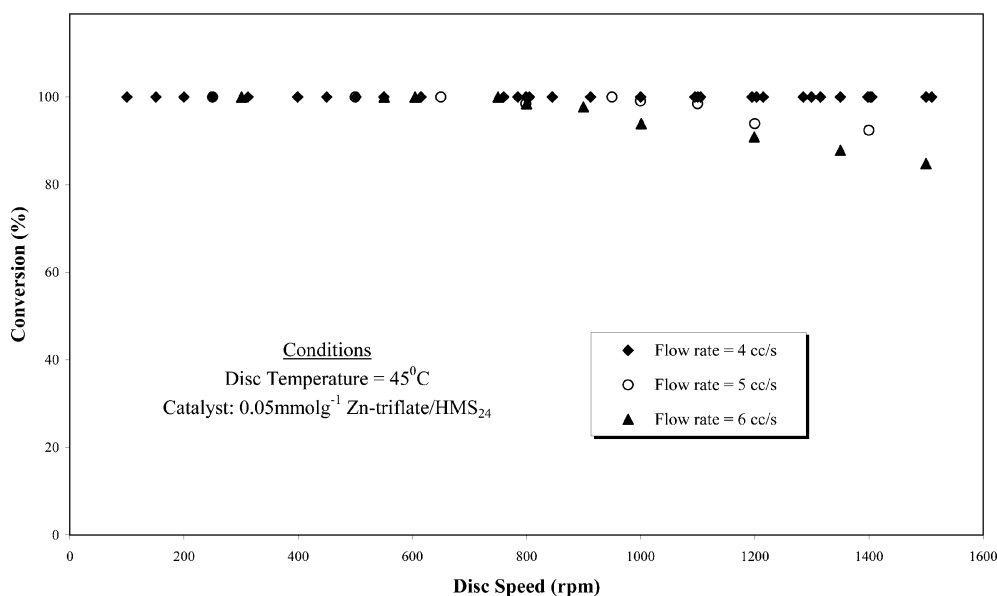


Fig. 6 Conversion results for the  $0.05 \text{ mmol g}^{-1} \text{ Zn(OTf)}_3\text{-HMS}_{24}$ .

had internal heating/cooling capability as well as temperature controlled jacketed walls. The catalyst ( $0.05 \text{ mmol g}^{-1} \text{ Zn(OTf)}_3\text{-HMS}_{24}$ ) was coated on the disc surface using an epoxy based glue. A thin layer of a two-component glue was spread on the disc and the catalyst sprinkled over it. After application the coated disk was left for 24 hours to allow the adhesive to fully dry and form a thin layer of the catalyst on the surface. Tests were performed using a disc temperature of  $45^\circ\text{C}$  by feeding the reactant which contained 1 g of  $\alpha$ -pinene oxide (Aldrich 99%) in 100 ml of 1,2-dichloroethane (Aldrich 98%) and 0.5 g of decane (Aldrich 99%) (internal standard). The feed was introduced at the centre of the disc and streamed across the catalysed surface in the form of thin highly sheared films. Product was continuously collected *via* exit pipes located at the bottom of the reactor. Thermocouples were located at selected positions to continuously measure the temperatures of the disc, feed and product. The collected samples were immediately analysed.

#### Analysis of samples

Samples collected from the SDR runs were analysed using an UNICAM Series 610 Gas Chromatograph, with a HP1 packed

column. The measured concentration values were used for calculating the conversion and selectivity of the runs. The GC was calibrated by using solutions of  $\alpha$ -pinene oxide in 1,2-dichloroethane in addition to known concentration solutions of campholenic aldehyde. The accuracy of the data collected was within  $\pm 1\%$ .

#### Results

Experimental results in the form of product conversion and selectivity are presented in this section for all the test runs carried out during the study. Tests were completed using rotational rates between 100–1500 rpm (corresponding to a centrifugal acceleration of 1–250 g) with flow rates of 4, 5 and  $6 \text{ cc s}^{-1}$  with the reactor surface temperature being maintained at  $45^\circ\text{C}$ . As can be seen in Fig. 6, 100% conversion was achieved for most of the runs with selectivity ranging from 20–75% towards campholenic aldehyde, as shown in Fig. 7. For flow rates 5 and  $6 \text{ cc s}^{-1}$  the conversion achieved is less than 100% as the rotational speed is increased beyond 800 rpm. This can be attributed to residence time effects. The residence time of the fluid on the disc decreases with increased rotational

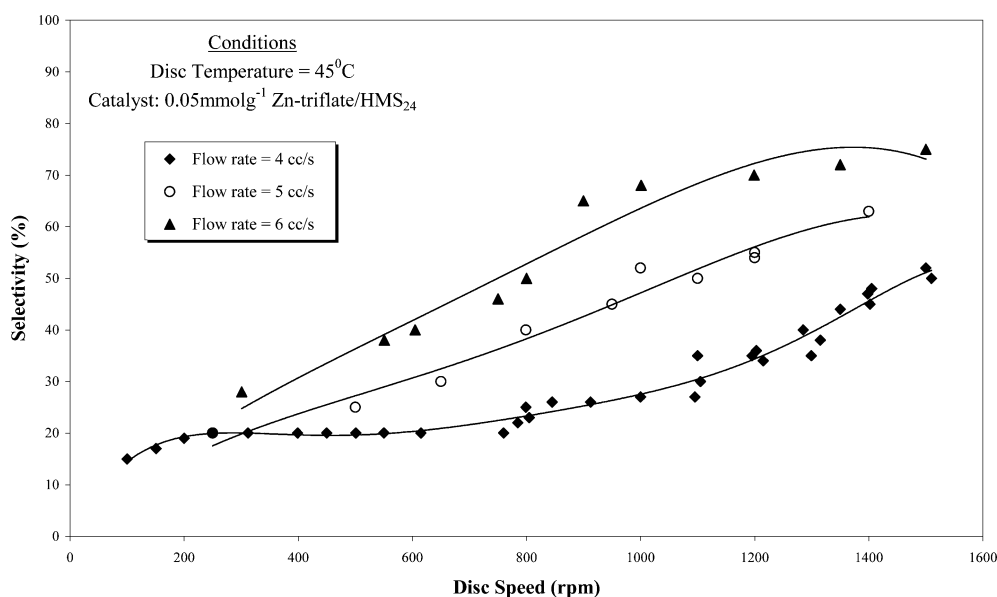


Fig. 7 Selectivity results for the  $0.05 \text{ mmol g}^{-1} \text{ Zn(OTf)}_3\text{-HMS}_{24}$ .



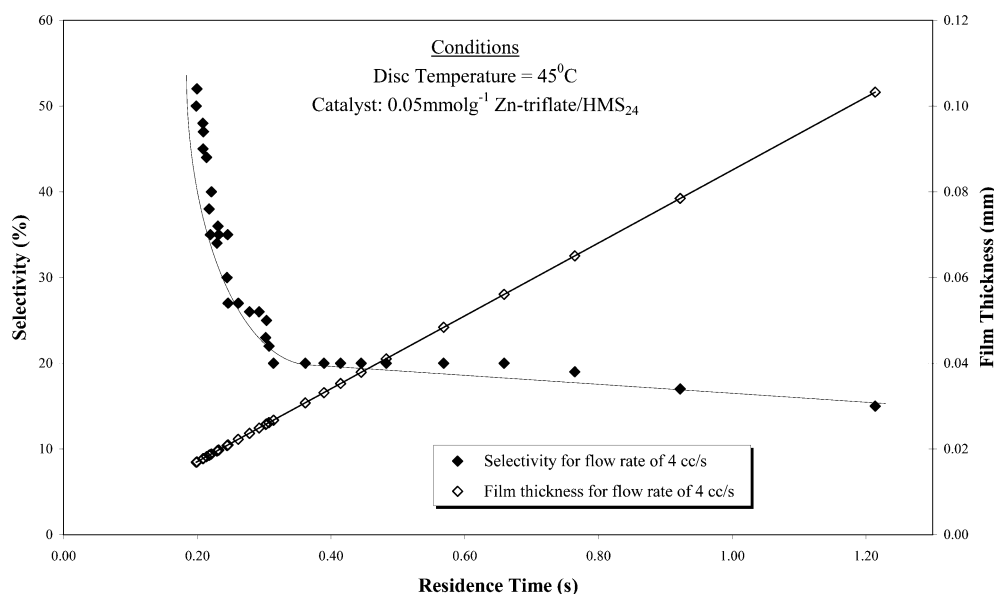


Fig. 8 Selectivity towards aldehyde and film thickness dependence on residence time.

speeds, therefore at these elevated rotational rates there is not sufficient time for the reaction to proceed to completeness. Fig. 7 shows the selectivity achieved for all the runs investigated and it is clear that the selectivity increases from 20 to 70% as the rotational rate is adjusted from 300 to 1500 rpm for the flow rate of 6 cc s<sup>-1</sup>. However the selectivity achieved for flow rates of 4 and 5 cc s<sup>-1</sup> is less than 50% over this rotational range. The selectivity profile obtained for all the experiments suggest that for a given flow rate increasing the rotational speed of the disc increases the selectivity of the process. This means that the selectivity is increasing when the residence time is short (less than 0.2 s as shown in Fig. 8).

The relationship between selectivity towards campholenic aldehyde and residence time on the disc as well as film thickness and residence time are shown in Figs. 8 and 9 respectively.

## Conclusions

This study has investigated a novel catalyst which was immobilised on the surface of a SDR. An earlier investigation

using a photocatalytic<sup>9</sup> rotating surface for treating chlorophenol had showed that provided catalysts can be immobilised on a reactor surface and heating and cooling facilities can be incorporated, SDRs can provide a useful module to perform catalytic reactions. Using a well designed SDR with good heat and mass transfer capabilities, rearrangement of  $\alpha$ -pinene using an immobilised catalyst system was studied and the findings have several implications. Firstly the high shear rates between the reaction medium and the catalyst has resulted in faster reaction rates allowing the reaction to achieve near completion in less than one second. Average shear rates as high as 13000 s<sup>-1</sup> were achieved on the disc surface in comparison to about 300 s<sup>-1</sup> in a conventional batch reactor. Secondly it has been shown that using the SDR technology the selectivity of the process may be influenced by controlling the residence time of the reaction which minimises the numerous side reactions that could take place. Thirdly this processing concept provides an opportunity to achieve product which is free of catalyst. This implies that the downstream separation process which is often used to recover the catalyst from the product can be eliminated, thereby providing scope for significant reduction in the energy

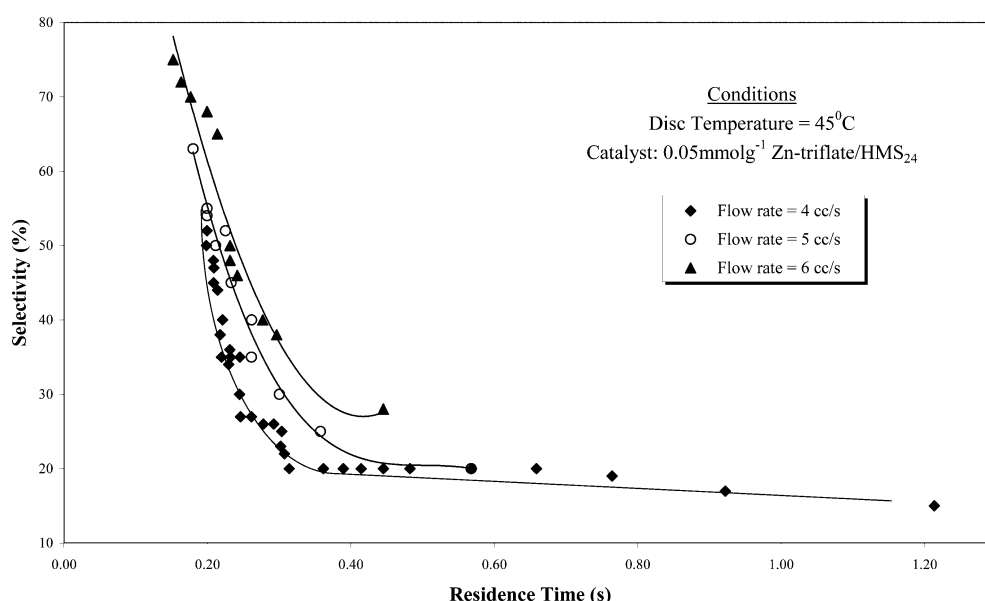


Fig. 9 Selectivity towards aldehyde dependence on residence time for different flow rates.

**Table 1** Comparison between batch and spinning disc reactor

	Batch process	SDR process
Process time/s	3600	~1
Processed feed/g h <sup>-1</sup>	1	60
Conversion (%)	50	85
Selectivity (%)	80	75
Additional notes	Catalyst separation	No loss of catalyst. Continuous process

consumption of the process. This study has also highlighted that the immobilised catalyst remains active over a considerable period of time. This knowledge, coupled with the fact that the use of SDR technology offers the opportunity for continuous rather than batch mode of operation, implies that the proposed process may reduce hold up and inventory making the operation much safer. A comparison between the conventional process using batch reactor technology and the intensified approach using SDR technology has been presented in Table 1. This comparison slightly favours the SDR performance because even though the amount of catalyst immobilised on the disc surface was extremely small compared to what was used in the batch vessel, the catalyst to reactant concentration was twice as much in the SDR than for the batch. This is because at any given time only a small amount of reactant comes in contact with the immobilised catalyst surface as the SDR process was operated on a continuous basis. In addition the SDR technology also offers good heat transfer rates<sup>10</sup> and may allow the use of higher operating temperatures resulting in faster reaction rates and therefore even smaller reactor size or disc diameter. This will further reduce the residence time and improve selectivity. It may be concluded that by selecting the appropriate catalyst immobilised on the surface of the SDR it may be possible to achieve a continuous process for the rearrangement of  $\alpha$ -pinene oxide to campholenic aldehyde. The findings of the present study indicate that the vision of realising a truly intensified chemical plant using green chemistry to achieve greener technology is a real possibility

## Acknowledgements

The authors gratefully acknowledge the financial contribution made by the EPSRC, UK and the Royal Academy of Engineering for supporting this activity.

## References

- 1 J. B. Lewis and G. W. Hedrick, Reaction of  $\alpha$ -pinene oxide with zinc bromide and rearrangement of 2,2,3-trimethyl-3-cyclopentene products derived therefrom, *J. Org. Chem.*, 1965, **30**, 4271.
- 2 K. Wilson, A. Renson and J. H. Clark, Novel heterogeneous zinc triflate catalysts for the rearrangement of  $\alpha$ -pinene oxide, *Catal. Lett.*, 1999, **61**(1–2), 51–55.
- 3 A. Aoune and C. Ramshaw, Process Intensification: Heat and Mass Transfer Characteristics of Liquid Films on Rotating Discs, *Int. J. Heat Mass Transfer*, 1999, **42**(14), 2543–2556.
- 4 K. V. K. Boodhoo, W. A. E. Dunk and R. J. Jachuck, Influence of Centrifugal Field on Free-Radical Polymerisation Kinetics, *J. Appl. Polym. Sci.*, 2002, **85**, 2283–2286.
- 5 P. Leveson, W. A. E. Dunk and R. J. Jachuck, Numerical Investigation of Kinetics of Free-Radical Polymerisation on Spinning Disk Reactor, *J. Appl. Polym. Sci.*, 2003, **90**, 693–699.
- 6 K. V. K. Boodhoo and R. J. Jachuck, Process Intensification: Spinning Disc Reactor for Condensation Polymerisation, *Green Chem.*, 2000, **2**, 235–244.
- 7 G. Trippa, P. Hetherington, and R. J. J. Jachuck, Process Intensification: Precipitation of Calcium Carbonate from the Carbonation Reaction of Lime Water using a Spinning Disc Reactor, in *15th Int. Symp. Ind. Cryst.*, Sorrento, Italy, 2002.
- 8 M. Vicevic, R. J. J. Jachuck and K. Scott, Process Intensification for Green Chemistry: Rearrangement of  $\alpha$ -pinene oxide on the Spinning Disc Reactor, in *4th Int. Conf. Process Intensif. Chem. Ind.*, BHR Group, Brugge, Belgium, 10–12 September 2001.
- 9 H. C. Yatmaz, C. Wallis and C. R. Howarth, The Spinning Disc Reactor – Studies on a Novel TiO<sub>2</sub> Photocatalytic Reactor, *Chemosphere*, 2001, **42**, 397–403.
- 10 R. J. J. Jachuck and C. Ramshaw, Process Intensification – Heat-Transfer Characteristics Of Tailored Rotating Surfaces, *Heat Recovery Syst. CHP*, 1994, **14**(5), 475–491.